

TECHNISCHE UNIVERSITÄT MÜNCHEN

Lehrstuhl für Molekulare Ernährungsmedizin

The developmental role of brown adipose tissue and brown-like adipocytes (brite) in murine neonates

David Lasar

Vollständiger Abdruck der von der Fakultät Wissenschaftszentrum Weihenstephan für Ernährung, Landnutzung und Umwelt der Technischen Universität München zur Erlangung des akademischen Grades eines

Doktors der Naturwissenschaften

genehmigten Dissertation.

Vorsitzender:

Univ.-Prof. Dr. M. W. Pfaffl

Prüfer der Dissertation:

1. Univ.-Prof. Dr. M. Klingenspor

2. Univ.-Prof. A. Schnieke, PhD

Die Dissertation wurde am 18. Juni 2014 bei der Technischen Universität München eingereicht und durch die Fakultät Wissenschaftszentrum Weihenstephan für Ernährung, Landnutzung und Umwelt am 15. September 2014 angenommen.

A theory can be proved by experiment; but no path leads from experiment to the birth of a theory.

- *Albert Einstein (The Sunday Times 18th July 1976)*

Table of contents

I List of figures	5
II List of tables	8
III List of abbreviation	9
Summary	12
1 Introduction	14
1.1 White and brown adipose tissue	14
1.2 Adipose tissue during murine development	16
1.3 Brown like adipocyte in white adipose tissue	17
1.4 Brown adipose tissue and brite occurrence in humans	19
1.5 Aims and scopes of this study	21
2 Material & Methods	23
2.1 Animal treatment	23
2.2 Animal experimentation	23
2.3 Perfusion of animals	25
2.4 Isolation of genomic DNA for genotyping of the UCP1 knockout mice	26
2.5 Polymerase Chain Reaction (PCR) targeting UCP1	26
2.6 Phenol-chloroform RNA extraction	27
2.7 Quantitative Reverse Transcription - Polymerase Chain Reaction (qRT-PCR)	28
2.8 Next generation sequencing.....	29
2.9 Combined Methylation sensitive high resolution melting (MS-HRM) and pyrosequencing of the UCP1 enhancer region.....	29

2.10 Protein extraction with RIPA-buffer	31
2.11 Western Blot.....	32
2.12 Histology - Hematoxylin & Eosin stain (H&E) and Immuno-histo-chemistry (IHC)	33
2.13 Hematoxylin & Eosin stain (H&E)	33
2.14 Immuno-Histo-Chemistry (IHC)	34
2.15 Immunofluorescence of UCP1-GFP reporter mice	34
2.16 Statistics.....	35
3 Results	36
3.1 Postnatal britening correlates with fat mass development.....	36
3.2 Maternal care modulates postnatal britening and fat pad development	49
3.3 Thermoneutrality reduces britening in white fat and leads to a brown fat hypertrophy	57
3.4 Epigenetic modifications are transiently reduced upon britening of white adipose tissue.....	65
3.5 Next Generation Sequencing based transcriptome analysis reveals putative genes involved in white fat britening	69
4 Discussion	77
5 References	87
IV Acknowledgments	94
V Curriculum Vitae	95
VI A Statement under Oath/Eidesstattliche Erklärung	98

I List of figures

Figure 1 Immunohistochemical detection of UCP1 positive adipocytes	15
Figure 2 Schematic draw of the respiratory chain within brown adipocyte mitochondria.....	16
Figure 3 Current model of brown and white adipocyte differentiation compared to skeletal muscle lineage.....	18
Figure 4 Schematic draw of a gravity driven perfusion system	25
Figure 5 Schematic draw of electric transfer arrangement using a semi-dry system	32
Figure 6 Postnatal body mass development of C57BL6/N (B6) and 129S6sv/ev (129) mice. .	36
Figure 7 Postnatal development of body mass and body composition of C57BL6/N (B6) and 129S6sv/ev (129) mice.	37
Figure 8 Body composition in proportion to body mass of C57BL/6N (B6) and 129S6sv/ev (129) mice.	38
Figure 9 Postnatal development of fat pad mass of C57BL6/N (B6) and 129S6sv/ev (129) mice.	39
Figure 10 Fat pad mass in proportion to body mass of C57BL6/N (B6) and 129S6sv/ev (129) mice.	40
Figure 11 Hematoxylin and eosin (H&E) staining of rWAT and iBAT of C57BL6/N (B6) and 129S6sv/ev (129) mice.	41
Figure 12 Immunohistochemical detection of UCP1-positive adipocytes in rWAT and iWAT of C57BL6/N (B6) and 129S6sv/ev (129) mice.	42
Figure 13 Immunofluorescence detection of UCP1-expressing adipocytes in iBAT and rWAT of C57BL6/N GFP reporter mice.	43
Figure 14 Expression of brown adipocyte marker genes in postnatal retroperitoneal white adipose tissue (rWAT) and inguinal white adipose tissue (iWAT) of C57BL6/N (B6) and 129S6sv/ev (129) mice.	45
Figure 15 Immunoblots of brown fat marker in iWAT and iBAT of C57BL6/N (B6) and 129S6sv/ev (129) mice.	46
Figure 16 Expression of PRDM16 and PGC1 α of C57BL6/N (B6) and 129S6sv/ev (129) mice.	47
Figure 17 Development of fat pad mass and brown fat marker expression of C57BL6/N (B6), 129S6sv/ev (129), AKR/J and SWR/J mice.....	48

Figure 18 Postnatal body mass development of cross fostered (CF) C57BL6/N (B6) and 129S6sv/ev (129) mice.	49
Figure 19 Postnatal development of fat pad masses of cross fostered (CF) C57BL6/N (B6) and 129S6sv/ev (129) mice.	50
Figure 20 Fat pad mass in proportion to body mass of cross fostered (CF) C57BL6/N (B6) and 129S6sv/ev (129) mice.	52
Figure 21 Expression of brown adipocyte marker genes in cross fostered (CF) postnatal retroperitoneal white adipose tissue (rWAT) and inguinal white adipose tissue (iWAT) of C57BL6/N (B6) and 129S6sv/ev (129) mice.	54
Figure 22 Expression of standardized brown adipocyte marker genes in cross fostered (CF) and normal fostered (NF) postnatal retroperitoneal white adipose tissue (rWAT) and inguinal white adipose tissue (iWAT) of C57BL6/N (B6) and 129S6sv/ev (129) mice.	56
Figure 23 Postnatal body mass of thermoneutral kept C57BL6/N (B6) and 129S6sv/ev (129) mice.	58
Figure 24 Postnatal body composition of thermoneutral kept C57BL6/N (B6) and 129S6sv/ev (129) mice.	58
Figure 25 Body composition of thermoneutral kept C57BL6/N (B6) and 129S6sv/ev (129) mice in proportion to body mass.	59
Figure 26 Postnatal fat pad masses of thermoneutral kept C57BL6/N (B6) and 129S6sv/ev (129) mice.	60
Figure 27 Fat pad mass in proportion to body mass of thermoneutral kept C57BL6/N (B6) and 129S6sv/ev (129) mice.	61
Figure 28 Postnatal lean masses of normal fostered and thermoneutral kept C57BL6/N (B6) and 129S6sv/ev (129) mice.	62
Figure 29 Immunohistochemical detection of UCP1-positive adipocytes in iBAT and iWAT of thermoneutral kept C57BL6/N (B6) and 129S6sv/ev (129) mice.	63
Figure 30 Expression of brown adipocyte marker genes in postnatal retroperitoneal white adipose tissue (rWAT) of thermal neutral kept C57BL6/N (B6) and 129S6sv/ev (129) mice. .	64
Figure 31 Schematic representation of the UCP1 enhancer region and its putative binding factors.	65
Figure 32 Schematic representation of a “U”-shaped methylation pattern	66

Figure 33 Methylation of the UCP1 enhancer region in postnatal retroperitoneal white adipose tissue (rWAT) and interscapular brown adipose tissue (iBAT) of C57BL6/N (B6) and 129S6sv/ev (129) mice.....	67
Figure 34 Normalized expression of UCP1 in postnatal retroperitoneal white adipose tissue (rWAT) of C57BL6/N (B6) and 129S6sv/ev (129) mice.....	69
Figure 35 Normalized expression of brown adipocyte marker genes in postnatal retroperitoneal white adipose tissue (rWAT) of C57BL6/N (B6) and 129S6sv/ev (129) mice.	70
Figure 36 Normalized expression of candidate genes in postnatal retroperitoneal white adipose tissue (rWAT) of C57BL6/N (B6) and 129S6sv/ev (129) mice.....	72
Figure 37 Normalized expression of negatively correlating candidate genes in postnatal retroperitoneal white adipose tissue (rWAT) of C57BL6/N (B6) and 129S6sv/ev (129) mice.	76

II List of tables

Table 1 Composition of diets.....	23
Table 2 Anesthesia protocol.....	25
Table 3 Composition of Tail-Lysis buffer	26
Table 4 PCR batch composition.....	26
Table 5 PCR program for genotyping UCP1 knockout animals	26
Table 6 Composition of RNA loading buffer.....	27
Table 7 Composition of a 1% formaldehyde gel for RNA separation	27
Table 8 Composition of qRT-PCR reaction mixture.....	28
Table 9 qRT-PCR program for gene expression analysis	28
Table 10 qRT-PCR Primer list.....	28
Table 11 Composition of RIPA-buffer.....	31
Table 12 List of primary antibody.....	32
Table 13 Time schedule for ethanol/xylene dehydration array.....	33
Table 14 Program for Hematoxylin-Eosin Staining	33
Table 15 Relative differences in body mass, eWAT, iWAT, rWAT and iBAT mass of cross fostered C57BL6/N and 129S6sv/ev mice expressed as percentage of normally fostered C57BL6/N and 129S6sv/ev mice.	51
Table 16 Relative differences in body mass, eWAT, iWAT, rWAT and iBAT mass of thermoneutral kept C57BL6/N and 129S6sv/ev mice expressed as percentage of normally fostered C57BL6/N and 129S6sv/ev mice.....	60
Table 17 List of reference genes correlating to postnatal browning in retroperitoneal white adipose tissue.....	70
Table 18 List of candidates with a high coefficient of variation	71
Table 19 List of candidates with a higher mean at P20 in 129S6sv/ev	73
Table 20 List of candidates with a higher mean at P20 in C57BL6/N	73
Table 21 List of candidates with negative correlation sorted by the coefficient of variation .	75

III List of abbreviation

129	129S6sv/ev Tac
ADP	adenosine diphosphate
ATP	adenosine triphosphate
B6	C57BL6/N
BAT	brown adipose tissue
BM	body mass
BMI	body mass index
bp	base pair
brite	brown in white
°C	degree Celsius
cAMP	cyclic adenosine monophosphate
CF	cross-fostered
CIDEA	cell death-inducing DFFA-like effector a
CREB	cAMP response element-binding
COX	cytochrome-c-oxidase
CV	coefficient of variation
d	days
Da	Dalton
DAB	3,3'-Diaminobenzidine
DAPI	4',6-diamidino-2-phenylindole
DIO	diet induced obesity
DNA	Deoxyribonucleic acid
e⁻	electron
ECL	enhanced chemoluminescence
eWAT	epididymal white adipose tissue
FDG	fluorodesoxyglucose
FGF	fibroblast growth factor

g	gram
GFP	green fluorescence protein
h	hours
H⁺	hydrogen ion
H&E	Hematoxylin & Eosin
IHC	Immuno-histo-chemistry
iWAT	inguinal white adipose tissue
ko	knockout
mg	milligram
ml	milliliter
MIM	mitochondrial inner membrane
min	minutes
MOPS	3-morpholinopropane-1-sulfonic acid
mRNA	messenger ribonucleic acid
Myf5	myogenic factor 5
NADH	nicotinamide adenine dinucleotide
NF	normal fostered
NGS	next generation sequencing
NMR	nuclear magnetic resonance
NST	non-shivering thermogenesis
P_i	pyrophosphate
P10	postnatal day 10
P20	postnatal day 20
P30	postnatal day 30
PAGE	polyacrylamide gel electrophoresis
PET/CT	positron emission tomography / X-ray computed tomography
PFA	Paraformaldehyde
PKA	protein kinase A
qRT-PCR	quantitative Reverse Transcription - Polymerase Chain Reaction

RIPA	Radioimmunoprecipitation assay
RNA	Ribonucleic acid
RT	room temperature
s	seconds
SD	standard deviation
SDS	Sodium dodecyl sulfate
TRIS	2-Amino-2-hydroxymethyl-propane-1,3-diol
rWAT	retroperitoneal white adipose tissue
TN	thermoneutral
Ttest	Student's t-test
WAT	white adipose tissue
UCP1	uncoupling protein 1

Summary

Nonshivering thermogenesis is mediated by the brown adipose tissue a specialized organ to dissipate energy provided by food into heat to maintain body temperature of neonates and small mammals. The heat is produced by uncoupling the mitochondrial oxidative phosphorylation that is dependent on uncoupling protein 1 (UCP1). During the postnatal development of mice certain white adipose tissue depots show a transient occurrence of brown adipocytes. These called brite (brown in white) adipocytes share several characteristics with classical brown adipocytes including a multilocular appearance and the expression of UCP1. The occurrence of brite adipocytes in adult mice can be chemically mediated by β_3 -adrenergic stimulation or naturally by prolonged cold exposure. Interestingly during postnatal development white fat depots show a strong brite occurrence with a maximum at postnatal day 20.

In the present study, pups of inbred mouse strains during the first 30 days of life were compared to analyze postnatal briteening. The strains C57BL6/N and 129S6sv/ev are known for their different propensity to diet-induced obesity. In both strains a transient reversible briteening that means a transition from white to brown adipocyte morphology could be observed in retroperitoneal and inguinal adipose tissue depots. Comparing pups of both strains show an increased abundance of multilocular and UCP1 positive cells from postnatal day 10 to 20 in 129S6sv/ev. In parallel the fat pad masses of the two fat depots attenuated upon briteening. However epididymal white and interscapular brown adipose tissue show a steady increased mass gain during the first 30 days of life. During this period, 129S6sv/ev pups developed a significantly higher total body fat mass than C57BL6/N.

Getting new insights of the occurrence of postnatal briteening the breeding conditions of both strains were manipulated by cross fostering and by changing the ambient temperature. Cross fostering, switching the pups from a 129S6sv/ev mother to a C57BL6/N mother and vice versa shows a maternal influence on briteening. The significant strain difference higher in 129S6sv/ev at postnatal day 20 is diminished either on fat pad mass gain or the abundance of brite adipocytes in retroperitoneal and inguinal white adipose tissue. Changing maternal care leads to an increase in fat pad mass gain in C57BL6/N, but the expression of brown adipocyte markers was not significantly increased. However in both strains the fat pad growth attenuation still remains. To validate whether the modulated briteening phenomenon is a

result of maternal care or genetic predisposition, pups of both strains were raised in a 30 °C environment to diminish postnatal browning. Animals of both strains drastically increase total body fat mass that can also be observed on the individual fat pad development. However these animals show a reduced browning but the strain difference of brown adipocyte marker gene expression is still higher in 129S6sv/ev. These manipulations show a stronger effect provided by maternal care.

To determine whether a genetic predisposition still interacts in the postnatal browning a methylation analysis of both strains of the UCP1 enhancer region in retroperitoneal white adipose tissue of normal fostered mice were performed. This analysis shows a significant reduced methylation pattern in 129S6sv/ev. To elucidate which genes are possible markers, inhibiting or enhancing white adipose tissue browning a Next Generation Sequencing based transcriptome analysis revealed new factors that are differentially expressed in both strains.

Based on these results the naturally occurrence of browning in white adipose tissues is a phenomenon that is both genetically inherited and specifically modulated by maternal care. The postnatal imprinting might be a possibility to modify the capacity of white adipose tissue browning in adults to increase resting energy expenditure.

1 Introduction

1.1 White and brown adipose tissue

In mammals, two different types of adipose tissue occurs, white (WAT) and brown (BAT) adipose tissue. They serve opposite functions in energy balance.

White adipose tissue stores excess energy in the form of lipids, and provide thermal and mechanical insulation. During food deprivation this storage serves as a long-term energy reserve. It is the only known tissue that can change its mass considerably even after childhood during adulthood (Hausman et al., 2001; Spiegelman and Flier, 1996). A major factor for this variability in adipose mass is the ability of white adipocytes to dramatically enlarge in size. White adipocytes are unilocular, containing one big lipid droplet per cell and can reach a diameter of larger than 120 μm (Fig. 1 A). However adipocyte size is also limited and *de novo* adipogenesis is required to further increase mass (Gesta et al., 2007). Adipogenesis ensures the maintenance and adipocyte turnover of adipose tissue (Spalding et al., 2008). It is a two-step process in which pluripotent stem cells become committed preadipocytes and subsequently differentiate into mature adipocytes (Pittenger et al., 1999; Rangwala and Lazar, 2000; Rosen and MacDougald, 2006).

Brown adipose tissue was first described in 1551 by Konrad Gessner, who stated that this tissue was “neither fat, nor flesh [nec pinguitudo, nec caro] — but something in between”. Around 410 years later in 1961, R. E. Smith showed a thermogenic function of BAT in the interscapular region in rats. Brown fat was initially identified in newborns and smaller hibernating animals (Gesta et al., 2007). It can mainly be found in the axillar, interscapular, subscapular and the suprasternal region. Compared to white, brown adipocytes are smaller and multilocular, containing several small lipid droplets. These cells can reach a diameter at a maximum of about 30-40 μm (Fig. 1 B). They serve to dissipate heat by oxidizing lipids and thereby provide a means of non-shivering thermogenesis. Within BAT a dense capillary network ensures the necessary supply of oxygen and substrates to produce heat that is distributed by the Sulzer’s vein into the body to defend body temperature, e.g. in cold ambient temperature (M. Klingenspor, 2011). Because thermogenesis is an energy wasting phenomenon, BAT activity is hormonal and centrally controlled and only responds to

appropriate stimuli, e.g. cold acclimatization (Lockie et al., 2012; Morrison et al., 2012; Silva, 1995).

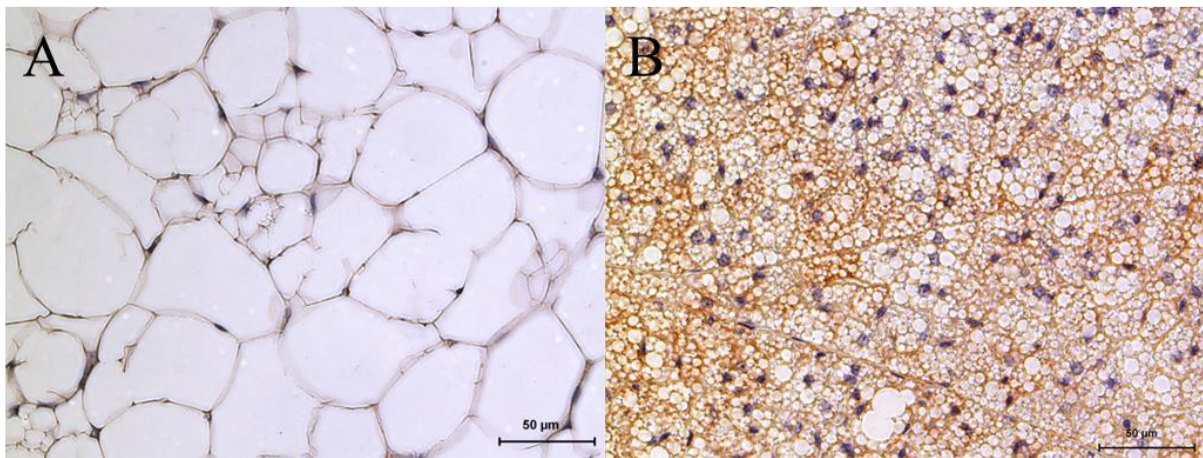


Figure 1 Immunohistochemical detection of UCP1 positive adipocytes

White (A) and brown (B) adipocytes in murine adipose tissues. Immunohistochemical detection of uncoupling protein 1 (UCP1) positive adipocytes in epididymal white adipose tissue and in interscapular brown adipose tissue of 129S6sv/ev mice. Nuclei were stained with hematoxylin. Scale bars = 50 µm.

A highly specific protein for brown adipocytes is the uncoupling Protein 1 (UCP1). It was firstly described as an unknown polypeptide with a molecular weight of approximately 32kDa. Its protein abundance was highly increased in mitochondrial extracts of BAT from cold acclimatized rats (Ricquier and Kader, 1976). Beyond question, UCP1 interacts with the respiratory chain (Fig. 2). Briefly, the respiratory chain is fueled by the citric acid cycle with highly energetic electrons that are transferred from the carrier molecules NADH and FADH₂ to complex I and II. Their high negative redox potential is used by complex I, III and IV to transport protons (H⁺) from the mitochondrial matrix into the intermembrane space. Except for brown adipocytes, the resulting membrane potential is used by the adenosine triphosphate (ATP) synthase to produce ATP from adenosine diphosphate (ADP) and inorganic phosphate (Pi). UCP1, a mitochondrial inner membrane carrier uncouples oxidative phosphorylation in mitochondria to dissipate the electrochemical gradient and establish a thermogenic proton leak (Aquila et al., 1985; Heaton et al., 1978; Inokuma et al., 2006). Also other uncoupling proteins are known, UCP2 or UCP3 (Fleury et al., 1997). Those share high rates of homology in the amino acid sequence and protein structure like the trinomial architecture or the GDP binding site (Borecky et al., 2001; Nedergaard et al., 2001). In isolated brown adipocytes of UCP1 knockout mice, UCP1 is essential for norepinephrine-induced thermogenesis (Matthias et al., 2000). However also free fatty acids released from norepinephrine-induced lipolysis in BAT can mimic the thermogenic effect of UCP1 (Bieber et

al., 1975; Matthias et al., 2000; Nedergaard and Lindberg, 1979; Prusiner et al., 1968). The underlying molecular mechanism of free fatty acid induced uncoupling is not fully understood.

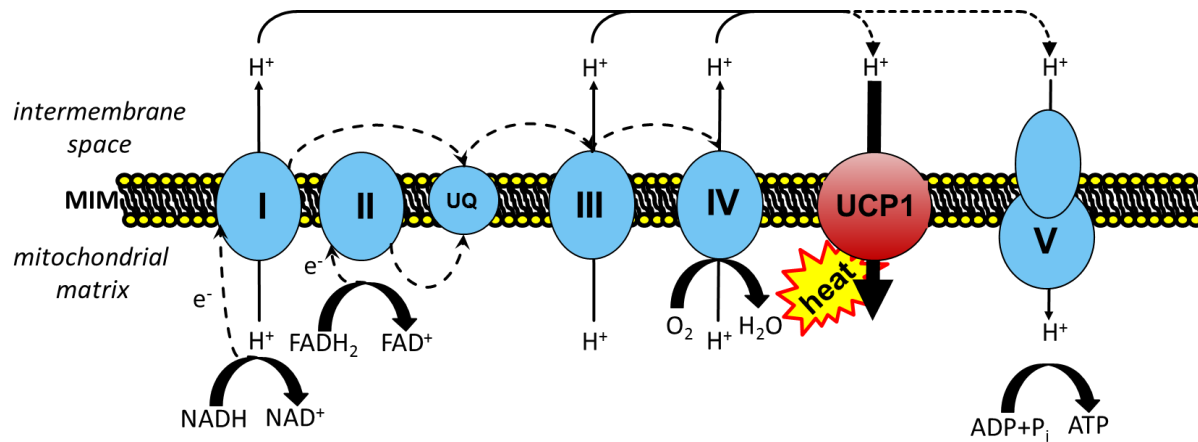


Figure 2 Schematic draw of the respiratory chain within brown adipocyte mitochondria.

Shown is the respiratory chain in brown adipocyte mitochondria. All four complexes (I-IV), the ATP synthase (V) and the uncoupling protein 1 (UCP1) are located in the mitochondrial inner membrane (MIM). Electrons (e^-) are transferred to complex I and II. Their transport along the respiratory chain is marked by dashed lines. The downgrading of the energy rich electron leads the transport of protons (H^+) into the intermembrane space. UCP1 uncouples oxidative phosphorylation by transporting protons back into the mitochondrial matrix and dissipate the electrochemical gradient. This transport of protons produces heat.

The ablation of UCP1 in mice leads to a monolocularization of BAT and a thermogenic deficiency. Surprisingly, UCP1 ablated mice show an increased occurrence of multilocular cells in WAT, possibly trying to compensate the thermogenic deficiency (Granneman et al., 2003; Meyer et al., 2010). A defective brown fat thermogenesis contributes to obesity (Himms-Hagen, 1985). Obesity is a result of a deleterious and long-term accumulation of fat mass, by storing excess energy in form of triglycerides into adipose tissue and is defined by a Body Mass Index (BMI) above 30. The World Health Organization (WHO) categorizes obesity as one of the major health risks next to cancer and AIDS. Obesity increases the risk for a number of other syndromes, e.g. cancer, arteriosclerosis and especially diabetes type 2 (Berghofer et al., 2008; Organization). Reducing food intake, increasing physical activity or thermogenesis are efforts to reduce obesity. They would lead to a reduction of the lipid content in white adipose tissue and result into a shift of the energy balance towards an increased energy expenditure (Rothwell and Stock, 1979).

1.2 Adipose tissue during murine development

Directly after birth, very few white adipocytes can be found in the retroperitoneal (rWAT) and inguinal (iWAT) region. These adipocytes already contain significant amounts of lipid whereas

the emergence of lipid storage in the epididymal region (eWAT) starts at postnatal day 7 (Han et al., 2011). Nevertheless the pre- and postnatal development of WAT and the functional and structural processes of adipogenesis in animals has not been studied to any large extent. Brown adipose tissue, e.g. the interscapular brown adipose tissue (iBAT), develops early during fetal development and is in principal fully functional at birth (Skala et al., 1970; Xue et al., 2007). In newborn sheep, BAT nonshivering thermogenesis already amounts to 33% of total thermogenesis and even up to 70% in a newborn rat (Hahn and Skala, 1972; Skala et al., 1970). Postnatal cold exposure induces further growth and stimulates an increase in thermogenic capacity and in the density of sympathetic innervation (Nisoli et al., 1998). Beyond cold exposure, the drastic switch in nutrient composition from umbilical glucose to maternal milk fat seems to act as a major cue in increased BAT capacity, acting via expression of the endocrine fibroblast growth factor 21 in the liver (Hondares et al., 2010). During murine ontogeny, white and brown adipocytes are derived from distinct progenitor cell populations. Brown adipocytes emerge from mesenchymal Myf5-positive stem cells of the muscle lineage whereas the progenitors of white adipocytes are Myf5-negative (Seale et al., 2008).

1.3 Brown like adipocyte in white adipose tissue

Brown adipocytes do not only occur in classical brown adipose tissue depots but also interspersed within white adipose tissue depots. This cell type has been termed “brite” (brown in white) or “beige” (Barbatelli et al., 2010; Petrovic et al., 2010; Seale et al., 2008). Like white adipocytes, brite cells can originate from Myf5-negative progenitors but their developmental origin is still elusive (Sanchez-Gurmaches et al., 2012). In adult mice, cold exposure (Young et al., 1984) and β -adrenergic stimulation (Guerra et al., 1998) increase the recruitment of brite cells but it is controversial whether they are a product of transdifferentiation of white adipocytes, or emerge from unknown progenitors or both (Fig. 3). Here transdifferentiation means a transition of a mature white adipocyte into a brite adipocyte without detouring to an undifferentiated state (Zhou and Melton, 2008). However, within white adipose tissue depots a subpopulation of precursor cells were found that can yield either brite or white adipocytes, depending on the stimulus (Lee et al., 2012).

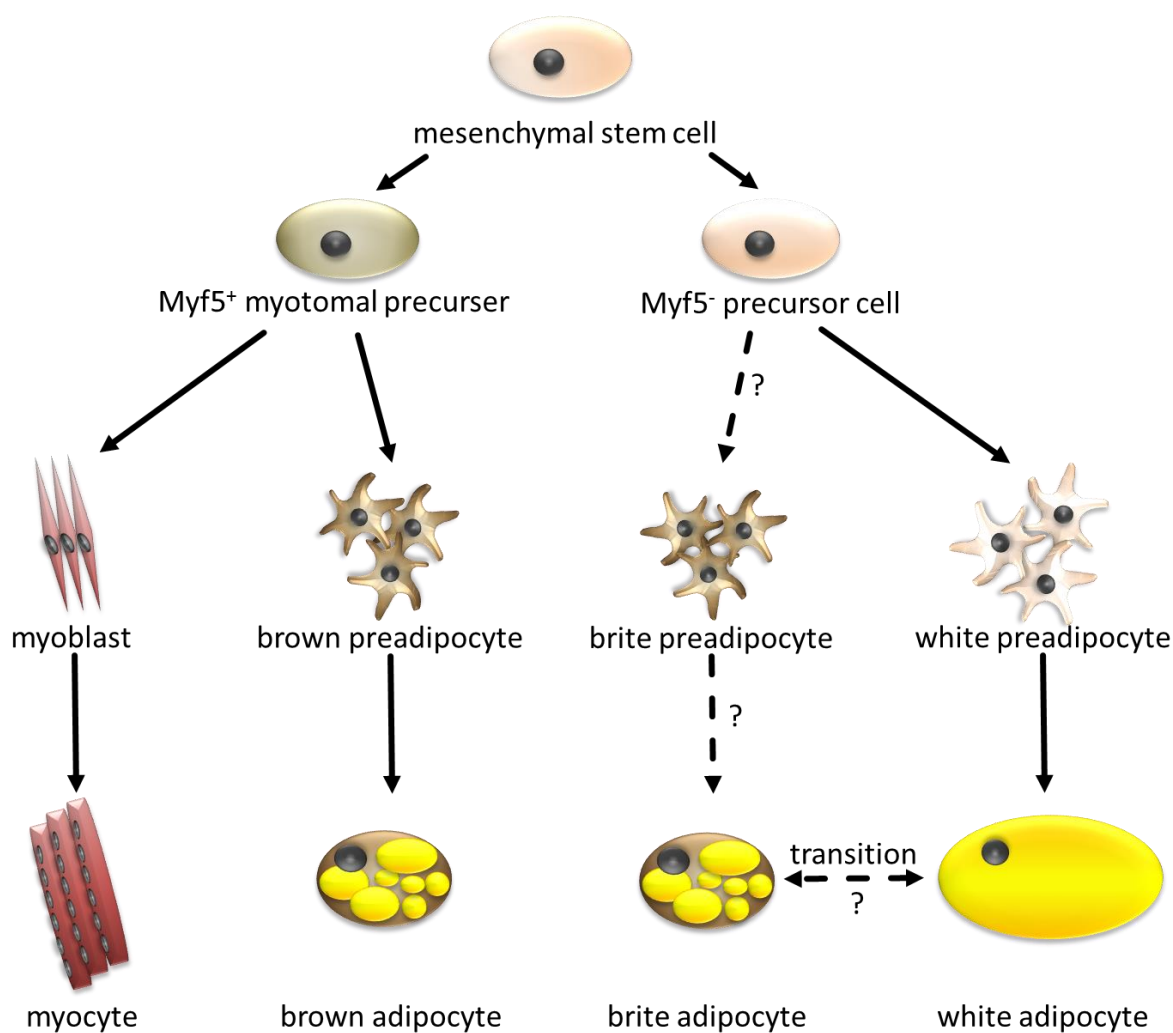


Figure 3 Current model of brown and white adipocyte differentiation compared to skeletal muscle lineage.

Shown is the current model of adipocyte and muscle cell differentiation originating from mesenchymal stem cells. The continuous arrows display the established and known cell differentiation pathways. The dashed arrows show a putative mechanism of brite adipocyte formation, by differentiation from brite preadipocytes or the transition of mature white adipocytes. The question marks show the still unknown mechanisms of a putative brite adipocyte precursor cell line and the putative transition from a mature white into a brite adipocyte.

During murine postnatal development, these brite cells spontaneously emerge around weaning (Lasar et al., 2013; Xue et al., 2007). Besides environmental and endocrine manipulation of white adipose tissue leading to its britening, several studies show that britening is not a monogenetic causality, but a complex meshwork of several factors. To get a better understanding and to identify specific factors, necessary for britening of white fat, genetically modified animal models have been generated that revealed factors that positively or negatively affect britening. Several pathways implicated in britening were identified by genetic manipulation. The most prominent known and dominant pathway in BAT that upon chronic activation leads to britening of white adipose tissue is the β_3 -receptor mediated norepinephrine pathway (Bourova et al., 2000; Chaudhry et al., 1994; Gerhardt et al., 1999).

Briefly, upon β_3 -receptor stimulation adenylate cyclase converts ATP into cyclic AMP (cAMP) that binds protein kinase A and phosphorylates the transcription factor cAMP response element-binding protein (CREB) in the nucleus (Thonberg et al., 2002). Another factor that is phosphorylated by protein kinase A is p38 mitogen activated protein kinase (MAPK). MAPK can phosphorylate the activating transcription factor 2 (ATF2) that promotes the expression and phosphorylation of peroxisome proliferator-activated receptor gamma coactivator 1-alpha (PGC1 α), the main regulator of mitochondrial biogenesis that itself drives UCP1 expression (Cao et al., 2004; Enslin et al., 1998; Robidoux et al., 2005). Another pathway mediating browning and influencing WAT morphology is developmental programming. The main regulator, switching from a progenitor cell into a brown adipocyte is PRD1-BF-1-RIZ1 homologous domain containing protein-16 (PRDM16). Overexpression of PRDM16 in WAT leads to an increased brown adipocyte formation (Seale et al., 2008; Seale et al., 2007). Also by manipulating the lipolytic pathway, browning in WAT can occur. A predominantly expressed factor in brown adipocytes is Cell death inducing DNA fragmentation factor, alpha subunit like effector A (CIDEA) (Nordstrom et al., 2005). An ablation of this factor leads to absence of multilocular adipocytes in WAT (Zhou et al., 2003). In simplified terms, browning of white adipose tissue is defined by the increased appearance of multilocular cells and an increase of specific brown adipocyte marker genes, e.g. UCP1 or CIDEA. Beyond question, the key factor or factors transforming a white adipocyte into a thermogenic active brown adipocyte is still not found.

1.4 Brown adipose tissue and brown occurrence in humans

Most information about BAT originates from animal studies. For humans it was initially claimed that BAT is functional only in neonates. However, active BAT in adult humans was observed in patients with malignant tumors using fluorodeoxyglucose (FDG) positron emission tomography (PET) combined with X-ray computed tomography (CT), short PET/CT (Cohade et al., 2003; Minotti et al., 2004). Sites of FDG uptake that correspond to BAT in adult humans are mainly found in the neck and the supraclavicular region. These regions showed a substantial and bilateral FDG uptake upon cold stimulation. Additional depots can be found in the mediastinum or the paravertebral and suprarenal region (Bar-Shalom et al., 2004; Truong et al., 2004). However these regions are not found in every subject, not even in every human

that is positive for FDG uptake in the neck and the supraclavicular region (Nedergaard et al., 2007). Newer studies using PET/CT validate and show the occurrence of a considerable amount of BAT in human (Cypess et al., 2009; Nedergaard et al., 2007; van Marken Lichtenbelt et al., 2009; Virtanen et al., 2009). Isolated tissue samples of the neck or supraclavicular region that show high uptake of FDG contain numerous UCP1 expressing adipocytes (Saito et al., 2009; van Marken Lichtenbelt et al., 2009). Cold exposure is a strong stimulant for BAT activation in humans. Energy expenditure studies on patients after simulated thermoneutral conditions of 27 °C and an acute cold exposure of 19 °C for 2 h showed a positive correlation of energy expenditure with BAT activity (Saito et al., 2009). In mice the activity of BAT is driven by adrenergic stimulation, e.g. ephedrine. However, ephedrine does not stimulate BAT activity in humans. It is assumed that cold exposure specifically activates the sympathetic pathway. Thus, agents that mimic cold activation of BAT could be a promising approach to increase BAT activity (Cypess et al., 2012; Vosselman et al., 2012). Another compound that increases resting metabolic rate in humans and induces brite adipocyte occurrence in mice WAT are capsinoids (Kawabata et al., 2009; Whiting et al., 2012). Patients with BAT have a higher increase in energy expenditure upon capsinoid intake compared to subjects without BAT (Yoneshiro et al., 2012). In rats these capsinoids activate the transient receptor potential channel 1 (TRPV1) in the upper digestive tract that results in an increased sympathetic tone to BAT (Ono et al., 2011). Nevertheless, pharmacological studies on humans are rare, considering the ethical background and agents that specifically activate BAT in humans are so far not known.

Comprehensive expression analysis on marker gene expression of classical murine BAT and human BAT show that human BAT expression resembles that of brite adipocytes (Sharp et al., 2012; Wu et al., 2012). None of the classical murine BAT markers, like *Zic1*, *Lhx8*, *Ebf3*, *Eva1* or *Fbxo31*, were found in human BAT (Walden et al., 2012; Wu et al., 2012). A recent study shows that isolated preadipocytes from human neck are capable of differentiating into brite adipocytes *in vitro* (Lee et al., 2014). Markers typical for mice brite adipocytes *Tmem26*, *CD137*, *Tbx1*, *Hoxc9*, *Cited1* and *Fgf21* were found in human BAT depots (Sharp et al., 2012; Walden et al., 2012; Wu et al., 2012). A metabolic function of these brite adipocytes has not been fully resolved yet. It is shown that brite adipocytes have a similar thermogenic capacity like brown adipocytes, when fully stimulated (Wu et al., 2012). Possibly, these cells would contribute to energy expenditure by burning lipids. Thus, the cellular transformation from

white adipocytes into fat oxidizing brite cells in human get particular interest in obesity research (Guerra et al., 1998; Himms-Hagen, 1989).

1.5 Aims and scopes of this study

Interestingly, the occurrence of brite adipocytes in mice WAT has been associated with obesity resistance, enhanced fat oxidation, energy expenditure, and improved systemic insulin sensitivity (Almind et al., 2007; Guerra et al., 1998). A highly suitable model system to study the recruitment of brite adipocytes is their natural emergence and disappearance during postnatal fat development (Xue et al., 2007). In murine neonates, the rWAT displays this drastic morphologic change during the first 30 days of life. In this depot large amounts of brown adipocytes appear at day 20 but are absent 10 days earlier or later. The morphological plasticity is known to differ in several inbred mouse strains (Xue et al., 2007) and is influenced by maternal nutrition (Delahaye et al., 2010). In this study the phenomenon is described in detail and therefore inbred mouse strains were compared to address the question whether postnatal browning is associated with the rate of WAT growth and total body fat accumulation during the first four weeks of life. As for 129S6sv/ev mice a high potential for brite recruitment is anticipated (Almind et al., 2007) and this strain is less prone to diet-induced obesity than C57BL/6N (Almind and Kahn, 2004; Matyskova et al., 2008) those two strains were chosen for comparison.

The first aim in this study was to examine the postnatal development of body mass and body fat mass as well as expansion of adipose tissue mainly in the two strains 129S6sv/ev and C57BL6/N using morphological, immunohistochemical and expression analyses of selected brown fat marker genes. Here it is demonstrated that maternal care during postnatal development influences WAT development and the brite cell occurrence within distinct depots.

The second aim is to understand whether the strain specific browning of WAT is a result of genetic predisposition or maternal imprinting. A next generation based sequencing approach of retroperitoneal WAT of both strains during postnatal development elucidates a difference within genes that correlate to the expression of brown adipose tissue marker. The inheritance of a strain specific brite adipocyte occurrence could be influenced by environmental

manipulations in both strains, but could not be completely eliminated. Thus, the genetic background is a crucial factor for the attendance of white adipose tissue browning.

In a broader context this animal study reinforces the necessity of maternal care influencing the postnatal development that may affect adult life with respect to diet induced obesity. Figuratively to human, maternal care may not change genetics and the inheritability but may affect them by maternal imprinting and strengthen or diminish the propensity towards diet induced obesity.

2 Material & Methods

2.1 Animal treatment

Mice of the C57BL6/N, 129S6sv/ev, AKR/J and SWR/J strains were bred and kept in our own specific-pathogen-free facility with regular hygiene monitoring according to FELASA criteria. The founder breeding pairs were originally obtained from Charles River Laboratories International Inc. (C57BL6/N), Taconic Farms, Inc. (129S6sv/ev Tac) and from The Jackson Laboratory Inc. (AKR/J & SWR/J). All mice were kept at a room temperature of 23 °C ± 1 °C with a relative humidity of 50 - 60 % and a 12 h light/dark cycle. They were fed a regular chow diet *ad libitum* (Tab. 1).

Table 1 Composition of diets

Components:	Regular chow diet
Crude protein (N x 6,25)	22%
Crude fat	4.50%
Crude fiber	3.90%
Crude ash	6.80%
N free extracts	50.80%
Starch	34%
Sugar	5%

To sacrifice mice cervical dislocation was employed on pups at the age of day 10 and CO₂ asphyxiation was used on pups at the age of day 20 and 30 or on adult mice. All animal experimentation was conducted according to the German animal welfare law and approved by the government of Oberbayern, Germany.

2.2 Animal experimentation

Postnatal development was analyzed to distinguish differences in body mass and body composition. For the study of postnatal development the mice of C57BL6/N, 129S6sv/ev, AKR/J and SWR/J were fed a regular chow diet *ad libitum* and pups at postnatal day 10, 20 and 30 (P10, P20 and P30) were weighed and the body composition was determined by nuclear magnetic resonance (NMR) spectroscopy (MQ 7.5 NMR analyzer, Bruker). During the entire postnatal period of 30 days pups remained with their mothers and were not weaned. During the entire postnatal period up to 30 days pups remained with their mothers and were not weaned. The following organs were dissected from male mice: epididymal white adipose

tissue (eWAT), inguinal white adipose tissue (iWAT), retroperitoneal white adipose tissue (rWAT), interscapular brown adipose tissue (iBAT), a part of liver and blood plasma samples were collected for our analyses. For the experiments only male mice were used. Litters with a size of fewer than 5 and more than 9 were excluded to avoid a growth advantage or disadvantage.

To analyze whether the maternal care influences the postnatal development in a strain dependent manner, a cross-foster experiment was performed. In the cross-foster study adult female and male mice of C57BL6/N and 129S6sv/ev were single caged for three days. Time mating were performed in which female mice were transferred to single caged males for 7 days and were then single caged again. This was intended to reduce cannibalistic behavior against unfamiliar pups. After delivery pups were switched from their original mother to the foster mother of the other strain directly after birth. Just litters with a number of pups per strain that were equally matched or diverging by ± 1 were switched 12 h – 18 h after birth. This was intended to reduce the maternal stress and to reduce the possibility of a growth advantage by one of the strains. Litters with a size of fewer than 5 and more than 9 were excluded to avoid a growth advantage or disadvantage. During the entire postnatal period of up to 30 days, pups remained with their mothers and were not weaned. The following organs were dissected at P10, P20 and P30 from male mice: eWAT, iWAT, rWAT, iBAT, a part of liver and blood plasma samples were collected for analyses.

The ambient temperature affects non shivering thermogenesis. To analysis whether an increased ambient temperature affects postnatal development, pregnant mice were single caged and kept for 2 days before delivery at an ambient temperature of $30\text{ }^{\circ}\text{C} \pm 1\text{ }^{\circ}\text{C}$, a humidity of 50 % and were fed a regular chow diet *ad libitum*. Reducing maternal stress and cannibalism, the cages were not changed or moved until pups gained an age of 7 days. Pups at postnatal day 10, 20 and 30 were weighed and the body composition was determined by NMR spectroscopy (MQ 7.5 NMR analyzer, Bruker). During the entire postnatal period of up to 30 days, pups remained with their mothers and were not weaned. Litters with a size of fewer than 5 and more than 9 were excluded to avoid a growth advantage or disadvantage. The following organs were dissected at P10, P20 and P30 from male mice: eWAT, iWAT, rWAT, iBAT, a part of liver and blood plasma samples were collected for analyses.

2.3 Perfusion of animals

For establishing and validating the UCP1 immunohistochemistry, perfused animals were used. Cross reactions of the primary or the secondary antibody with unspecific targets like erythrocytes or thrombocytes or other cells in the vascularization system can cause false positive background signals. This phenomenon is often observed in tissues with a strong vascularization. Especially serum albumin shows a high cross reactivity to certain antibodies (Renshaw, 2007). Perfusion of animals can avoid these false positive background signals by flushing them out. Each mice was narcotized with a Ketamin-Xylazin mixture that was intraperitoneally injected with 10 μ l per gram of body mass (Tab. 2).

Table 2 Anesthesia protocol

Ketamin-Xylazin	used for 16.25ml
Ketamin 100mg/ml	1ml
2% Xylazin	0.25ml
0.9% NaCl	6ml

The ribcage was opened and a thin syringe was entered into the left ventricle. The right atrium was severed as a blood drain. First the animal was perfused with a 0.9 % sodium chloride solution until the blood flow and liver brightens. Afterwards the animal was perfused with 4 % paraformaldehyde solution until the body contracts (Fig. 4).

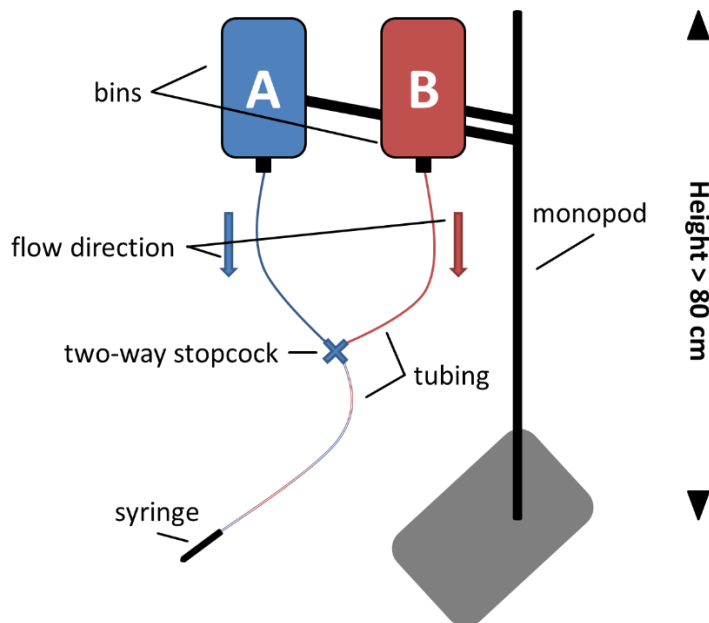


Figure 4 Schematic draw of a gravity driven perfusion system

Shown is the schematic arrangement of a gravity driven perfusion system. Two bins installed at a monopod at a height of 80 cm containing 0.9 % sodium chloride (A) and 4 % paraformaldehyde (B). Both bins are connected via silicone tubing (1 x 3 mm) to a two-way stopcock. From the stopcock a tubing ends in a syringe that enters the left ventricle.

2.4 Isolation of genomic DNA for genotyping of the UCP1 knockout mice

Tail tips were dissolved in 500 µl tail-lysis buffer freshly supplemented with 0.4 mg/ml Proteinase K (Fermentas) at 55 °C over night (Tab. 3). DNA was precipitated with 500 µl isopropanol by intense shaking and centrifuged for 15 min at 12000 g. The pellet was washed three times with 70 % ethanol and a centrifugation step at 12000 g for 5min each. Genomic DNA was dissolved in 40µl nuclease-free water.

Table 3 Composition of Tail-Lysis buffer

Tail-Lysis buffer	used for 200ml
TRIS	242.3mg
KCl	745.6mg
Gelatin	20mg
Nonidet P40	900µl
10x MOPS buffer	900µl
ddH ₂ O	ad 200ml

2.5 Polymerase Chain Reaction (PCR) targeting UCP1

UCP1 knockout animals were used as controls in the immunohistochemistry approach. Isolated genomic DNA was used in a PCR according to Table 4 and Table 5 using the primers (5'-3'): WT Forward CCCCTGTCAGGTGGGAT; WT Reverse. CACCCACATTGTCCATGAAG and Neo Reverse: AGGGGAGGAGTAGAAGGTGG. The estimated sizes were 371bp for wildtype and 198bp for mutant.

Table 4 PCR batch composition

Initial solution	used for 20µl
2x Immomix	10 µl
Primer R [10 pmol/µl]	1,0 µl
Primer F [10 pmol/µl]	1,0 µl
Primer R [10 pmol/µl]	1,0 µl
H ₂ O bidest. steril	7 µl
Verdau	1 µl

Table 5 PCR program for genotyping UCP1 knockout animals

Step	Temperature [°C]	Time [s]	Cycles
Initialization	95	600	
Denaturing	94	30	} 35 x
Annealing	58	40	
Elongation	72	60	
Final elongation	72	420	

2.6 Phenol-chloroform RNA extraction

Snap frozen tissues were homogenized in 1 ml Trisure (Bioline) and for 25 sec by a homogenizer (Micra D-9; Micra). For tissues that contain fat the homogenate was incubated for 5 min at RT and subsequently centrifuged for 5min at 2500 g at 4 °C. Lipids will form a layer on top of the homogenate. By piercing through this layer and transferring the homogenate into a new reaction tube enables a separation and removal of fat that would disturb the following process. To the homogenate 200 µl of chloroform were added and the solution was gently mixed for 15 sec and afterwards incubated for 3min. The solution was centrifuged for 15 min at 12000 g at 4 °C. This prolonged centrifugation step results in a phase separation: at the bottom the green colored phenol-chloroform organic phase, in the middle a small white phase containing protein and the top aqueous phase that contains the nucleic acids. The top phase was mixed with 500 µl of 75 % EtOH and gently mixed and incubated for 2 min. Afterwards the ethanol solution was transferred to columns of the SV Total RNA Isolation System (Promega) and proceeded according to the manufacturer's protocol. RNA was eluted in 30 µl nuclease-free water and concentration was measured spectrophotometrically (Infinite 200 NanoQuant, Tecan). For quality assessment by visualization of the 28S and 18S ribosomal RNA (rRNA) bands 2 µl of RNA mixed with 8 µl of RNA loading buffer were loaded into a 1 % denaturing RNA-formaldehyde agarose gel that was used for gel electrophoresis for 40 min at 100 V (Tab. 6 & 7). Alternatively integrity was assessed using a gel chip based method (Agilent 2100 Bioanalyzer; Agilent Technologies) by random sampling. Eluted RNA was stored at -80 °C.

Table 6 Composition of RNA loading buffer

RNA loading buffer	used for 320µl
formamide	200µl
37% formaldehyde	64µl
10x MOPS buffer	40µl
ethidium bromide	8µl
H2O	8µl

Table 7 Composition of a 1% formaldehyde gel for RNA separation

1% formaldehyde gel	used for 100ml
agarose	1g
H ₂ O	72ml
10x MOPS buffer	10ml
37% formaldehyde	18ml

2.7 Quantitative Reverse Transcription - Polymerase Chain Reaction (qRT-PCR)

The cDNA synthesis was performed with the Quantitect Reverse Transcription Kit (Qiagen), utilizing oligo-dT and random primer, using 500 ng RNA in a volume of 20 μ l. Quantitative PCR was performed in a Roche Lightcycler 480 II (Roche) in 384 well plates (4titude) with Sensi Mix no Rox (Bioline) and 1 μ l of 1:20 diluted cDNA in a volume of 12.5 μ l. The qRT-PCR for the analysis of gene expression was performed according to Table 8. Primers were synthesized by Eurofins (MWG Operon) (Tab. 10). Gene expression levels of the samples were calculated from a standard curve that was generated from pooled cDNA of all samples of each tissue and diluted in eight 1:2 steps. Standards were measured in duplicates while the sample cDNAs were measured in triplicates. The RNA abundance of each gene was normalized to a housekeeper. Samples were measured according to Table 9.

Table 8 Composition of qRT-PCR reaction mixture

Initial solution	Final volume 12.5 μ l
Sensimix SYBR NoRox	6.25
Primer forward	1
Primer reverse	1
Nuclease-free water	3.25
cDNA	1

Table 9 qRT-PCR program for gene expression analysis

Step	Temperature [°C]	Time [s]	Cycles
Initialization	95	600	
Denaturing	97	10	} 45 x
Annealing	52	15	
Elongation	72	20	
Melting curve	from 60 to 90	1200	

Table 10 qRT-PCR Primer list

GUSB forward	ACTATGGGCATTTGGAGGTG
GUSB reverse	ACTCCTCACTGAACATGCGA
UCP1 forward	GGGCCCTTGTAACAACAAA
UCP1 reverse	GTCGGTCCTTCCTTGGTGTA
CIDEA forward	TGCTCTTCTGTATCGCCCAGT
CIDEA reverse	GCCGTGTTAAGGAATCTGCTG
COX7A1 forward	CCGACAATGACCTCCCAGTA
COX7A1 reverse	TGTTTGTCCAAGTCTCCAA
Actin forward	AGAGGGAAATCGTGCGTGAC
Actin reverse	CAATAGTGATGACCTGGCCGT
PRDM16 forward	TGCTAAGCCTTCACCGTTCT
PRDM16 reverse	GAAGTTGAACGGGTGGTGAG
PGC1 α forward	GGACGGAAGCAATTTTCAA
PGC1 α reverse	GAGTCTGGGAAAGGACACG

2.8 Next generation sequencing

RNA transcriptome analysis next generation sequencing was performed by Dr. Karol Szafranski from the working group of Prof. Dr. M. Platzer, Fritz Lipmann Institute in Jena, Germany. RNA isolated as described in 2.3.3 of rWAT of C57BL6/N and 129S6sv/ev mice at postnatal day 10, 20 and 30 was used for RNA-sequencing (RNA-seq). RNA-seq libraries were prepared using TruSeq RNA Sample Prep kit v2, pooled in to 7 libraries per lane and sequenced for 50 nt using TruSeq SBS kit v3-HS to result in a depth of at least 25 million read pairs per sample. Gene expression analysis was performed by mapping the next generation sequencing reads to the mouse genome (Genomatix Mining station; Genomatix) by applying the library version NCBI build 37 and the EIDorado version 08-2011 (seed mapping type "deep", 92 % minimum alignment quality). Only unique hits were subjected to differential expression analysis utilizing the Genomatix Genome Analyzer. Data were processed in Excel 2013 (Microsoft). Transcripts with a sum in all samples under 2000 reads were removed from the analysis.

Searching for genes that resemble the transient appearance of UCP1 during postnatal development with a maximum of expression at P20, the normalized expression of each transcript of 129S6sv/ev at P10 to P30 were correlated to the normalized expression of five brown fat specific factors UCP1, CIDEA, COX7A1, CPT1b and FABP3. The mean of the five correlation coefficients was determined and used to remove the transcripts below 0.75 and higher -0.75. Using the coefficient of variation (CV) transcripts were removed below 35 %. A case analysis was performed to clarify whether C57BL6/N or 129S6sv/ev has a higher normalized expression value at P20 that is confirmed by using a two-sided Student's t-test with a p-value < 0.05.

2.9 Combined Methylation sensitive high resolution melting (MS-HRM) and pyrosequencing of the UCP1 enhancer region

For the methylation analysis genomic DNA was extracted from rWAT and iBAT of C57BL6/N and 129S6sv/ev mice using a DNA column assembly (SV Genomic DNA Purification System; Promega) according to the manufacturer's protocol with slight variations for fat tissues. After tissue digestion the homogenate was centrifuged for 5 min at 2500 g at 23 °C. Lipids will form a layer on top of the homogenate. By piercing through this layer and transferring the

homogenate into a new reaction tube enables a separation and removal of fat that would obstruct the binding matrix of the spin column. Before adding the Lysis Buffer and proceeding according to the manufacturer's protocol the homogenate was incubated at 55 °C for 5 min. To reduce the loss of DNA integrity, samples were eluted in two steps each using 250 µl nuclease free water according to the manufacturer's protocol. Afterwards samples were concentrated in a vacuum concentrator (Eppendorf 5301 Concentrator Centrifugal Evaporator; Eppendorf).

Local DNA methylation analyses using MS-HRM and pyro-sequencing were executed by Veronika Pistek, institute of physiology as described in Fürst et al., 2012 with slight variations (Fürst et al., 2012b). MS-HRM PCR primers and subsequent pyro-sequencing sequencing primers (PSQ primer see below) were created on in-silico bisulfite converted DNA using the PyroMark Assay Design Software 2.0 (Qiagen). 500ng DNA were used for bisulfite conversion of eWAT, iBAT and rWAT. For the High-Resolution-Melt PCR the following two primer pairs were used to cover all six postulated CpG sites in the UCP1 enhancer region (Kozak et al., 1994). Therefore primer pair one (PP1) covers the first four CpG-sites resulting in a 256 bp long amplicon and primer pair two (PP2) covers the last two CpG-sites resulting in a 152 bp amplicon. For the Pyrosequencing PCR primers (PSQ) of Shore et al. 2010 were used.

HRM Primer:

PP1 For 1-4 = GTGATGTTTTGTGGTTTGAGTGTATATATTTGTTTAGTG
Rev1-4 = Bio-AACTAATATCCCCAAAAATCTAATTTCTACTCTTCTAAC

PP2 For 5-6 = TTTTGGGGGTAGTAAGGTTAAT
Rev 5-6 = BIO-TATTACCCAACAAAACTTTCC

Pyrosequencing Primer:

PSQ S1 = TTGTTTAGTGATTTTGTGAAA
S2 = TTTTTGTTTTGAGTTGATA

2.10 Protein extraction with RIPA-buffer

Snap frozen tissue was homogenized in RIPA-buffer (max 200 μ l per 50 mg tissue) with a homogenizer (Micra D-9; Micra) and subsequently incubated for 10 min at 4 °C (Tab. 11). The homogenate was centrifuged for 15 min at 2000 g at 4 °C and the fat layer was removed. This step was repeated as long as the complete fat layer is removed. Afterwards the homogenate is centrifuged for 15 min at 15000 g at 4 °C and the supernatant is transferred into a new reaction tube and stored at -80 °C. Additionally the remaining pellet can be used by either resuspending it in RIPA-buffer or in 4 x SDS-loading buffer. Protein concentrations were determined by Micro BCA protein assay kit (Pierce), they were determined in duplicates in a 96-plate according to the manufacturer's protocol. For the standard curve BSA concentrations diluted in RIPA-buffer of: 200, 40, 20, 10, 5, 2.5, 1, 0.5 and 0 μ g/ml were used. Samples were measured at 590 nm absorbance using a microplate reader (Tecan Infinite 200 PRO NanoQuant; Tecan).

Table 11 Composition of RIPA-buffer

RIPA-buffer	stock concentraion	used for 10 ml
20mM Tris-HCl pH8	1 M	200 μ l
1% NP-40	10 %	1000 μ l
150mM NaCl	5 M	300 μ l
10mM NaF	1 M	100 μ l
1mM Na-ortho-vanadate	100 mM	100 μ l
1mM Na-pyrophosphate	100 mM	100 μ l
ddH ₂ O		7900 μ l
Sigma Protease inhibitor 2 (Prod.No. 042M4052)		100 μ l
Roche complete mini (Prod.No. 04693124001)	1 pill	1 per 10ml

2.11 Western Blot

For protein separation according to molecular weight 40 µg of protein per sample were loaded on a 12.5 % sodium-dodecyl-sulfate polyacrylamide gel (SDS-PAGE) based on a discontinuous Laemmli system (Laemmli, 1970). Separated proteins were electro-blotted from the SDS-gel onto a nitrocellulose membrane using a semi-dry system (BIORAD) with 2 mA per 1 cm² membrane for 1 h (Fig. 5).

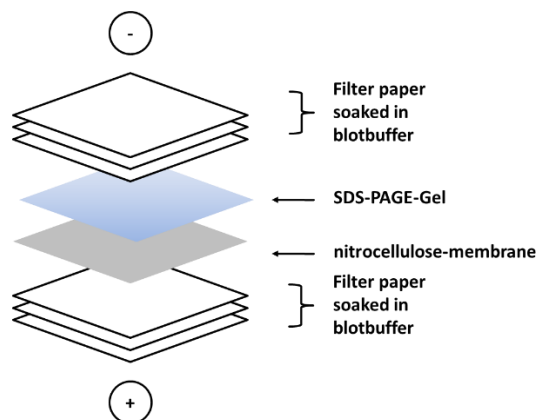


Figure 5 Schematic draw of electric transfer arrangement using a semi-dry system

Shown is the schematic arrangement to blot the proteins from the SDS-PAGE-Gel onto the nitrocellulose membrane using three layers of blotbuffer soaked filter paper to perform an equal electric field.

After blocking for 1 h with 3 % BSA in TBS, membranes were incubated with primary antibody in TBS-T according to the antibody with or without 0.3 % BSA overnight at 4 °C (Tab. 12). Membranes were rinsed three times in PBS-T each 7 min and incubated with secondary antibody solution (1:20,000; LI-COR Bioscience) in TBS-T at room temperature for 1 h. After secondary antibody incubation membranes were rinsed three times in PBS-T each 7 min and target proteins were detected by using an Odyssey Infrared imaging System (LI-COR Bioscience).

Table 12 List of primary antibody

targeted protein	host	vendor/Reference	product code
Actin	mouse	Millipore	#MAB1501
COXIV	rabbit	Cell Signaling	#4844
UCP1 for IHC	rabbit	Abcam	ab10983
UCP1 for WB	rabbit	self-made	(Meyer et al., 2004)
CIDEA	rabbit	self-made	(Hirschberg, 2012)

2.12 Histology - Hematoxylin & Eosin stain (H&E) and Immuno-histo-chemistry (IHC)

Dissected tissues were directly incubated in 4 % para-formaldehyde solution with 0.0024 % picric acid for 48 h. Fixated tissues were dehydrated in an increasing ethanol/xylene series and then infiltrated with Paraplast (Leica):

Table 13 Time schedule for ethanol/xylene dehydration array

Bin no.	bin content	incubation time
1	70 % EtOH	1 h
2	70 % EtOH	1 h
3	80 % EtOH	1 h
4	80 % EtOH	1 h
5	90 % EtOH	1 h
6	90 % EtOH	1 h
7	99 % EtOH	1 h
8	99 % EtOH	1 h
9	Xylene	1 h
10	Xylene	1 h
11	Paraplast	1 h
12	Paraplast	1 h

Infiltrated tissue samples were paraffin embedded and cut with a rotary microtome (Leica). 2.5 µm sections were mounted onto Poly-D-Lysine coated microscopic slides (Thermo) and dried: for H&E 20 min at 60 °C and for IHC 24 h at 37 °C.

2.13 Hematoxylin & Eosin stain (H&E)

Dried sections were transferred into a Multistainer (Leica) for standardized coloration and a Hematoxylin and Eosin stain (Carl Roth) was performed for nuclei and cytosolic staining (Tab. 14). Stained sections were mounted in Roti-Mount (Carl Roth).

Table 14 Program for Hematoxylin-Eosin Staining

Bin no.	bin content	incubation time [min]
1	Xylene	3
2	Xylene	3
3	100 % EtOH	2
4	96 % EtOH	2
5	70 % EtOH	1
6	distilled Water	1
7	Hematoxylin	5
8	Flow Water Station	4
9	Eosin	2
10	70 % EtOH	1
11	96 % EtOH	1
12	100 % EtOH	1
13	100 % EtOH	1.5
14	Xylene	1.5
15	Xylene	2
16	Xylene	2

2.14 Immuno-Histo-Chemistry (IHC)

Slides for IHC were heated at 70 °C for 7 min to melt the paraffin surrounding the tissue. Deparaffination was performed in xylene and a stepwise decreasing ethanol concentration array (99 %, 80 % and 70 %). Slides were heated to 90 °C for 20 min in 20 mM sodium-citrate and 10 min in 10 mM sodium-citrate for epitope retrieval, then rinsed in PBS for 5min and subsequently incubated in 3 % H₂O₂. After rinsing for 5min in PBS sections were incubated with 2.5 % normal goat serum in PBS blocking solution for 1 h at RT and rinsed 3 times for 5 min in PBS. Sections were incubated overnight with 1:500 diluted primary antibody in 0.25 % normal goat serum in 0.1 % PBS-T at 4 °C. After rinsing 3 times 5min each in 0.1 % PBS-T, sections were incubated for 1h at RT with 1:100 diluted HRP conjugated secondary antibody. Afterwards sections were rinsed 3 times in 0.1 % PBS-T 5 min each and incubated with DAB enhanced Mix (Leica) for 2 min per section. DAB reaction was stopped by rinsing the sections in ddH₂O. Subsequently sections were incubated for 3 min in hematoxylin and rinsed with ddH₂O until the pH changes that results in a color change from magenta to light blue. Sections were then dehydrated with an increasing ethanol/xylene gradient (70 %, 80 %, 99 % and xylene) for 2 min each. Sections were mounted in Roti-Mount.

2.15 Immunofluorescence of UCP1-GFP reporter mice

The UCP1-GFP reporter mice were generated and previously described (Rosenwald et al., 2013). Transgenic male mice were gavaged for five days at postnatal day 15 with 0.01 mg/μl tamoxifen, 2 mg tamoxifen per animal, dissolved in sunflower oil. At postnatal day 20 transgenic and non-transgenic litter mates were killed by CO₂ asphyxiation and rWAT and iBAT were dissected. Directly after dissection tissues were rinsed in PBS for 10 min and afterwards incubated with stirring in 4 % PFA for 2 h at 4 °C. Afterwards tissues were rinsed in PBS with stirring over night at 4 °C and dehydrated in 30 % Succrose in PBS for 24 h. Tissues were snap frozen on dry ice. In a Cryostat (Thermo NX 70, Thermo) with low profile blades (Leica) at a cutting angle of 10 °, object temperature ≤ -25 °C for BAT and ≤ -35 °C for WAT and blade temperature at -30 °C 7 μm sections were made. OCT was just used to attach the tissue to the base plate and not to mount the tissue into an OCT-block, because OCT gets brittle at -35 °C and rolls oneself up. Sections were mounted on Poly-D-Lysin slides (Thermo) and stored at 4 °C for drying for 30 min. Sections were mounted in Vectashield HardSet with DAPI

(Reactolab) and analyzed on an SP2 confocal microscope (Leica). Background was adjusted using samples from GFP negative littermates.

2.16 Statistics

Graphs were created with GraphPad Prism Version 5 (GraphPad Software, Inc.). Two-way ANOVA analyses were performed with Sigma Plot (Sigma Plot 12.5, Systat Software Inc.). Data were log transformed in case of deviation from normal distribution measured by a Shapiro-Wilk test. Multiple comparisons were performed with the Holm–Sidak post hoc test. Student's t-tests for the comparison of two groups were performed with Excel 2013 (Microsoft).

For the cross-fostering and thermoneutrality experiments, the resulting data of these animals were compared to the data of the normal fostered animals that are firstly described (starting at 3.1). To distinguish the treated animals to the normal fostered, the normal fostered were mentioned and abbreviated with B6 NF or 129 NF.

3 Results

3.1 Postnatal britening correlates with fat mass development

Britening, a transition from white adipose tissue to a brown adipose tissue like morphology, occurs transiently during postnatal development of mice. To investigate whether the postnatal britening influences fat mass development, mice of the 129S6sv/ev and C57BL6/N strain were studied at postnatal days 10, 20 and 30 (P10, P20 & P30).

In a cohort of over 600 animals, body mass was determined. At all three time points 129S6sv/ev show a small but significant elevation in body mass compared to C57BL6/N (Fig. 6).

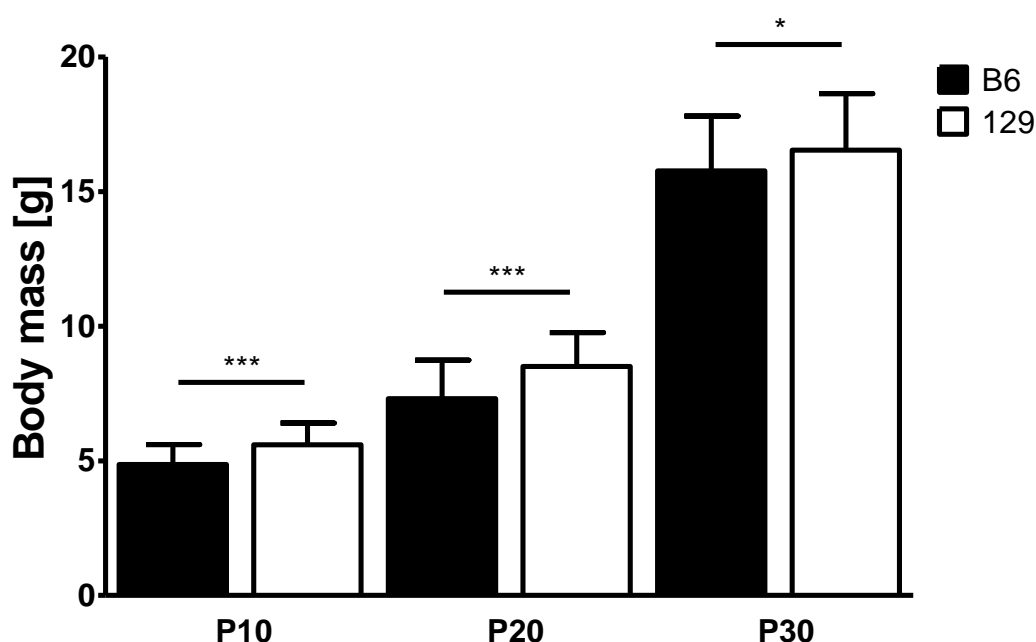


Figure 6 Postnatal body mass development of C57BL6/N (B6) and 129S6sv/ev (129) mice.

Body mass development of C57BL6/N (B6, black bars) and 129S6sv/ev (129, white bars) mice at indicated time points. Bars depict mean values \pm SD of $n = 128$ B6 P10, 110 B6 P20, 118 B6 P30, 106 129 P10, 74 129 P20, 68 129 P30 individual samples per group. Statistical significant differences are the result of two-way-ANOVA, * illustrates a significant strain difference at the displayed time points, * $p < 0.05$; *** $p < 0.001$.

In a smaller cohort, body composition was also measured to determine the contribution of fat and lean mass to the observed difference in body mass. In this second cohort a subtle elevation of body mass was also found 129S6sv/ev compared to C57BL6/N though not significant at P10 ($p = 0,431$) or P20 ($p = 0,078$) (Fig. 7A). However, total body fat mass was significantly increased by approximately 35 % at P20 and 15 % at P30 in 129S6sv/ev compared to C57BL6/N. Lean mass was decreased at P10 and P30 but not at P20 in 129S6sv/ev compared to C57BL6/N (Fig. 7 B).

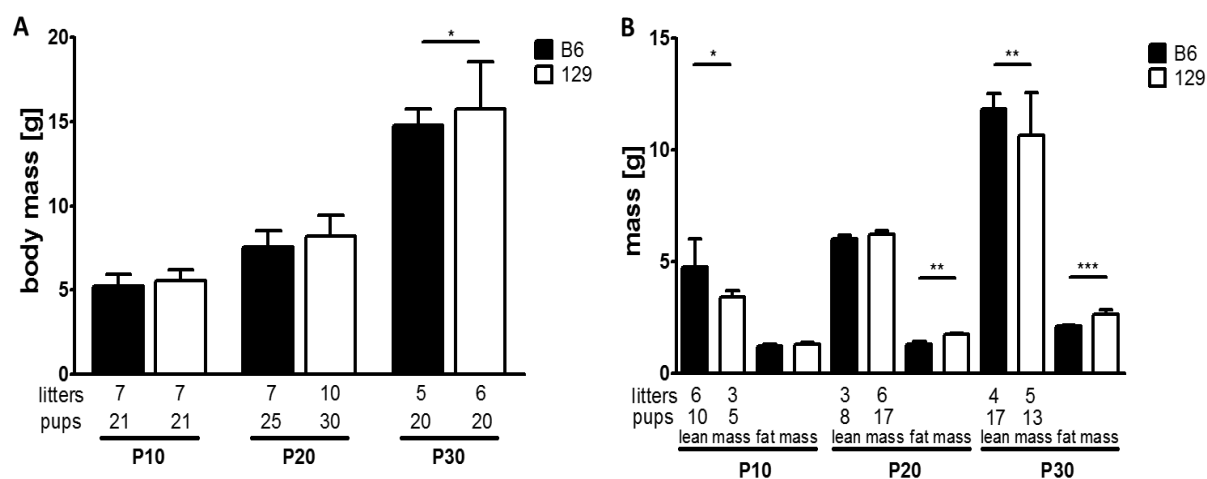


Figure 7 Postnatal development of body mass and body composition of C57BL6/N (B6) and 129S6sv/ev (129) mice. Body mass development (A) at indicated time points and lean mass and fat mass distribution (B). Bars depict mean values \pm SD. The number of litters and pups are as indicated. The postnatal days 10 to 30 of age are abbreviated P10, P20 and P30, indicating the respective postnatal day of life. Statistical significant differences are the result of two-way-ANOVA, * illustrates a significant strain difference at the displayed time points, * $p < 0.05$; ** $p < 0.01$; *** $p < 0.001$.

Possibly, lean and fat mass are higher in 129S6sv/ev mice compared to C57BL6/N that have a similar body mass. By correlating individual lean and fat masses to their respective body mass, differences in body composition between mice of each strain with a similar body mass can be observed. Lean mass in C57BL6/N was slightly higher when plotted against the individual body mass for each mouse (Fig. 8 A). Both strains showed a proportional correlation of lean mass to body mass from P10 to P30. For total fat mass plotted against its individual body mass, 129S6sv/ev displayed an elevated fat mass compared to C57BL6/N. For both strains a proportional growth of fat mass was found at each individual time point, but not continuously from P10 to P30. Therefore a regression between P10 and P20 could not be clearly extrapolated (Fig. 8 B). In both strains the increase of body mass from P10 to P20 was not accompanied by an increase of total fat mass.

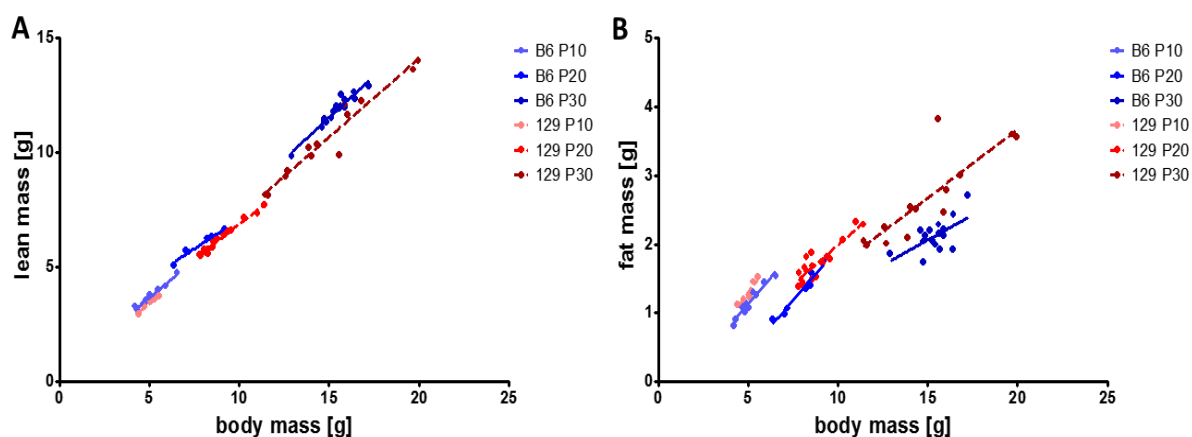


Figure 8 Body composition in proportion to body mass of C57BL/6N (B6) and 129S6sv/ev (129) mice.

Lean mass (A) and fat mass (D) at postnatal days 10 (P10), 20 (P20) and 30 (P30) plotted against the respective body mass. Each symbol represents an individual fat mass and lean mass. Continuous lines represent the linear regression within B6 and dashed lines the linear regression of 129 samples within a distinct postnatal day.

To determine whether the difference in total body fat mass at P20 and P30 is reflected in changes in the regional distribution of the intraperitoneal and subcutaneous fat depots epididymal, inguinal, retroperitoneal white adipose tissue (eWAT, iWAT, rWAT) and interscapular brown adipose tissue (iBAT) were dissected and weighed from pups at all three time points of age, P10-30 (Fig. 9). At P10 no differences between strains could be observed in any of the dissected tissues. From P10 to P20, 129S6sv/ev exhibited a significantly increased fat mass growth of rWAT, iWAT, eWAT and iBAT as compared to C57BL6/N. From P20 to P30 both strains further increased fat pad mass in rWAT, iWAT and eWAT. Again, this increase was more pronounced in 129S6sv/ev compared to C57BL6/N (Fig. 9).

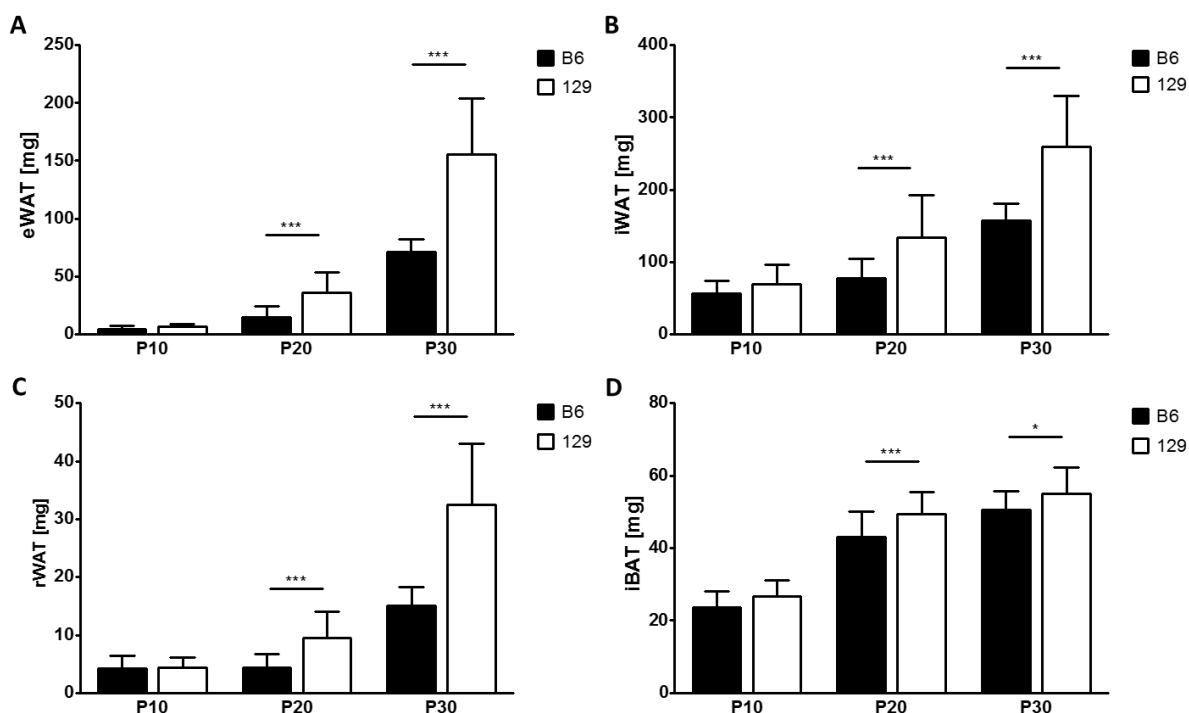


Figure 9 Postnatal development of fat pad mass of C57BL6/N (B6) and 129S6sv/ev (129) mice.

Mass of epididymal white adipose tissue (eWAT) (A), inguinal white adipose tissue (iWAT) (B), retroperitoneal white adipose tissue (rWAT) (C) and interscapular brown adipose tissue (iBAT) (D) depots are shown. Bars depict mean values \pm SD of $n = 21$ B6 P10, 25 B6 P20, 20 B6 P30, 21 129 P10, 30 129 P20, 20 129 P30 individual samples per group. The postnatal days 10, 20 and 30 of age are abbreviated P10, P20 and P30, indicating the respective postnatal day of life. Statistical significant differences are the result of two-way-ANOVA, * illustrates a significant strain difference at the displayed time points, * $p < 0.05$; *** $p < 0.001$.

To analyze the contribution of individual fat pads to the strain difference in total body fat mass, individual fat pad masses were plotted against body mass for each mouse. The resulting scatter plots demonstrated that eWAT increases almost continuously with body mass in both strains. In 129S6sv/ev the slope was greater compared with C57BL6/N and accumulated a higher fat pad mass at postnatal day 20 and 30 (Fig. 10 A). In rWAT and iWAT, however, such a proportional growth of depot mass was not found. The depot mass was proportional to body mass within the data points of a single separate day, but the P20 regression could not clearly be extrapolated from the P10 regression. In both strains the increase of body mass from P10 to P20 is not accompanied by an increase in iWAT and rWAT (Fig. 10 B and C). Thus, the relative contribution of these two fat pads to body mass decreases during early development. Comparing individual mice of similar body mass, 129S6sv/ev mice develop a higher rWAT and iWAT mass at postnatal day 20 and 30. The iBAT development correlates with the increase of body mass until post natal day 20 and reaches a plateau at day 30 (Fig. 10 D).

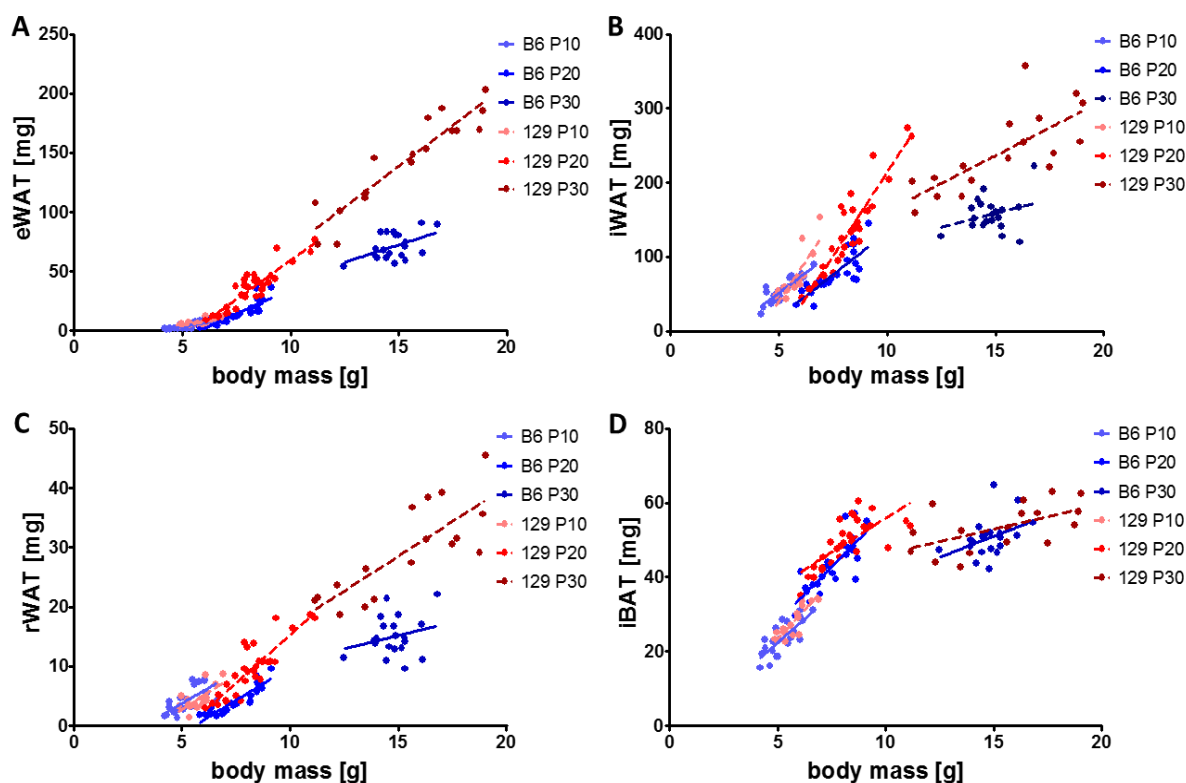


Figure 10 Fat pad mass in proportion to body mass of C57BL6/N (B6) and 129S6sv/ev (129) mice.

Epididymal white adipose tissue (eWAT) (A) inguinal white adipose tissue (iWAT) (B) retroperitoneal white adipose tissue (rWAT) (C) and interscapular brown adipose tissue (iBAT) (D) at postnatal days 10 (P10), 20 (P20) and 30 (P30). Each symbol represents an individual fat pad mass plotted against the respective body mass. Continuous lines represent the linear regression within B6 and dashed lines the linear regression of 129 samples within a distinct postnatal day group.

Investigating a possible cause for the observed growth attenuation of rWAT and iWAT, hematoxylin and eosin (H&E) staining were performed at P10, P20 and P30. Adult rWAT mainly displays a typical unilocular adipocyte morphology accompanied by a low grade of vascularization (Fig. 11 A). Vice versa, adult iBAT is highly vascularized and brown adipocytes show a multilocular appearance (Fig. 11 A). The histological HE staining during postnatal development revealed a changing plasticity in tissue morphology. At day 10, the adipocytes of rWAT were unilocular and exhibited a typical white morphology as compared to the adult rWAT control. At day 20, islets of smaller multilocular cells appeared similar to those usually seen in adult iBAT. This change was reversed until day 30 with adipocytes exhibiting unilocular appearance again. In rWAT of 129S6sv/ev mice the formation of multilocular islets was stronger compared to C57BL6/N mice (Fig. 11 B).

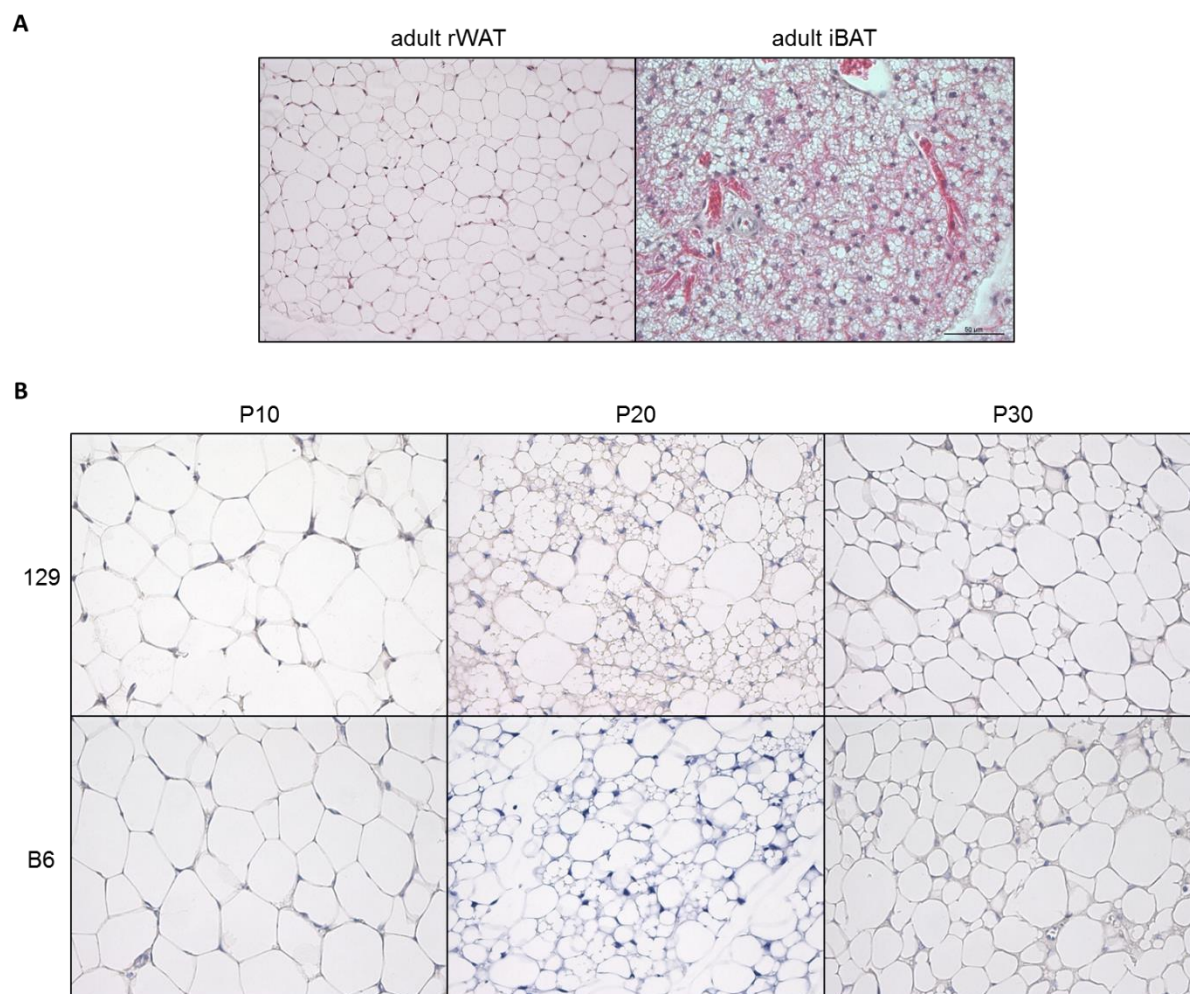


Figure 11 Hematoxylin and eosin (H&E) staining of rWAT and iBAT of C57BL6/N (B6) and 129S6sv/ev (129) mice.

H&E staining of adult rWAT and iBAT showing morphologic differences. A: shown are histological H&E staining of adult rWAT and iBAT of C57BL6/N. B: shown are histological H&E staining of rWAT and iWAT of B6 and 129 at indicated time points P10, P20 and P30 showing a transient appearance of multilocular cells.

Immunohistochemistry (IHC) for UCP1 in rWAT revealed that the multilocular cells at P20 were expressing UCP1. Interestingly in both strains, some small unilocular cells expressed UCP1 at P10, but not at P20 and P30. At P20, however, only multilocular cells seemed to be UCP1 immunoreactive (Fig. 12 A). At P30 only very few adipocytes with multilocular appearance could be found. The same transient pattern of multilocular UCP1 positive cells could be observed in iWAT in both strains (Fig. 12 B). Additionally in iWAT the dense islet formation seen at P20 was reduced by an increase in unilocular cells that do not express UCP1. In 129S6sv/ev mice, the formation of multilocular and UCP1 positive islets was stronger compared to C57BL6/N mice. The specificity of the immunohistochemistry was verified by incubation of iBAT samples with or without primary antibody against UCP1 from C57BL6/N wildtype and UCP1 knockout animals (Fig. 12 C).

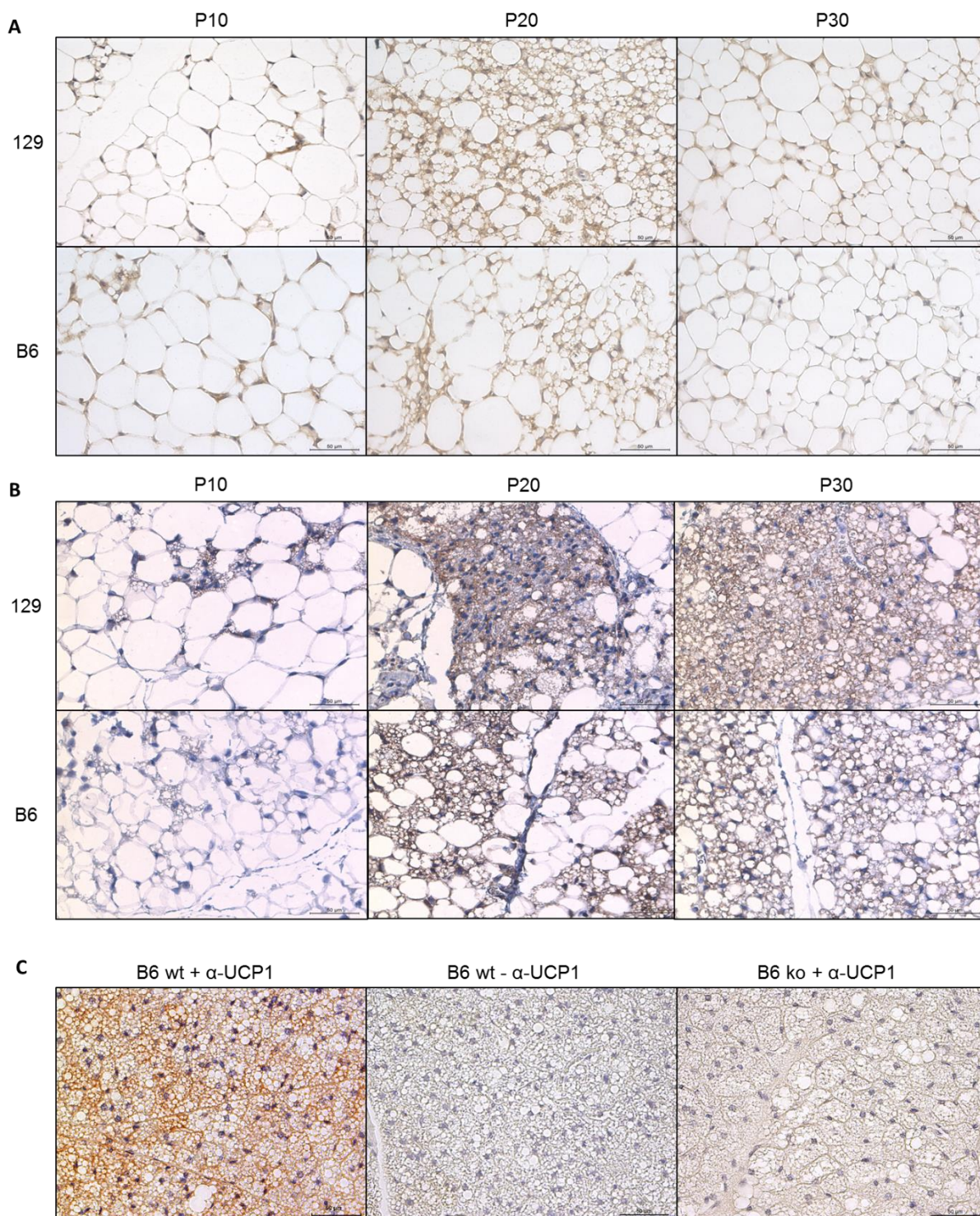


Figure 12 Immunohistochemical detection of UCP1-positive adipocytes in rWAT and iWAT of C57BL6/N (B6) and 129S6sv/ev (129) mice.

Morphologic change and IHC detection of UCP1-positive multilocular cells in rWAT (A) and iWAT (B) at the indicated time points, abbreviated P10, P20 and P30, indicating the respective postnatal day of life. Validation of IHC detection (C) in iBAT of wildtype (wt) C57BL6/N (B6) with (+ α -UCP1) and without primary antibody (- α -UCP1) and in iBAT of C57BL6/N UCP1 knockout (ko) mice; nuclei stain hematoxylin. Magnification \times 40; Scale bars: 50 μ m.

Immunofluorescence approaches on paraformaldehyde fixed and paraffin embedded adipose tissues are not possible, because of a strong auto-immunofluorescence. Therefore cryo-sectioning on rWAT and iBAT of Ucp1-GFP positive and negative animals at P20 were

performed (Fig. 13 A & B). The transgenic UCP1-GFP animals express GFP fused to the diphtheria toxin receptor (DTR) under the control of the UCP1 promoter. DTR is a cell membrane receptor. The activation of UCP1 in a cell leads to an increased expression of the fusion molecule DTR-GFP that accumulates in the cell membrane and shows a green fluorescent signal. In rWAT of these transgenic animals at P20, UCP1 positive cells are found forming islets surrounded by white adipocytes that do not show a fluorescent signal and therefore do not express UCP1.

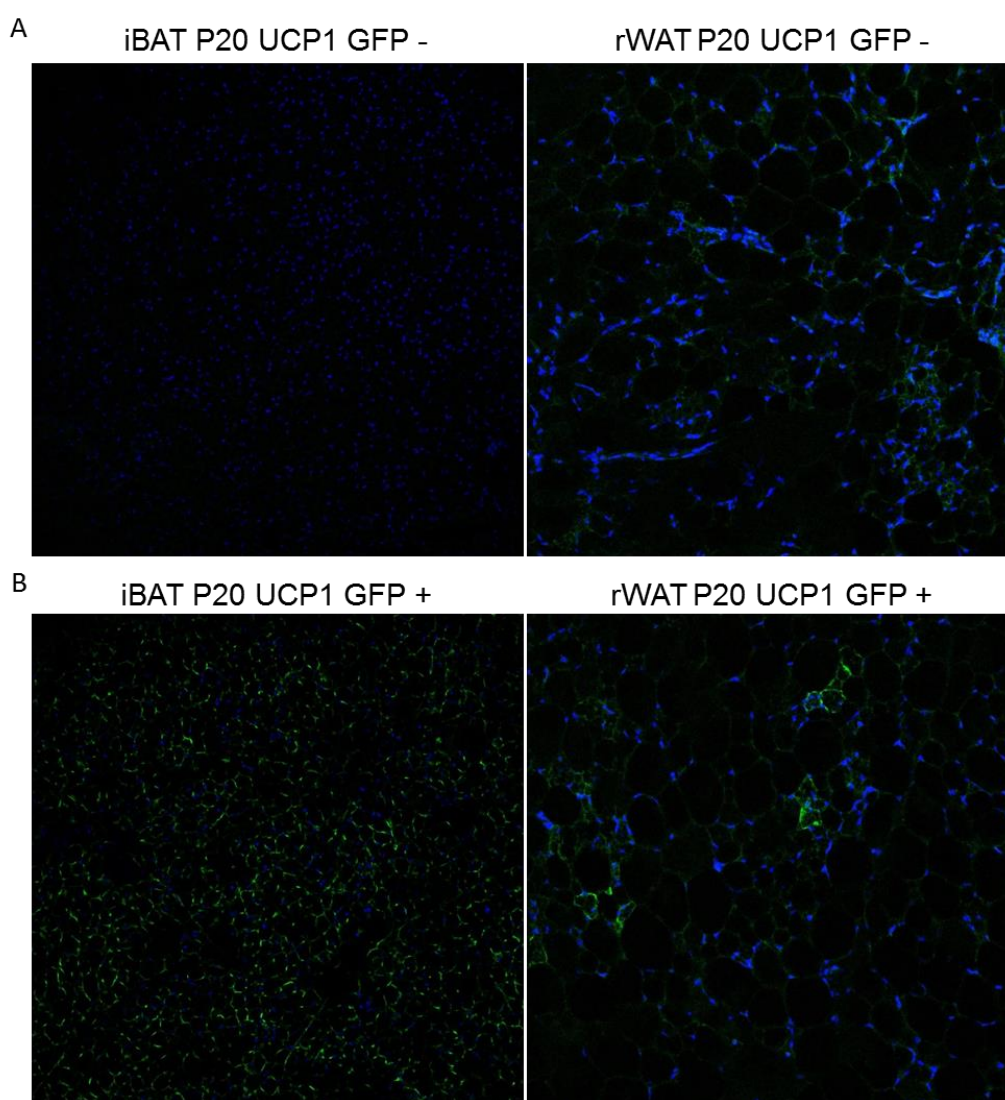


Figure 13 Immunofluorescence detection of UCP1-expressing adipocytes in iBAT and rWAT of C57BL6/N GFP reporter mice. Immunofluorescence detection of 5 days tamoxifen treated C57BL6/N GFP mice at P20. UCP1-expressing (green) adipocytes of iBAT and rWAT processed into 7 μ m cryosections of C57BL6/N UCP1-GFP negative (A) and positive (B) mice. Nuclei stained with DAPI (blue). Magnification x 40.

Taken together during the first 30 days of postnatal development rWAT and iWAT show a growth attenuation accompanied with a transient morphologic change from classical white fat to a brown fat like appearance with the formation of islets of multilocular and UCP1

positive cells. This transition from a white to a brown like tissue seen from P10 to P20 is here defined as “briteening” and it appears much stronger in 129S6sv/ev compared to C57BL6/N. However, 129S6sv/ev mice have a higher total body fat mass and higher fat pad masses in eWAT, rWAT and iWAT compared to C57BL6/N.

To verify that multilocular, UCP1 positive cells were indeed brite adipocytes the expression of further brown fat marker genes in rWAT and iWAT were analyzed by quantitative PCR. Beyond UCP1, the lipid droplet coating protein cell death-inducing DFFA-like effector a (CIDEA) and a subunit of cytochrome c oxidase (COX7A1) were chosen. Additionally two factors possibly involved in the recruitment of brown and brite adipocytes were analyzed: PR domain containing 16 (PRDM16) and peroxisome proliferator-activated receptor- γ coactivator 1- α (PGC1 α). The pattern of relative mRNA abundance for UCP1, CIDEA and COX7A1 was very similar regarding the transient appearance of multilocular UCP1 positive cells in the tissue. It increased from P10 to P20 and decreased from P20 to P30 in both tissues of C57BL6/N and 129S6sv/ev (Fig. 14).

Comparing the strains at P20, rWAT of 129S6 sv/ev mice displayed a 12-fold higher UCP1 level as compared to C57BL6/N mice. The same was true for CIDEA (6-fold) and COX7A1 (2.5-fold). Focusing on iWAT of C57BL6/N mice at P20, all three analyzed genes were more abundant as compared to rWAT. Similar to rWAT, 129S6sv/ev mice displayed 2-fold higher levels of UCP1 and CIDEA and 1.5-fold of COX7A1 than C57BL6/N. This analysis is well in line with the morphological changes observed in both fat pads and the increase of multilocular UCP1 positive cells on IHC sections.

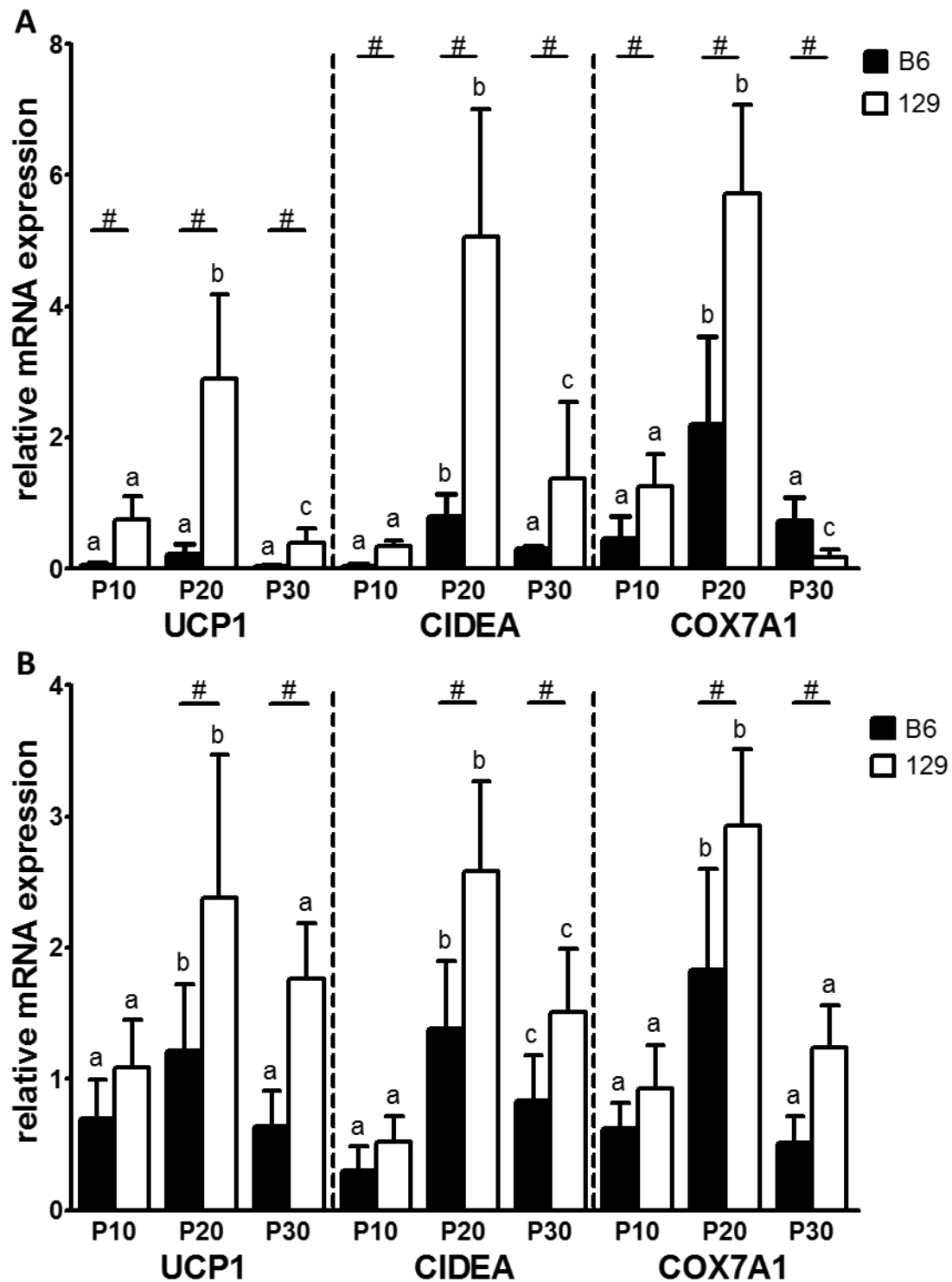


Figure 14 Expression of brown adipocyte marker genes in postnatal retroperitoneal white adipose tissue (rWAT) and inguinal white adipose tissue (iWAT) of C57BL6/N (B6) and 129S6sv/ev (129) mice.

Shown is the transcript abundance of UCP1, CIDEA and COX7A1 of B6 and 129 mice normalized to GUSB in rWAT (A) and iWAT (B) at the indicated time points. Bars depict mean values \pm SD of $n = 7-8$ individual samples per group. Statistical significant differences were analyzed by two-way-ANOVA, # illustrates a significant strain difference at the respective time point, $p < 0.05$; a, b, c illustrate differences within the strains between the displayed time points, $p < 0.05$.

Quantitative real time PCR shows the mRNA abundance of rWAT and iWAT at distinct time points. However, the protein abundance may vary by post transcriptional modifications, e.g. degradation and may influence the actual protein concentration. To investigate, whether the protein concentration of brown adipocyte marker changes during postnatal development, Western Blot analysis were performed. Due to low rWAT mass at P10 and P20 Western Blot analysis of individual samples was not possible. Western Blot analysis of UCP1 in iWAT largely resembles the pattern of the transient transcript abundance of the brown adipocyte markers measured by qRT-PCR with an increase of UCP1 from P10 to P20, a reduction from P20 to P30 and the strain difference in which 129S6sv/ev displays a higher UCP1 abundance at P10 and P20 compared to C57BL6/N (Fig. 15 A). UCP1 protein abundance in iBAT was measured without using a housekeeper like actin or Cox4 because the signals of both proteins were not constant, especially at P10 by using the same amount of 40 μ g per condition and lane (Fig. 15 B). A transient increase of UCP1 protein with a maximum at P20 could not be observed in iBAT.

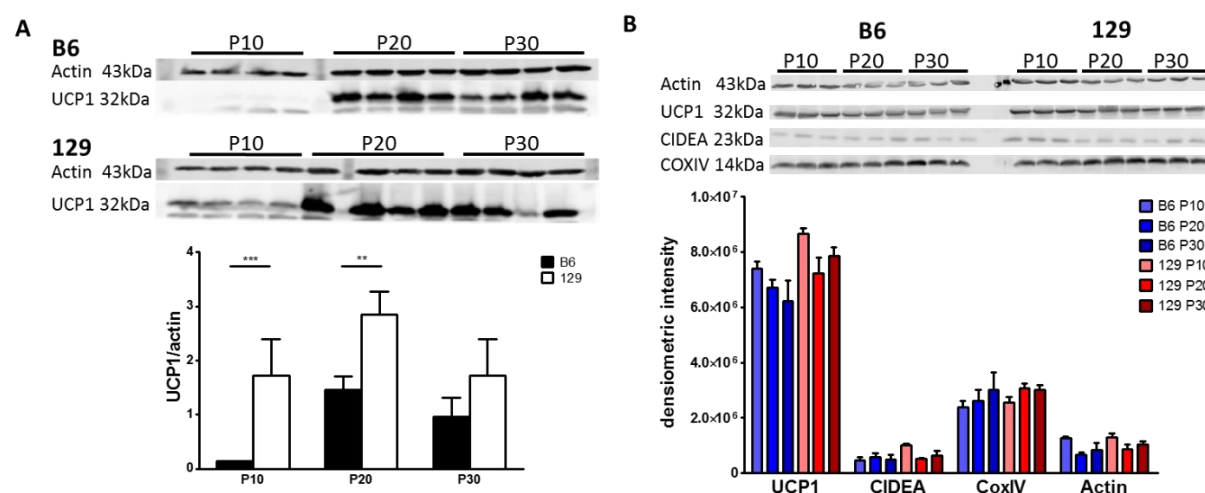


Figure 15 Immunoblots of brown fat marker in iWAT and iBAT of C57BL6/N (B6) and 129S6sv/ev (129) mice.

Immunoblot of iWAT (A) with densitometric quantification of pan-actin (43kDa) and UCP1 (32kDa). Panel (B) shows the immunoblot of iBAT with its densitometric quantification of pan-actin (43kDa), UCP1 (32kDa), CIDEA (23kDa) and COXIV (14kDa). Analysis of three individual depot samples of iWAT and iBAT of B6 and 129 at indicated time points of actin. Band intensities are represented as mean values \pm SD, $n = 4$ for iWAT and $n = 3$ for iBAT. Statistical differences were analyzed by two-way-ANOVA, ** $p < 0.01$; *** $p < 0.001$.

Next to markers that appear in mature brown adipocytes other known factors control the differentiation of brown adipocytes in brown adipose tissue. The coregulator PRDM16 is a crucial factor by determine the cell fate between muscle cells and brown adipocytes. The ablation of PRDM16 in precursors of brown adipocytes promotes muscle differentiation. Another crucial factor for brown adipocyte function in PGC1 α . This transcriptional coactivator is a master regulator of mitochondrial biogenesis. Mice lacking PGC1 α show a blunted

expression of genes that are involved in oxidative phosphorylation in the mitochondria. Investigating whether those factors also influence postnatal britening of white adipose tissue in a strain specific manner, their mRNA abundance during postnatal development was analyzed. The pattern of relative mRNA abundance for PRDM16 and PGC1 α corresponds to the transient appearance of multilocular UCP1 positive cells in rWAT, with a peak at P20. In iWAT the abundance of both genes within the strains was almost unaltered. However C57BL6/N displayed a higher PRDM16 mRNA abundance compared to 129S6sv/ev at all time points. No strain difference in PGC1 α mRNA abundance could be observed in either tissue (Fig. 16 A & B).

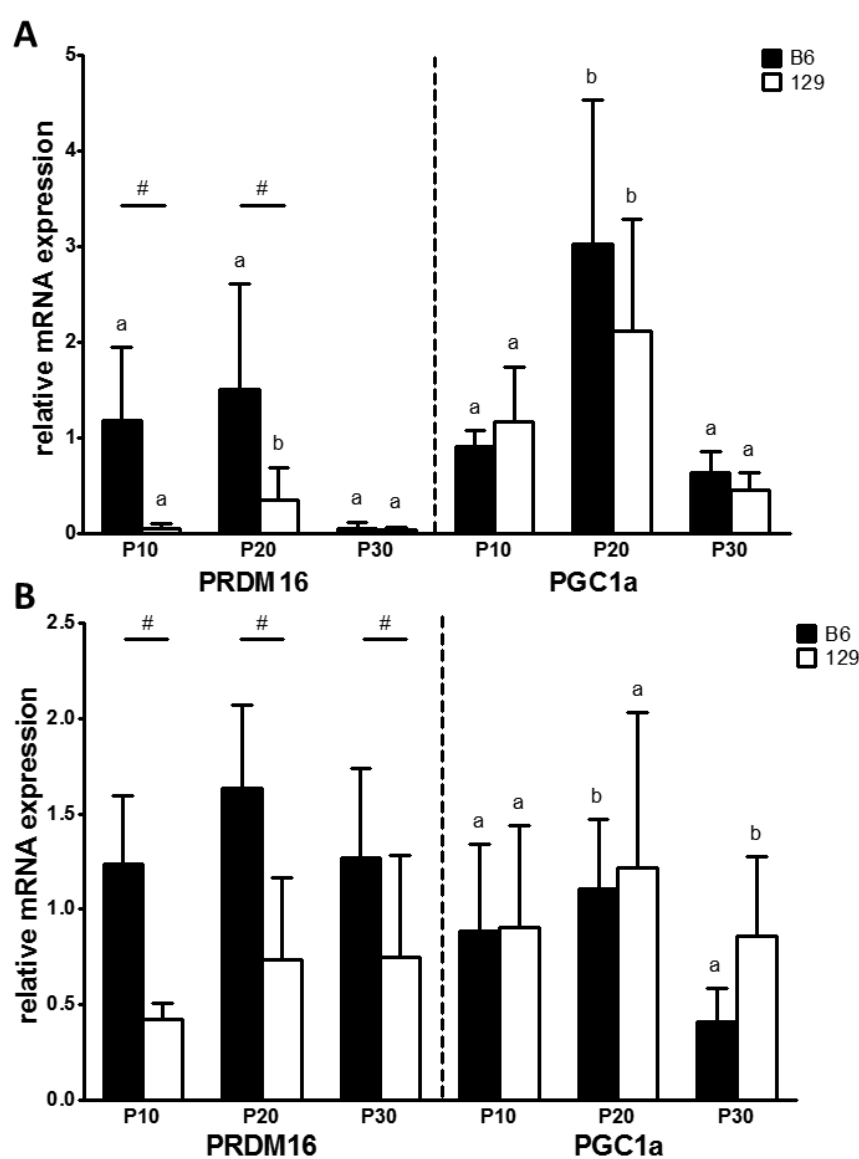


Figure 16 Expression of PRDM16 and PGC1 α of C57BL6/N (B6) and 129S6sv/ev (129) mice.

Transcript abundances of PRDM16 and PGC1 α in rWAT (A) and iWAT (B) B6 and 129 are normalized to GUSB in rWAT (A) and iWAT (B) at the indicated time points. Bars depict mean values \pm SD of $n = 8$ individual samples per group. Statistical significant differences were analyzed by two-way-ANOVA, # illustrates a significant strain difference at the respective time point, $p \leq 0.05$; a, b, c illustrate differences within the strains between the displayed time points, $p \leq 0.05$.

Analyzing whether the observed strain difference in postnatal fat pad development of C57BL6/N and 129S6sv/ev is also seen in other strains, SWR/J and AKR/J mice were analyzed at P20 with regard to their fat pad development and brown adipocyte marker gene abundance. AKR/J and SWR/J mice had a similar development of eWAT and rWAT as 129S6sv/ev with a trend toward lower fat pad mass. For iWAT development, AKR/J showed a fat pad mass similar to C57BL6/N, while SWR/J resembles 129Ssv/ev (Fig. 17 A). The iBAT mass was lower in AKR/J compared to the other three strains. 129S6sv/ev showed the highest fat pad masses. AKR/J had a similar level as C57BL6/N, whereas SWR/J had a significant higher UCP1 and CIDEA abundance compared to AKR/J (Fig. 17 B).

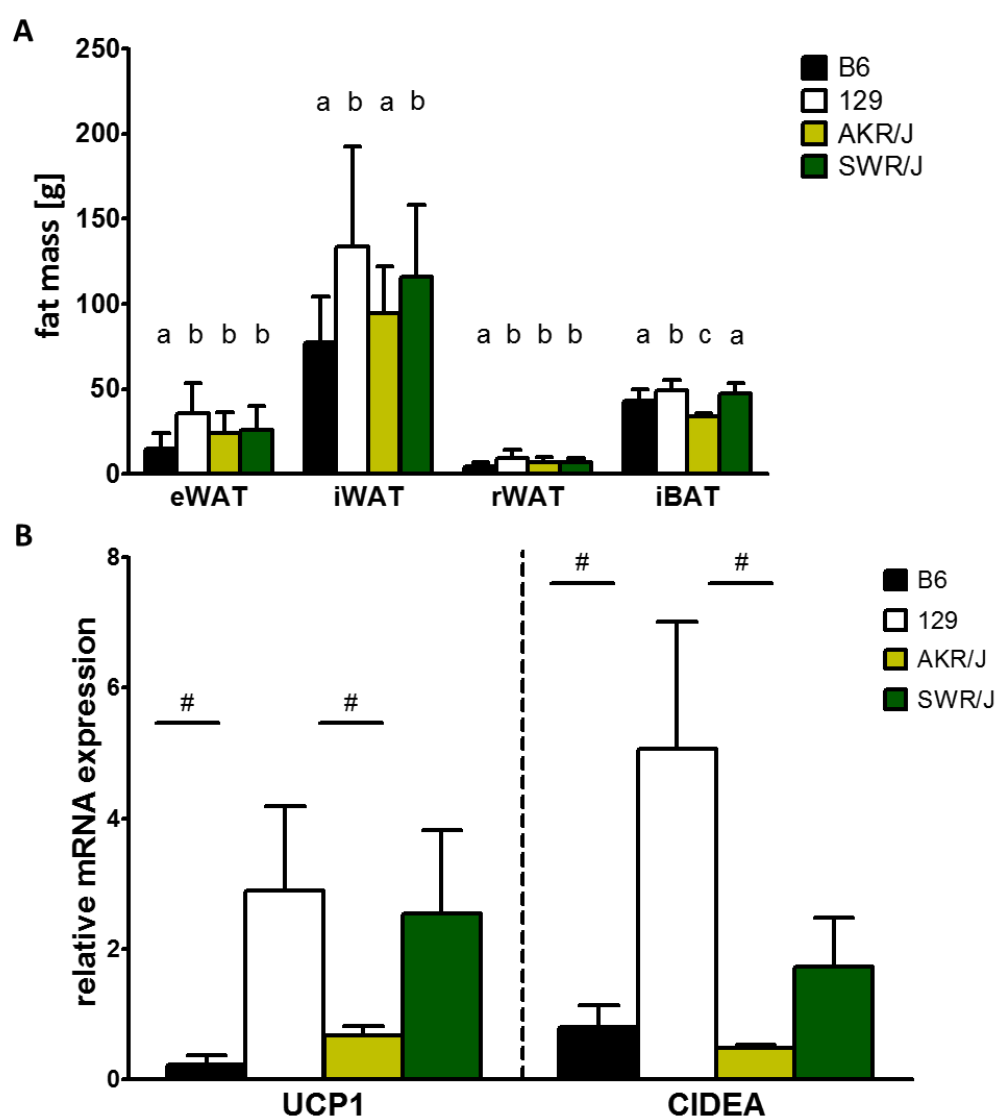


Figure 17 Development of fat pad mass and brown fat marker expression of C57BL6/N (B6), 129S6sv/ev (129), AKR/J and SWR/J mice.

(A) Mass of eWAT, iWAT, rWAT and iBAT depots of C57BL6/N, 129S6sv/ev, AKR/J and SWR/J mice at P20. (B) Relative expression of brown adipocyte marker genes UCP1 and CIDEA in rWAT. Bars depict mean values \pm SD of $n = 25$ B6, 30 129 P20, 8 AKR/J and 9 SWR/J individual samples per group for fat mass and $n = 7-8$ for gene expression data. Statistical significant differences are the result of two-way-ANOVA, * illustrates a significant strain difference at the displayed time points, * <0.05 ; *** <0.001 ; a, b, c illustrate differences between the strains at the displayed time points, $p \leq 0.05$.

Taken together, a strain difference in britening is not limited to the two strains initially observed but could be demonstrated in several strains of a different genetic background. Especially strains that are described to have a lower propensity towards diet induced obesity, show elevated fat pad masses with an elevated britening.

3.2 Maternal care modulates postnatal britening and fat pad development

Possibly, the transient postnatal britening effect of white adipose tissue originates from maternal care, e.g. grooming, warming and feeding. To determine whether maternal care is the major contributor of postnatal britening, C57BL6/N and 129S6sv/ev pups were cross-fostered and analyzed at the postnatal days P10, P20 and P30 of age. Cross-fostering means the switch of litters from one strain to a foster mother of another strain and *vice versa*. The litters are equally in number and age. The body mass development of both strains showed no differences at all three respective time points (Fig. 18). Normal fostered 129S6sv/ev mice displayed a subtle but not significant elevation body mass.

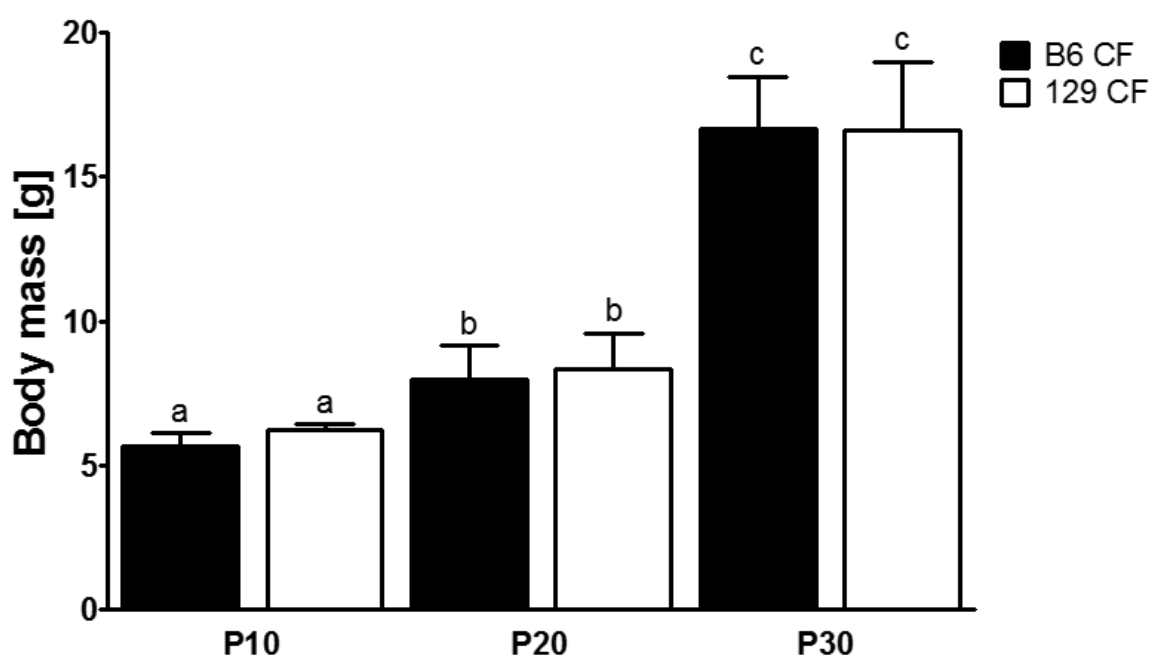


Figure 18 Postnatal body mass development of cross fostered (CF) C57BL6/N (B6) and 129S6sv/ev (129) mice.

Body mass development of cross fostered C57BL6/N (B6) in black bars and 129S6sv/ev (129) mice in white bars at indicated time points. Bars depict mean values \pm SD of n = 5 B6 P10, 15 B6 P20, 9 B6 P30, 7 129 P10, 14 129 P20, 12 129 P30 individual samples per group.

The adipose tissue depots eWAT, iWAT, rWAT and iBAT were dissected and weighed at all three stages of age, P10-30. In cross-fostered animals no difference in P10 fat pad mass could

be observed between strains. From P10 to P20, fat pad mass in eWAT, rWAT and iWAT showed a growth attenuation and was not further increased. An exception was iWAT of 129S6sv/ev. All three fat pads displayed significantly increase mass from P20 to P30. That was much more pronounced in 129S6sv/ev. The iBAT mass steadily increased and no strain differences could be observed at any time points (Fig. 19).

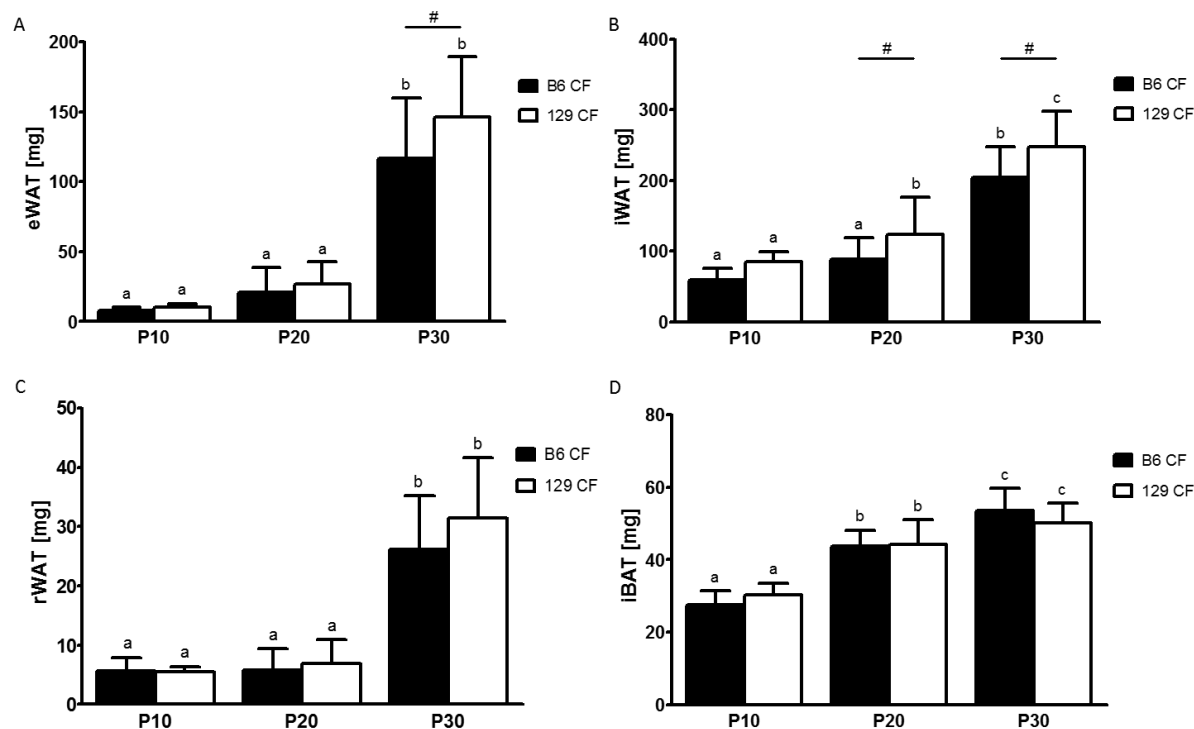


Figure 19 Postnatal development of fat pad masses of cross fostered (CF) C57BL6/N (B6) and 129S6sv/ev (129) mice.

Mass of epididymal white adipose tissue (eWAT) (A), inguinal white adipose tissue (iWAT) (B), retroperitoneal white adipose tissue (rWAT) (C) and interscapular brown adipose tissue (iBAT) (D) depots are shown. Bars depict mean values \pm SD of $n = 5$ B6 P10, 15 B6 P20, 9 B6 P30, 7 129 P10, 14 129 P20, 12 129 P30 individual samples per group. The postnatal days 10, 20 and 30 of age are abbreviated P10, P20 and P30, indicating the respective postnatal day of life. Statistical significant differences are the result of two-way-ANOVA, # illustrates a significant strain difference at the displayed time points, * <0.05 ; a, b, c illustrates differences within the strains, $p \leq 0.05$.

Normal fostered C57BL6/N and 129S6sv/ev mice showed a strain difference in body mass development from P10 to P30. Especially the development of distinct white adipose tissue depots displayed significant higher depot masses in 129S6sv/ev at P20 and P30 compared to C57BL6/N. To analyze the impact of cross-fostering on postnatal development, cross-fostered animals were compared to normal fostered animals. The comparison showed a reduced strain difference of body mass development within the cross-fostered animals. Interestingly the individual fat pad mass development of cross-fostered C57BL6/N mice is higher compared to normal fostered animals. Considering the relative changes from normal fostered to cross-fostered animals, both strains displayed a steady increase in body mass and fat pad

masses of eWAT, iWAT, rWAT and iBAT. However, cross-fostered C57BL6/N mice exhibited higher body mass, eWAT, iWAT, rWAT and iBAT masses compared to normal fostered C57BL6/N at P20 and P30. Interestingly cross-fostered 129S6sv/ev mice showed lower fat pad masses (Tab. 15).

Table 15 Relative differences in body mass, eWAT, iWAT, rWAT and iBAT mass of cross fostered C57BL6/N and 129S6sv/ev mice expressed as percentage of normally fostered C57BL6/N and 129S6sv/ev mice.

	B6 CF				
	BM [g]	eWAT[mg]	iWAT[mg]	rWAT[mg]	iBAT [mg]
P10	+8.35 %	+85.36 %	+6.11 %	+34.19 %	+17.19 %
P20	+5.76 %	+42.26 %	+14.37 %	+32.28 %	+1.43 %
P30	+12.64 %	+63.96 %	+30.27 %	+73.94 %	+5.94 %
	129 CF				
	BM [g]	eWAT[mg]	iWAT[mg]	rWAT[mg]	iBAT [mg]
P10	+12.12 %	+49.58 %	+23.75 %	+27.63 %	+13.92 %
P20	+1.64 %	-24.65 %	-7.28 %	-27.20 %	-10.63 %
P30	+5.22 %	-5.84 %	-4.81 %	-3.01 %	-8.91 %

To investigate, whether the reduced strain difference is caused by a different proportionality of fat pad mass and body mass, for each mouse the individual fat pad masses were plotted against their body mass (Fig. 19). The resulting scatter plots demonstrated that eWAT increased almost continuously with body mass in both strains. Interestingly 129S6sv/ev reached a higher eWAT mass at P30 when comparing animals of both strains with the same body mass (Fig. 20 A). In iWAT and rWAT a proportional growth of depot mass was not found from P10 to P30, similar to normal fostered animals. The depot mass was proportional to body mass within the data points of one separate day P10 or P20 respectively, but the P20 regression could clearly not be extrapolated from the P10 regression. In both strains the increase in iWAT and rWAT mass attenuated from P10 to P20 (Fig. 20 B and C). Comparing individual mice of similar body mass, no strain difference in a higher iWAT and rWAT mass could be observed at day 20. The iBAT development correlates with the increase of body mass until post natal day 20 and reaches a plateau at day 30 (Fig. 20 D).

Normal fostered 129S6sv/ev mice displayed a higher white adipose depot mass comparing to C57BL6/N mice of equal body mass. Interestingly cross fostering converged both strains, resulting in a higher fat pad mass gain in C57BL6/N. Compared to normal fostered mice, both cross-fostered strains showed a lower difference of total fat pad mass in eWAT, iWAT and rWAT, when comparing mice with an equal body mass.

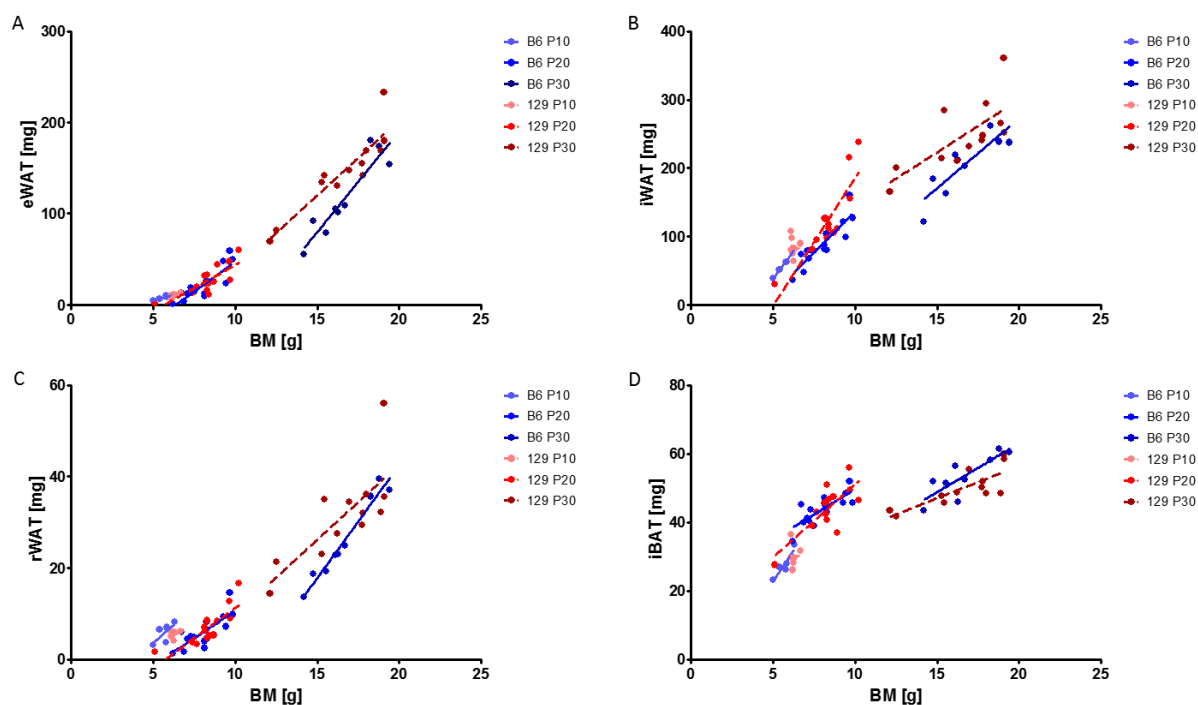


Figure 20 Fat pad mass in proportion to body mass of cross fostered (CF) C57BL6/N (B6) and 129S6sv/ev (129) mice.

The four panels show the mass of epididymal white adipose tissue (eWAT) (A) inguinal white adipose tissue (iWAT) (B) retroperitoneal white adipose tissue (rWAT) (C) and interscapular brown adipose tissue (iBAT) (D) at postnatal days 10 (P10), 20 (P20) and 30 (P30) of cross fostered C57BL6/N (B6) and 129S6sv/ev (129) mice. Each symbol represents an individual fat pad mass plotted against the respective body mass. Continuous lines represent the linear regression within B6 and dashed lines the linear regression of 129 samples within a distinct postnatal day group.

Shown in normal fostered mice, higher postnatal fat mass correlates with a higher abundance of brown adipocyte markers during the browning of white adipose tissue. Possibly, the increase of adipose tissue mass in cross-fostered C57BL6/N also results in higher abundance of brown adipocyte markers. To determine whether cross-fostering also affects the browning capability of both strains, qRT-PCR were performed of rWAT and iWAT in both strains for the brown fat markers UCP1, CIDEA and COX7A1. In rWAT C57BL6/N mice showed a subtle increase of UCP1 abundance from P10 to P20 that is reduced at P30. Interestingly 129S6sv/ev mice displayed a steady reduced expression from P10 to P30 of mitochondrial associated genes, UCP1 and COX7A1. The same pattern could be observed for COX7A1 in C57BL6/N. However a strain difference resulting in a significant higher expression in 129S6sv/ev could be observed at all time points for UCP1. For COX7A1 a significant strain difference could not be observed at P20 and P30. The gene expression of CIDEA showed a transient appearance from P10 to P30 with a maximum at P20 in both strains, with a significantly higher expression in 129S6sv/ev (Fig. 21 A). In iWAT of cross-fostered animals a transient expression could be observed for CIDEA and COX7A1 in both strains and in UCP1 for C57BL6/N. However a

significant strain difference at P20 could not be observed in the expression of all three genes (Fig. 21 B). By comparing normal fostered with cross-fostered animals, rWAT of cross-fostered C57BL6/N showed a transient pattern in UCP1 abundance, similar to normal fostered animals. They displayed a significantly higher UCP1 expression at P10 and P20 compared to normal fostered animals. The transient pattern of CIDEA was unaffected by cross fostering. The COX7A1 pattern in rWAT of cross fostered animals declined from P10 to P30. Interestingly, normal fostered animals had a transient expression with a maximum at P20. Similar to UCP1, cross-fostered C57BL6/N had a significantly higher COX7A1 abundance at P10. But the abundance at P20 was significantly higher in normal fostered animals (Fig. 21 A). However the increase of brown fat markers in white adipose tissue suggests a higher browning potential in cross-fostered C57BL6/N. In cross-fostered 129S6sv/ev mice UCP1 and COX7A1 abundance declined from P10 to P30. At P20 cross-fostered animals showed a reduced expression of both genes compared to normal fostered animals that reaches significance for COX7A1. The pattern of CIDEA abundance in cross fostered animals resembled the pattern of normal fostered animals. Interestingly cross-fostered mice showed a significant lower abundance at P20 (Fig. 21 B). This displays a possible lower browning potential for rWAT of cross-fostered 129S6sv/ev mice.

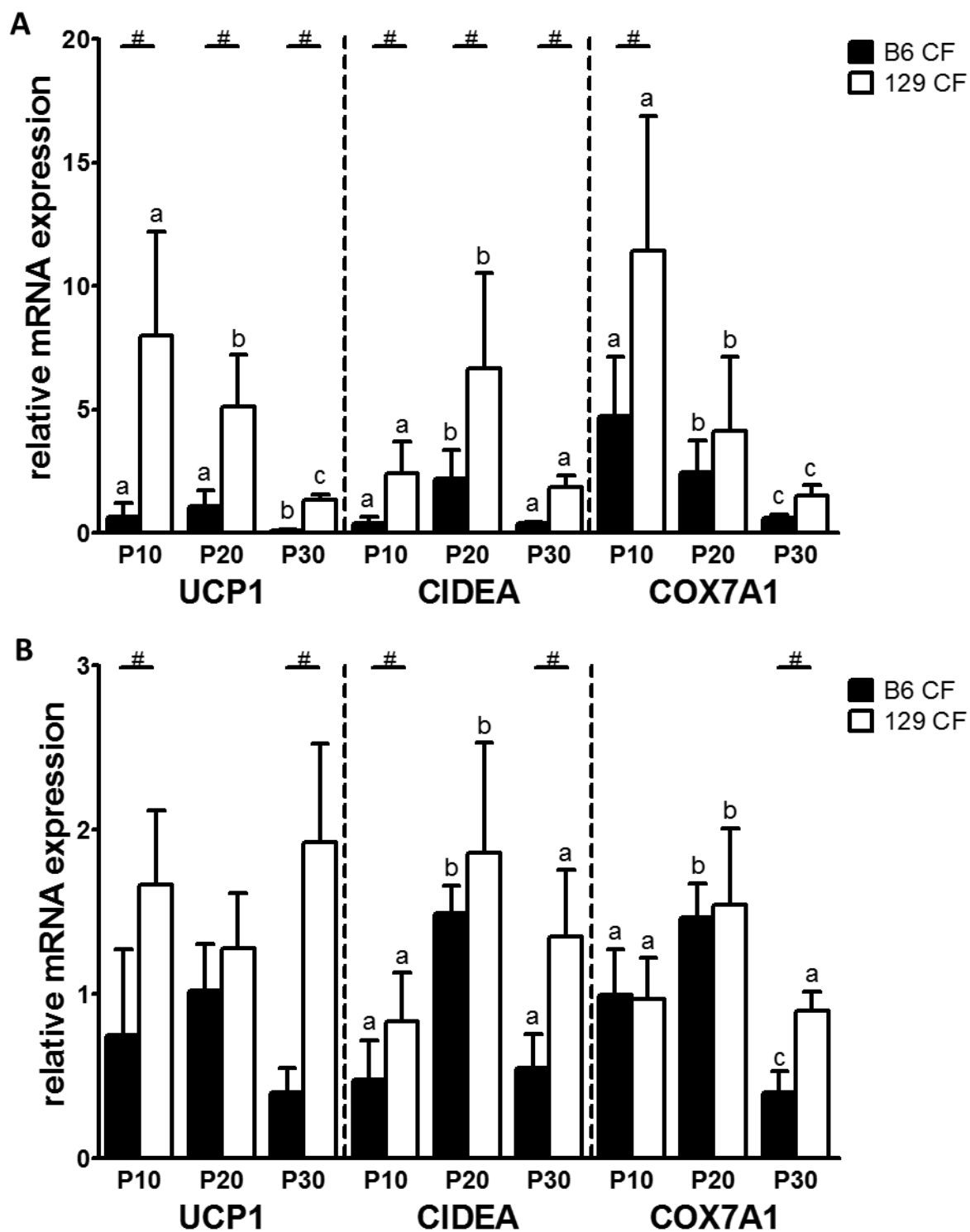
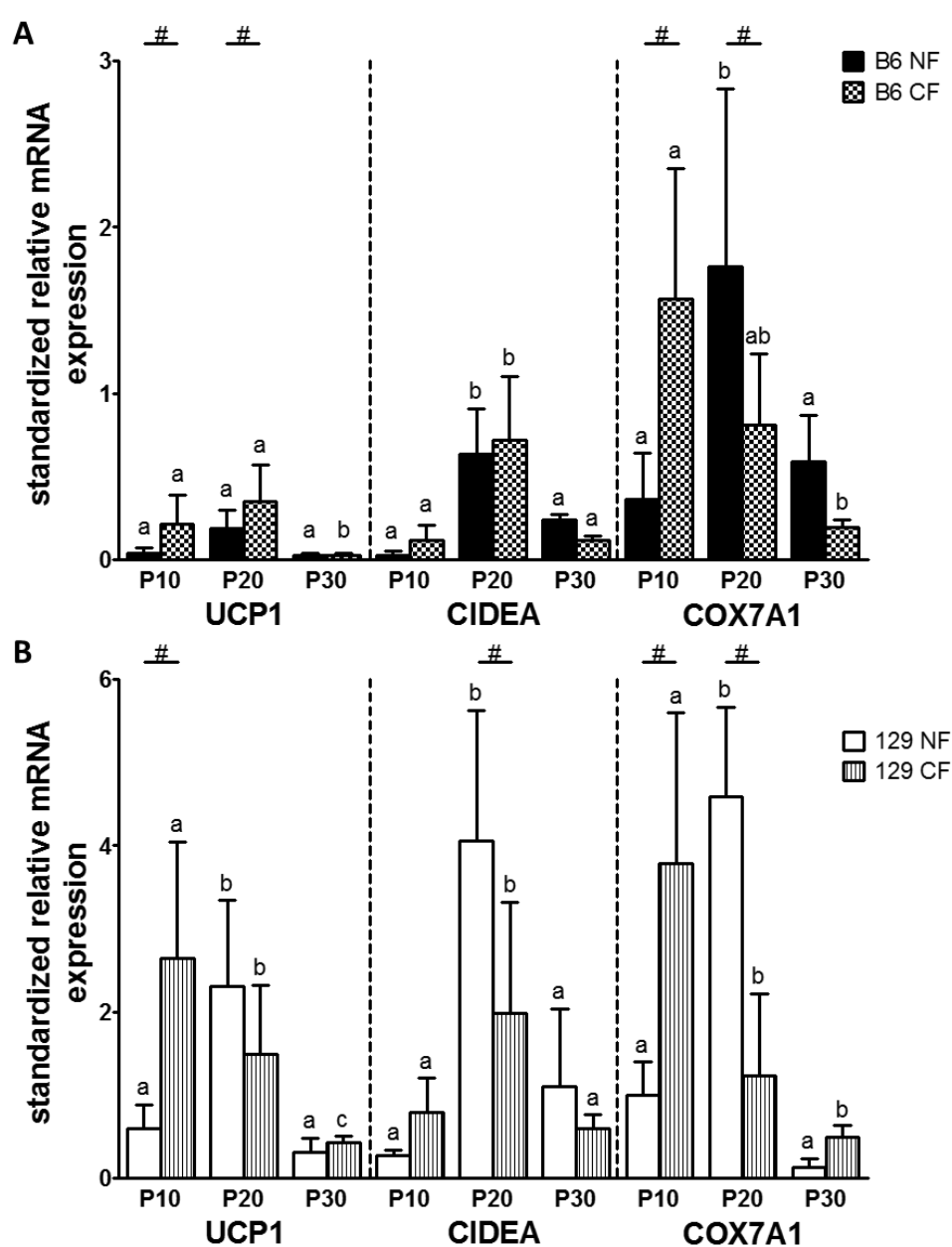


Figure 21 Expression of brown adipocyte marker genes in cross fostered (CF) postnatal retroperitoneal white adipose tissue (rWAT) and inguinal white adipose tissue (iWAT) of C57BL6/N (B6) and 129S6sv/ev (129) mice.

Shown is the transcript abundance of UCP1, CIDEA and COX7A1 of cross fostered B6 and 129 normalized to GUSB in rWAT (A) and iWAT (B) at the indicated time points. Bars depict mean values \pm SD of $n = 5-8$ individual samples per group. Statistical significant differences were analyzed by two-way-ANOVA, # illustrates a significant strain difference at the respective time point, $p < 0.05$; a, b, c illustrate differences within the strains at the displayed time points, $p < 0.05$.

In iWAT the expression of all three brown fat markers in cross fostered C57BL6/N animals show a similar pattern to normal fostered animals. However at P10 cross fostered animals show a subtle expression that reaches significance for COX7A1 (Fig. 22 C). Cross fostered 129S6sv/ev mice do not show a transient expression pattern for UCP1 that was observed in normal fostered animals. At P20 the expression was reduced in cross fostered animals. The expression of CIDEA and COX7A1 resembles the transient expression of normal fostered animals. However cross fostering leads to a significant reduction in COX7A1 at P20 (Fig. 22 D). The reduced effect of cross-fostering upon brown adipocyte marker expression in iWAT of both strains show a lower variability in affecting subcutaneous white adipose browning.



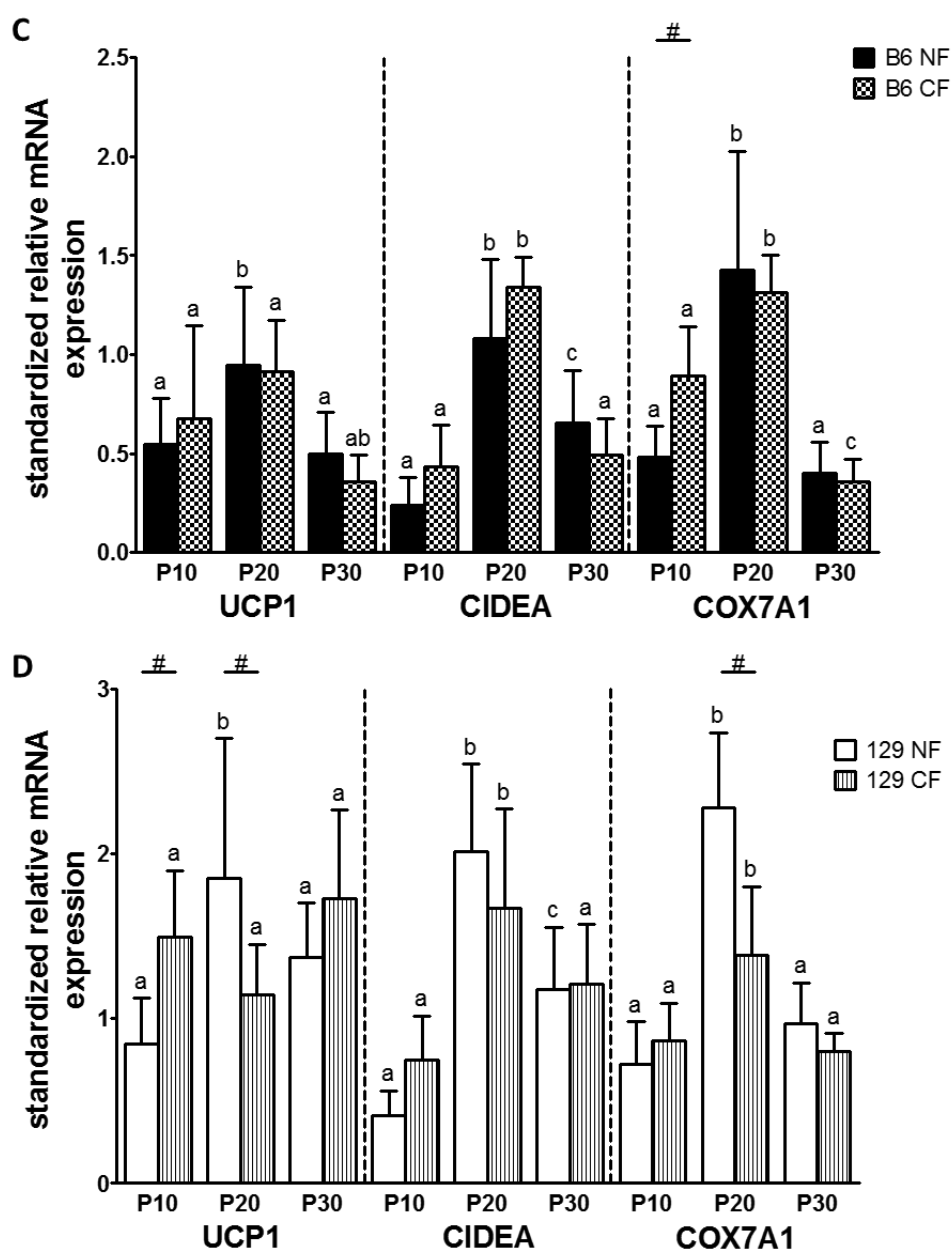


Figure 22 Expression of standardized brown adipocyte marker genes in cross fostered (CF) and normal fostered (NF) postnatal retroperitoneal white adipose tissue (rWAT) and inguinal white adipose tissue (iWAT) of C57BL6/N (B6) and 129S6sv/ev (129) mice.

Shown is the transcript abundance of UCP1, CIDEA and COX7A1 of cross fostered and normal fostered B6 and 129 normalized to GUSB and standardized to the mean of all expression values in rWAT (A & B) and iWAT (C & D)) at the indicated time points. Bars depict mean values \pm SD of $n = 5-8$ individual samples per group. Statistical significant differences were analyzed by two-way-ANOVA, # illustrates a significant strain difference at the respective time point, $p \leq 0.05$; a, b, c illustrate differences within the strains, $p \leq 0.05$.

Taken together, cross fostering affects the fat pad mass of mice from C57BL6/N and 129S6sv/ev. While cross-fostering in C57BL6/N leads to a higher fat pad mass, 129S6sv/ev animals displayed a lower fat pad mass at P20 and P30. Gene expression in white adipose tissue of cross-fostered mice showed a higher in C57BL6/N and in 129S6sv/ev mice a lower

brown adipocyte marker gene expression in rWAT. In normal fostered animals the transient expression pattern of brown adipocyte marker genes in white adipose tissue correlates with its browning. Therefore, the expression pattern revealed a higher browning potential in mice, e.g. C57BL6/N that are switched to a foster mother of a strain inheriting a strong browning potential or *vice versa*. However the lower influence of cross-fostering on iWAT browning compared to rWAT, shows the variability of browning in different adipose tissues. Interestingly, in a strain specific manner cross-fostering showed that maternal care directly influences adipose tissue mass and postnatal browning of pups.

3.3 Thermoneutrality reduces browning in white fat and leads to a brown fat hypertrophy

Cross-fostering affects the strain specific browning of white adipose tissue. Possibly, either the thermal micro environment or other maternal factors as grooming, the milk composition or the length of the interval in which the mother leaves the nest influences the postnatal development. Investigating if the higher white fat pad masses in C57BL6/N or the lower in 129S6sv/ev are an effect of the maternal thermal environment pregnant mice of both strains were transferred to a 30 °C environment 2 days before delivery. The environment of 30°C ambient temperature resembles thermoneutrality. Pups were kept at 30 °C and were analyzed and dissected at postnatal day P10, P20 and P30 of age. Body mass, body composition, eWAT, iWAT, rWAT and iBAT masses were determined. Body mass was significantly higher in 129S6sv/ev pups at P20 and P30 compared to C57BL6/N (Fig. 23).

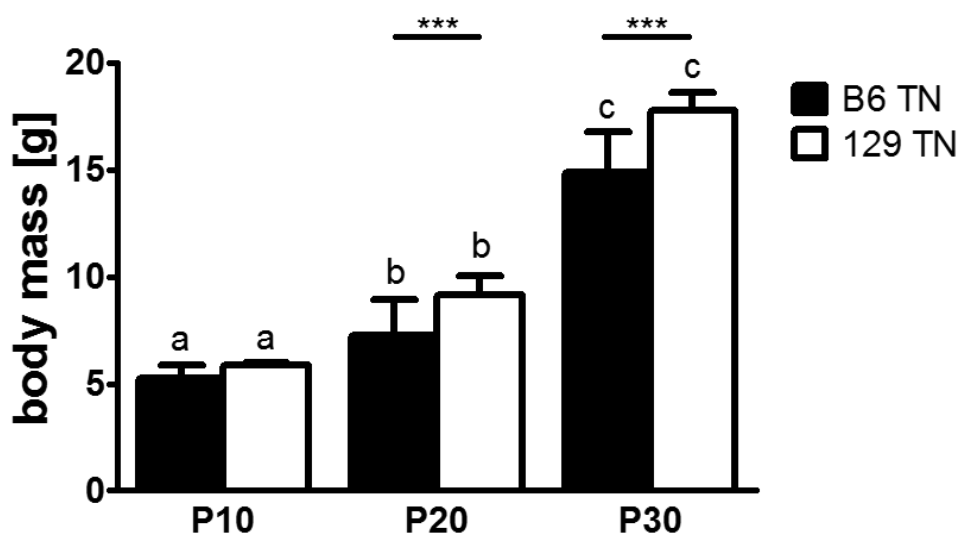


Figure 23 Postnatal body mass of thermoneutral kept C57BL6/N (B6) and 129S6sv/ev (129) mice.

Body mass development of C57BL6/N (B6) in black bars and 129S6sv/ev (129) mice in white bars, kept in 30°C ambient temperature at indicated time points. Bars depict mean values \pm SD of $n = 8$ B6 P10, 14 B6 P20, 12 B6 P30, 3 129 P10, 12 129 P20, 4 129 P30 individual samples per group. Statistical significant differences are the result of two-way-ANOVA, * illustrates a significant strain difference at the displayed time points, *** <0.001 ; a, b, c illustrates differences within the strains, $p \leq 0.05$.

Body composition showed that the increase of body mass of 129S6sv/ev was subject to a significantly higher fat mass at P20 and P30 accompanied by an increase in lean mass at P20. However total body fat mass was increased by approximately 37.5 % at P20 and 40 % at P30 in 129S6sv/ev compared to C57BL6/N, while lean mass was also increased by approximately 20 % at P20 (Fig. 24).

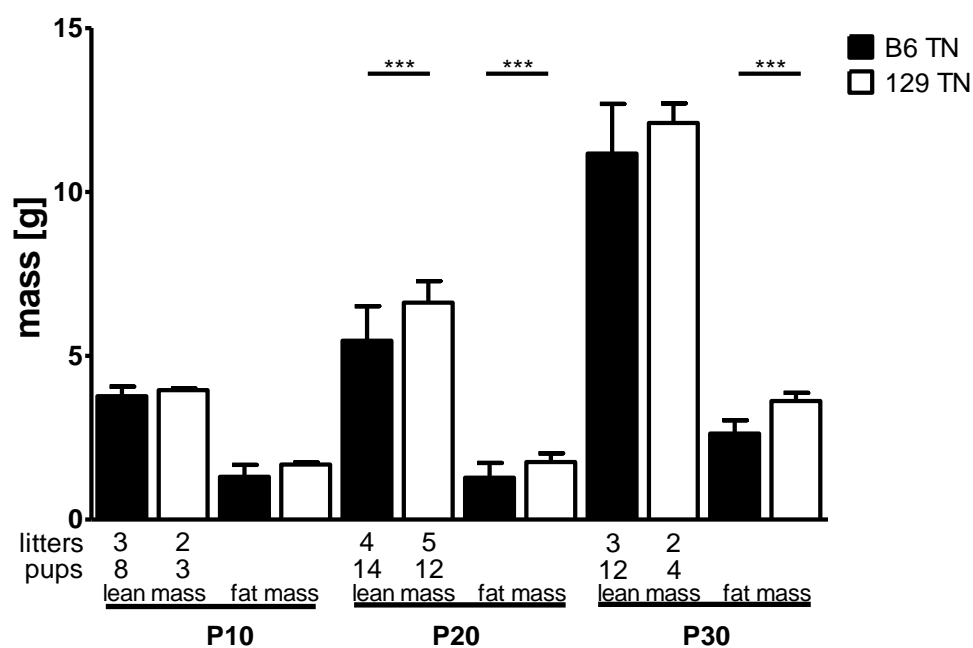


Figure 24 Postnatal body composition of thermoneutral kept C57BL6/N (B6) and 129S6sv/ev (129) mice.

Body composition at indicated time points of lean mass and fat mass distribution. Bars depict mean values \pm SD. The number of litters and pups are as indicated. The postnatal days 10 to 30 of age are abbreviated P10, P20 and P30, indicating the respective postnatal day of life. Statistical significant differences are the result of two-way-ANOVA, * illustrates a significant strain difference, *** <0.001 .

Lean mass at P30 in C57BL6/N was slightly but not significantly higher when plotted against the individual body mass for each mouse (Fig. 25 A). Nevertheless, both strains showed a linear regression of lean mass to body mass from P10 to P30. For total fat mass plotted against its individual body mass, 129S6sv/ev showed a higher fat mass compared to C57BL6/N. However, for both strains a proportional growth of fat mass was not found. Between P10 and P20 fat mass attenuated and a regression could not be clearly extrapolated (Fig. 25 B). In both strains the increased body mass from P10 to P20 was not accompanied by a higher total fat mass.

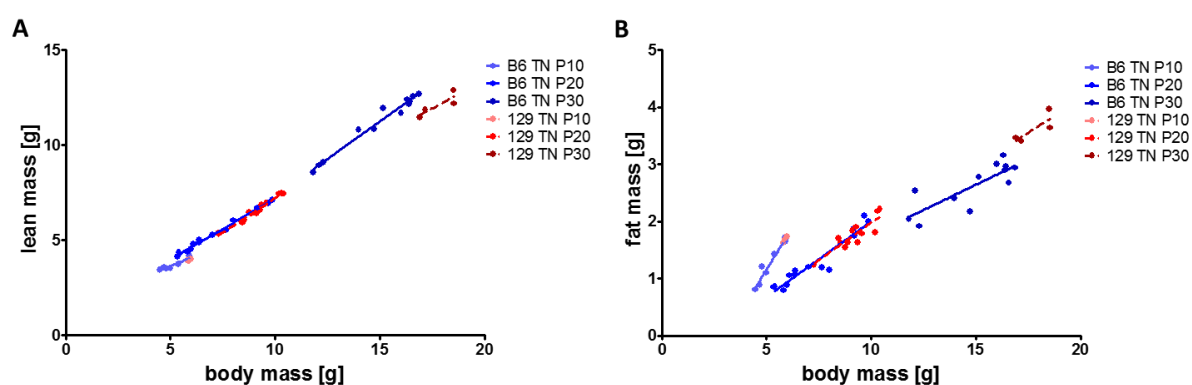


Figure 25 Body composition of thermoneutral kept C57BL6/N (B6) and 129S6sv/ev (129) mice in proportion to body mass. The two panels show the lean mass (A) and fat mass (D) plotted at postnatal days 10 (P10), 20 (P20) and 30 (P30) plotted against the respective body mass. Each symbol represents an individual fat mass and lean mass. Continuous lines represent the linear regression within B6 and dashed lines the linear regression of 129 samples within a distinct postnatal day group.

Illustrating whether the difference in total body fat mass at P20 and P30 is reflected in altered adipose tissue depot masses and changes in the regional distribution, eWAT, iWAT, rWAT and iBAT were dissected and weighed from pups at all three stages of age, P10-P30. At P10, no strain difference could be observed in any of the dissected tissues (Fig. 26). From P10 to P20, 129S6sv/ev exhibited a significant increase in fat mass growth of rWAT, iWAT, eWAT and iBAT as compared to C57BL6/N. From P20 to P30 both strains further increased fat pad mass in rWAT, iWAT and eWAT. Again, this increase was more pronounced in 129S6sv/ev compared to C57BL6/N (Fig. 25). Pertaining to brown adipose tissue 129S6sv/ev tended to grow more iBAT mass but this strain difference attained significance at P20. During the first 30 days of life body mass and fat pad masses are largely increasing in both strains, with enhanced overall growth rates in 129S6sv/ev mice compared to C57BL6/N.

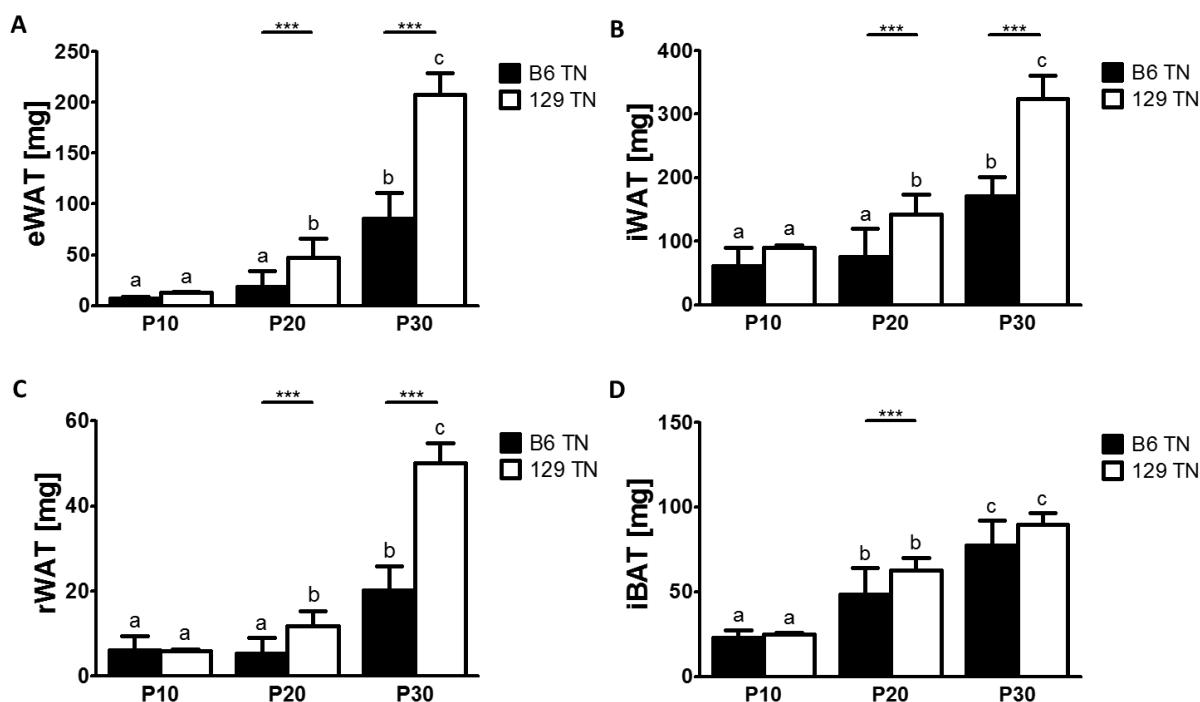


Figure 26 Postnatal fat pad masses of thermoneutral kept C57BL6/N (B6) and 129S6sv/ev (129) mice.

Mass of epididymal white adipose tissue (eWAT) (A), inguinal white adipose tissue (iWAT) (B), retroperitoneal white adipose tissue (rWAT) (C) and interscapular brown adipose tissue (iBAT) (D) depots are shown. Bars depict mean values \pm SD of $n = 8$ B6 P10, 14 B6 P20, 12 B6 P30, 3 129 P10, 12 129 P20, 4 129 P30 individual samples per group. The postnatal days 10, 20 and 30 of age are abbreviated P10, P20 and P30, indicating the respective postnatal day of life. Statistical significant differences are the result of two-way-ANOVA, * illustrates a significant strain difference, *** <0.001 .

Compared to normal fostered animals the thermoneutral kept mice of both strains had a higher fat mass from P10 to P30, while 129S6sv/ev also increase in body mass. Especially from P10 to P30 eWAT and rWAT in both strains displayed higher masses compared to normal fostered animals. Interestingly iBAT show an increased fat pad mass development in thermoneutral kept animals from P20 to P30 (Tab. 16). This increase could not be observed in cross fostered animals. In a non-strain specific manner thermoneutrality largely increase adipose tissue development.

Table 16 Relative differences in body mass, eWAT, iWAT, rWAT and iBAT mass of thermoneutral kept C57BL6/N and 129S6sv/ev mice expressed as percentage of normally fostered C57BL6/N and 129S6sv/ev mice.

	B6 TN				
	BM [g]	eWAT[mg]	iWAT[mg]	rWAT[mg]	iBAT [mg]
P10	+0.47 %	+59.26 %	+8.81 %	+44.49 %	-2.45 %
P20	-3.66 %	+26.43 %	-2.34 %	+20.88 %	+11.79 %
P30	+0.60 %	+20.06 %	+8.65 %	+35.18 %	+52.61 %
	129 TN				
	BM [g]	eWAT[mg]	iWAT[mg]	rWAT[mg]	iBAT [mg]
P10	+12.46 %	+94.23 %	+30.64 %	+38.16 %	-6.22 %
P20	+16.67 %	+49.94 %	+13.80 %	+36.58 %	+29.46 %
P30	+12.75 %	+33.48 %	+24.84 %	+54.43 %	+62.98 %

To investigate whether the strain difference in fat mass development in thermoneutral kept 129S6sv/ev and C57BL6/N mice is caused by a different proportionality of fat pad mass and body mass, for each mouse the individual fat pad masses were plotted against their body mass. The resulting scatter plots demonstrate that eWAT increases almost continuously with body mass in both strains. In 129S6sv/ev the slope was similar to C57BL6/N, but still 129S6sv/ev accumulated a higher fat pad mass at postnatal day 20 and 30 (Fig. 27 A). In iWAT and rWAT a proportional growth of depot mass was not found in both strains. The increase of body mass from P10 to P20 was not accompanied by an increase in iWAT and rWAT mass but with a growth attenuation (Fig. 27 B and C). Thus the relative contribution of these two fat pads to body mass decreases during early development. Comparing individual mice of similar body mass, 129S6sv/ev mice developed a higher rWAT and iWAT mass at postnatal day 20 and 30. The iBAT development correlated with the increase of body mass until post natal day 20. A plateau at day 30 like in normal or cross fostered animals cannot be observed (Fig. 27 D).

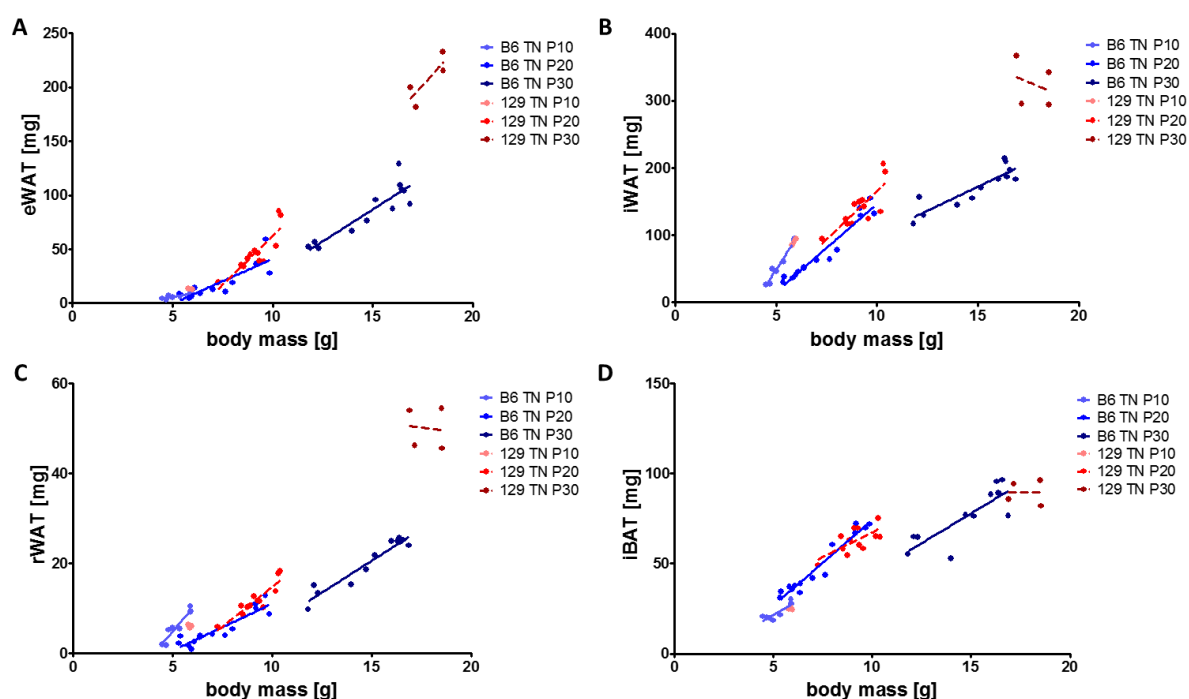


Figure 27 Fat pad mass in proportion to body mass of thermoneutral kept C57BL6/N (B6) and 129S6sv/ev (129) mice. The four panels show the mass of epididymal white adipose tissue (eWAT) (A) inguinal white adipose tissue (iWAT) (B) retroperitoneal white adipose tissue (rWAT) (C) and interscapular brown adipose tissue (iBAT) (D) at postnatal days 10 (P10), 20 (P20) and 30 (P30) of cross fostered C57BL6/N (B6) and 129S6sv/ev (129) mice. Each symbol represents an individual fat pad mass plotted against the respective body mass. Continuous lines represent the linear regression within B6 and dashed lines the linear regression of 129 samples within a distinct postnatal day group.

The pattern of adipose tissue masses plotted against their body mass from mice of both strains kept in thermoneutrality resembled the pattern of normal fostered mice. However

thermoneutrality increased adipose tissue mass (Tab. 16), while lean mass was unaffected, except for normal fostered C57BL6/N at P10 exhibiting a significantly higher lean mass (Fig. 28).

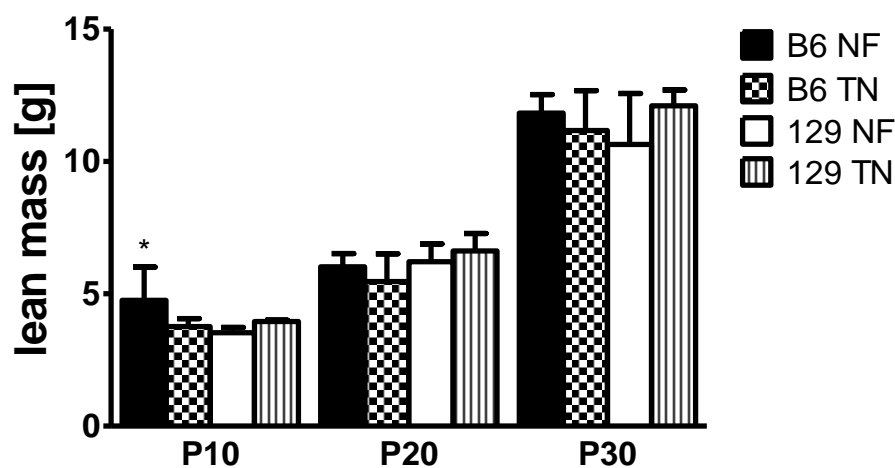


Figure 28 Postnatal lean masses of normal fostered and thermoneutral kept C57BL6/N (B6) and 129S6sv/ev (129) mice. Lean mass at indicated time points. Bars depict mean values \pm SD of $n = 4-18$. The postnatal days 10 to 30 of age are abbreviated P10, P20 and P30, indicating the respective postnatal day of life. Statistical significant differences are the result of two-way-ANOVA, * illustrates a significant strain difference, $* < 0.05$.

To determine the effect of thermoneutrality on postnatal hypertrophic iBAT and the presumable browning of iWAT in 129S6sv/ev and C57BL6/N, immunohistochemical analysis of iBAT and iWAT sections at P20 were performed. In both strains iBAT showed larger lipid droplets compared to normal fostered mice (Fig. 29 B). Possibly, thermoneutrality leads to a higher lipid accumulation in brown adipocytes. However these cells still expressed UCP1 (Fig. 29 A). In iWAT, multilocular UCP1 expressing cells also appeared at P20 as single cells and did not form islets compared to normal fostered mice. However in thermoneutral kept C57BL6/N the size of lipid droplets in iBAT and the number of UCP1 expressing, multilocular cells in iWAT was higher compared to 129S6sv/ev.

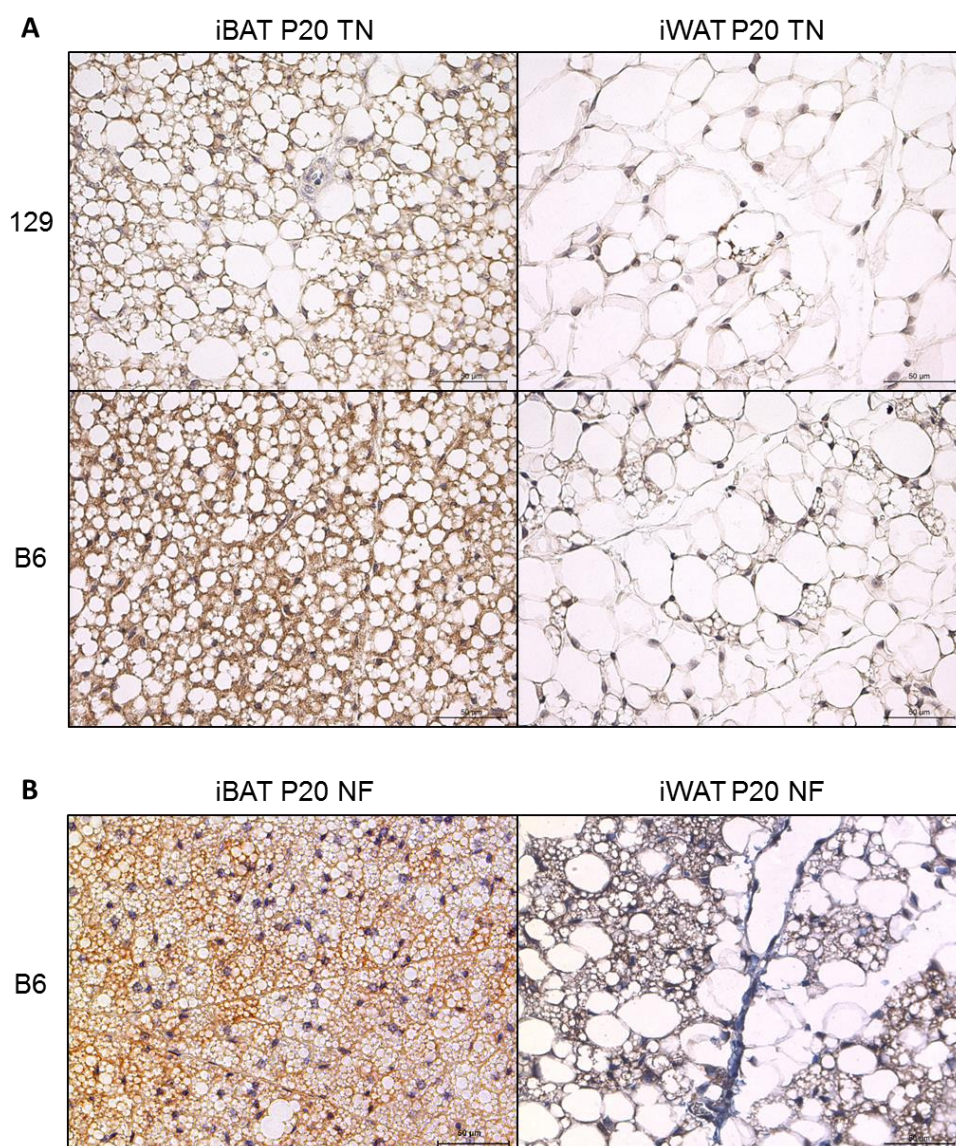


Figure 29 Immunohistochemical detection of UCP1-positive adipocytes in iBAT and iWAT of thermoneutral kept C57BL6/N (B6) and 129S6sv/ev (129) mice.

Morphologic and IHC detection of UCP1-positive multilocular cells in iBAT and iWAT at postnatal day 20, abbreviated P20; nuclei stain hematoxylin. Magnification $\times 40$; Scale bars: 50 μm .

To show whether thermoneutrality affects the browning capability of rWAT, qRT-PCR were performed for the brown fat markers UCP1 and CIDEA in both strains at P20. The abundance of UCP1 and CIDEA in thermal neutral kept C57BL6/N and 129S6sv/ev was significantly decreased compared to normal fostered animals. This reduction is much more pronounced in 129S6sv/ev (Fig. 30).

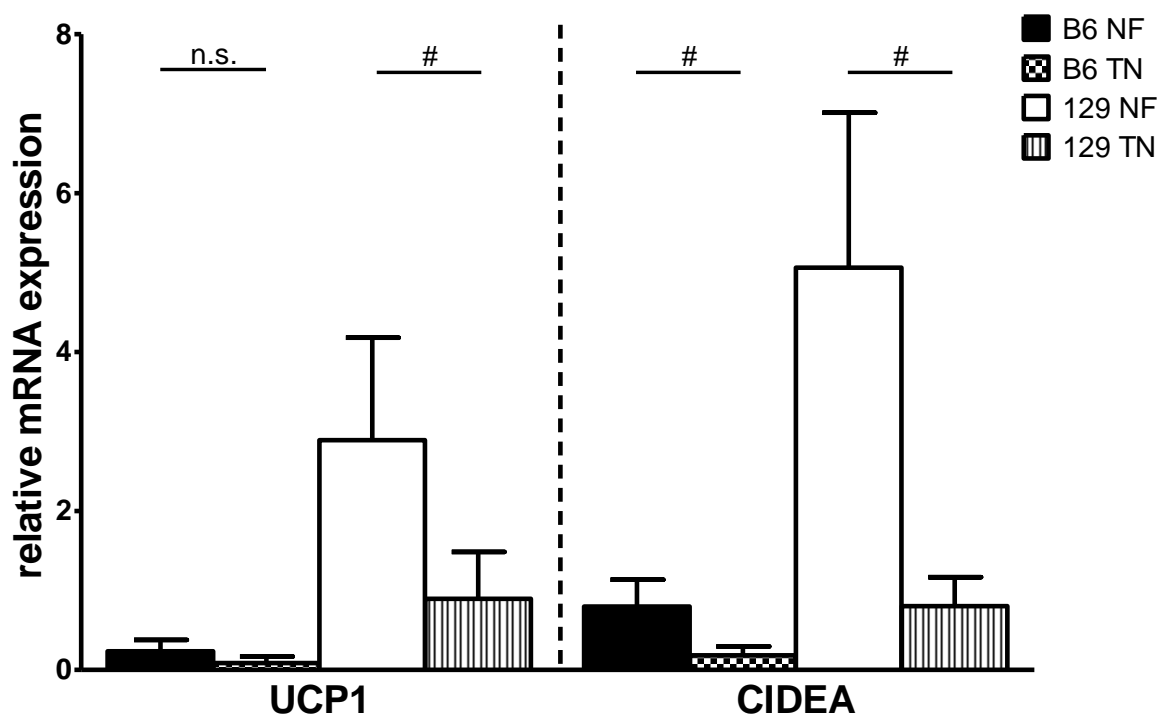


Figure 30 Expression of brown adipocyte marker genes in postnatal retroperitoneal white adipose tissue (rWAT) of thermal neutral kept C57BL6/N (B6) and 129S6sv/ev (129) mice.

Shown is the transcript abundance of UCP1 and CIDEA of B6 and 129 normalized to GUSB in rWAT at P20. Bars depict mean values \pm SD of $n = 7-8$ individual samples per group. Statistical significant differences were analyzed by two-way-ANOVA, # illustrates a significant strain difference, $p \leq 0.05$;

Taken together body mass and body composition of mice kept in thermoneutrality show higher fat pad masses compared to normal fostered animals. However these mice have higher masses in eWAT, iWAT and rWAT, the overall development is similar to normal fostered animals. Compared to normal fostered mice iBAT mass is increased. Immunohistochemistry showed larger lipid droplets, the result of an increased lipid accumulation within the cells leading to a higher tissue mass. Gene expression data of rWAT demonstrate a decrease of brown adipocyte marker genes at P20 in both strains compared to normal fostered animals. Possibly, the reduction in brown adipocyte marker gene expression leads to a lower browning in white adipose tissue kept in thermoneutrality.

3.4 Epigenetic modifications are transiently reduced upon britening of white adipose tissue

Cross fostering and thermoneutrality affects the postnatal britening of C57BL6/N and 129S6sv/ev. Cross fostering leads to a higher fat pad mass in C57BL6/N compared to 129S6sv/ev and normal fostered mice and reduces britening in rWAT and iWAT in both strains. Thermoneutrality increase adipose tissue growth in both strains compared to normal fostered mice. Additionally, immunohistochemistry and mRNA abundance of brown adipocyte marker genes show a lowered britening in rWAT at P20 in both strains. Both, cross-fostering and thermoneutrality aimed to investigate a maternal influence on the strain difference in postnatal britening. However, these experiments displayed a diminished strain difference. Possibly, environmental conditions can influence gene expression by methylation or demethylation of gene regulatory sequences. To investigate whether the Ucp1 enhancer in principle is subject to this kind of mechanism, a methylation analysis on the UCP1 enhancer region was performed on rWAT and iBAT of C57BL6/N and 129S6sv/ev mice at postnatal day 10, 20 and 30. This region contains six CpG sites that can be encompassed by two Methylation sensitive high resolution melting primer pairs. The amplicon of primer pair 1 (PP1) includes the first four and the primer pair 2 (PP2) the last two CpG sites. An additional genome analysis of both strains of this region revealed a single-nucleotide polymorphisms (SNPs) annotated as rs8236746. This SNP rs8236746 is a cytosine in 129S6sv/ev and an adenosine in C57BL6/N. Therefore, it generates a new CpG site in 129S6sv/ev (Fig. 31).

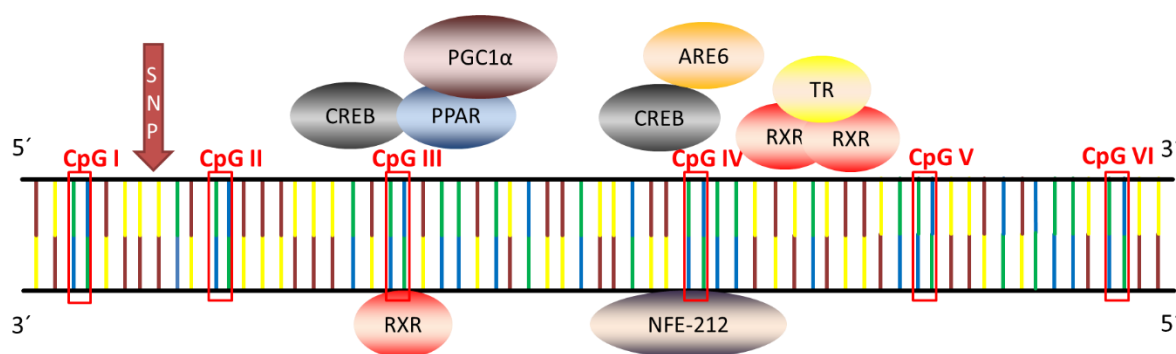


Figure 31 Schematic representation of the UCP1 enhancer region and its putative binding factors.

Shown is a scheme of an approximately 390 bp long UCP1 enhancer region on DNA level (colored). Six CpG sites located within this region are marked CpG I – VI and transcription factors that have been previously described binding this region: cAMP response element-binding protein (CREB), peroxisome proliferator-activated receptor (PPAR), Peroxisome proliferator-activated receptor gamma coactivator 1-alpha (PGC-1α), retinoic acid (RA), retinoid X receptor (RXR), thyroid hormone receptor (TR), brown fat response element (BRE) and nuclear factor erythroid derived 212 (NFE-212). The SNPs rs8236746 is marked by a red arrow. 5' and 3' are showing DNA orientation.

In rWAT, the overall methylation from CpG I to VI in both strains of the UCP1 enhancer region at each time point show a “U” shape with a minimal methylation at CpG II and III (Fig. 32). A

lower methylation rate at a CpG site in an enhancer region increases the possibility of transcription factor binding that leads to a higher gene expression.

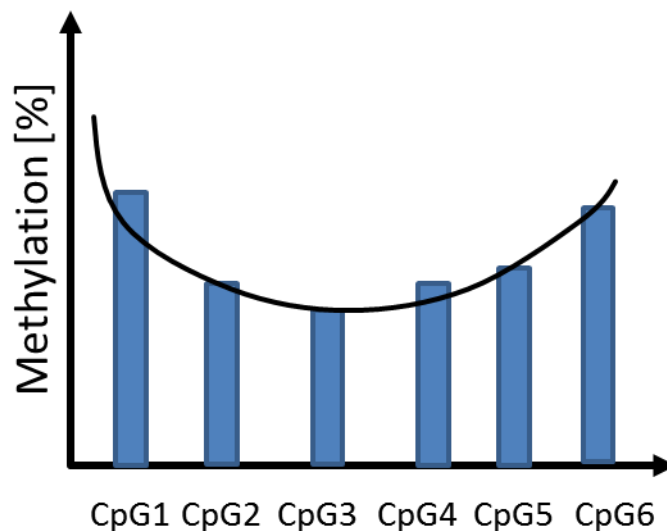


Figure 32 Schematic representation of a “U”-shaped methylation pattern

Within each CpG site a transient reduction of methylation from P10 to P30 can be observed with its minimum at P20 including the 129S6sv/ev SNP region (Fig. 33 A). Statistics like two way ANOVA of individual CpG sites did not clearly show a strain difference. At P20 both strains reach similar levels of methylation. However, it seems that the transiently lower methylation is more pronounced in 129S6sv/ev compared to C57BL6/N. To emphasize this difference, the methylation at P20 and P30 were normalized to P10 in each strain at each CpG site excluding the strain specific SNP in 129S6sv/ev. In rWAT, a lower decrease from P10 to P20 in 129S6sv/ev could be observed reaching significance in CpG II, V and VI compared to C57BL6/N (Fig. 33 B). In iBAT, the overall methylation in both strains displayed a similar “U” shape as observed in rWAT with subtly increased methylation rates in 129S6sv/ev. Nevertheless, a transient methylation from P10 to P30 within each CpG site could not be observed either in the mean of methylation or by a normalization (Fig. 33 C & D).

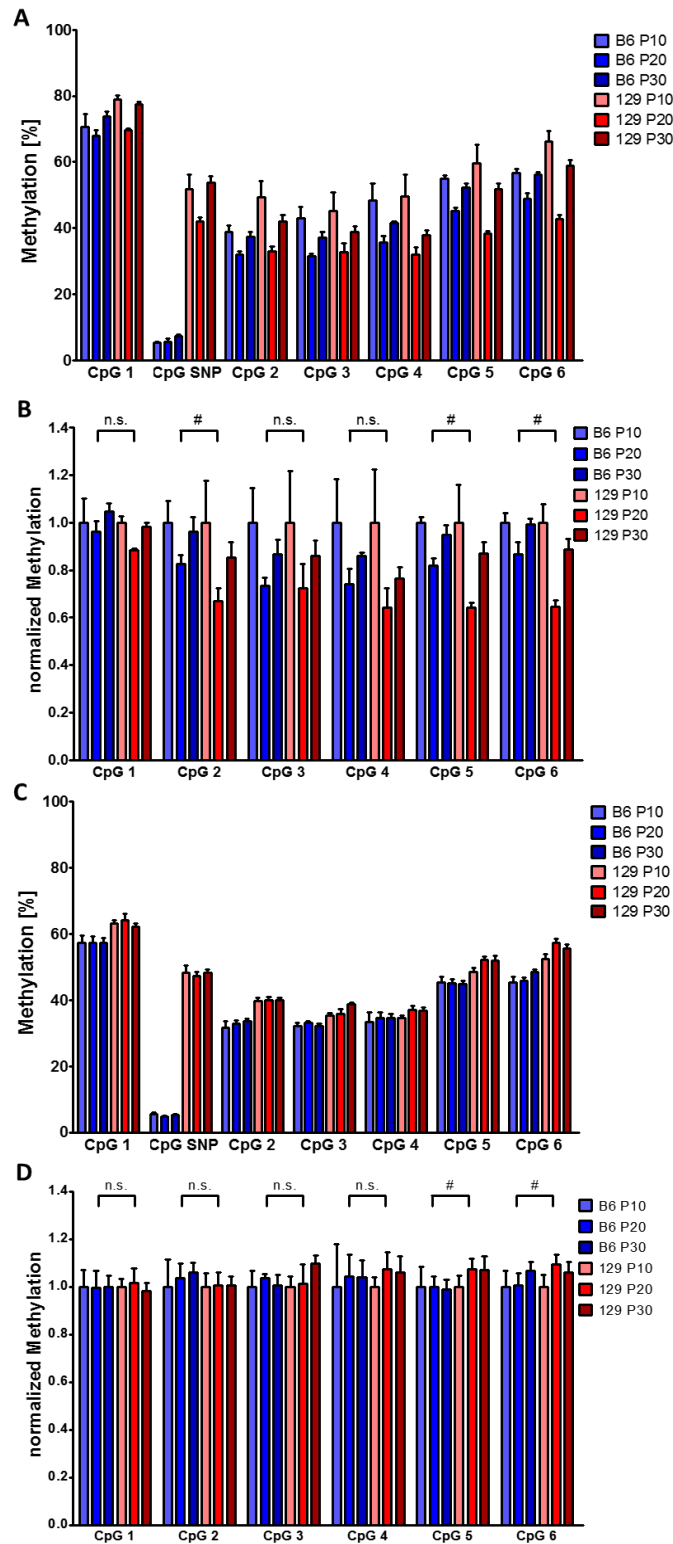


Figure 33 Methylation of the UCP1 enhancer region in postnatal retroperitoneal white adipose tissue (rWAT) and interscapular brown adipose tissue (iBAT) of C57BL6/N (B6) and 129S6sv/ev (129) mice.

Shown is the percentage methylation of rWAT (A) and iBAT (C) and the normalized methylation of rWAT (B) and iBAT (D). Normalization was performed to the mean value of P10 in each strain. Bars depict mean values \pm SD of $n=3$ for rWAT & $n=4$ for iBAT. Statistical significant differences at P20 were analyzed by a student T-test, # illustrates a significant strain difference, $p \leq 0.05$.

Taken together, the overall methylation rate between the CpG sites varies with a minimum at CpG II and III. In rWAT the specific transient reduction correlates with the transient browning, like the unchanged methylation pattern in iBAT correlates with the continuous UCP1 expression. However the reduction within the CpG sites is stronger in 129S6sv/ev compared to C57BL6/N that correlates with an increased UCP1 expression.

3.5 Next Generation Sequencing based transcriptome analysis reveals putative genes involved in white fat britening

While britening in white fat occurs, the methylation of the UCP1 enhancer region in rWAT is transiently reduced with a minimum at P20. This reduction negatively correlates with the transient UCP1 expression. The cross-foster experiment displayed a maternal influence upon white adipose tissue britening. Possibly, both maternal influence and a genetic predisposition influence britening of white adipose tissue. Analyzing which genes may correlate with postnatal britening of white adipose tissue a next generation sequencing (NGS) based transcriptome analysis of retroperitoneal adipose tissue of C57BL6/N and 129S6sv/ev mice at postnatal day P10, P20 and P30 were performed. Candidates for a correlation analysis were selected and sorted as described in 2.3.5. The UCP1 expression in C57BL6/N did not correlate with the transient britening phenomenon, because of an outlier. However excluding the outlier, normalized UCP1 expression displayed a transient expression in the NGS based transcriptome analysis (Fig. 34).

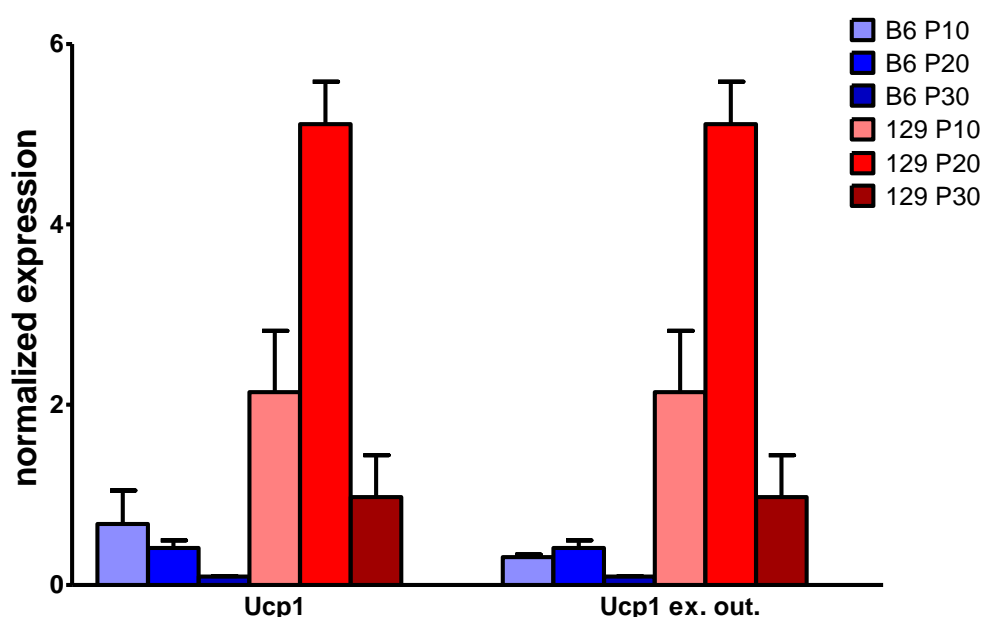


Figure 34 Normalized expression of UCP1 in postnatal retroperitoneal white adipose tissue (rWAT) of C57BL6/N (B6) and 129S6sv/ev (129) mice.

Shown is the normalized expression of the NGS based transcriptome analysis of UCP1 including and excluding an outlier (UCP1 ex. Out.) of retroperitoneal adipose tissue. Bars depict mean value \pm SD of $n = 3$ including the outlier and $n = 2$ excluding the outlier individual samples per group.

For further analysis the outlier was not excluded. Nevertheless the used reference genes UCP1, CIDEA, FABP3, COX7A1 and CPT1B correlate with the transient postnatal britening in rWAT of both strains (Fig. 35).

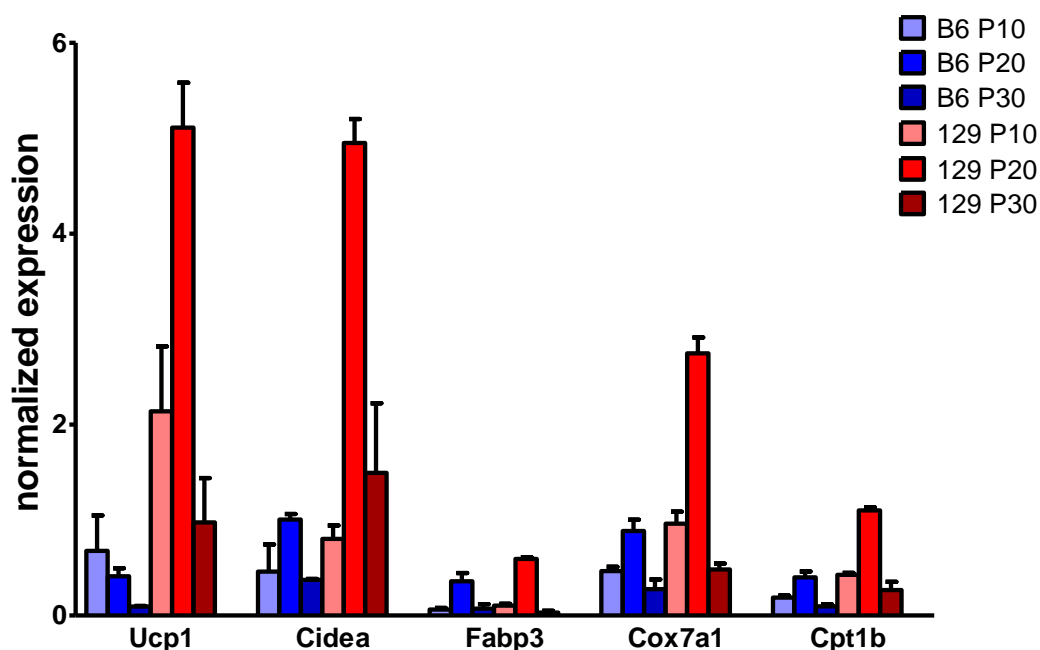


Figure 35 Normalized expression of brown adipocyte marker genes in postnatal retroperitoneal white adipose tissue (rWAT) of C57BL6/N (B6) and 129S6sv/ev (129) mice.

Shown is the normalized expression of the NGS based transcriptome analysis of reference genes of retroperitoneal white adipose tissue. Bars depict mean values \pm SD of $n = 3$ individual samples per group.

These genes were significantly higher expressed at P20 in 129S6sv/ev compared to C57BL6/N except for Fabp3 that was higher expressed in 129S6sv/ev but the difference did not reach significance (Tab. 17).

Table 17 List of reference genes correlating to postnatal britening in retroperitoneal white adipose tissue

Mean of correlation (mean cor) and coefficient of variation (CV%) were calculated for individual normalized expression data from P10 to P30 of C57BL6/N and 129S6sv/ev. A strain difference at P20 is analyzed by comparing the respective mean values of both strains. A student t-test illustrates whether a strain difference at P20 is significant.

Symbol	mean cor	CV [%]	129P20>B6P20	B6P20>129P20	Ttest
Ucp1	0.9336	118.61	Yes	No	0.01327
Cidea	0.9173	112.24	Yes	No	0.00286
Fabp3	0.9629	107.93	Yes	No	0.14098
Cox7a1	0.9595	89.60	Yes	No	0.02117
Cpt1b	0.9615	83.31	Yes	No	0.00236

To determine the top 25 candidates, that positively correlated to the selected reference genes and had a high coefficient of variation from P10 to P30 the list was arranged in descending order by the coefficient of variation (Tab. 18). The coefficient of variation is a measure of distribution within a gene during postnatal development. The higher the coefficient of variation, the higher was the regulation within this gene. The resulting table after sorting displayed several genes, including the five marker genes.

Table 18 List of candidates with a high coefficient of variation

Mean of correlation (mean cor) and coefficient of variation (CV%) were calculated for individual normalized expression data from P10 to P30 of C57BL6/N and 129S6sv/ev. A strain difference at P20 is analyzed by comparing the respective mean values of both strains. A student t-test illustrates whether a strain difference at P20 is significant.

Symbol	mean cor	CV [%]	129P20>B6P20	B6P20>129P20	Ttest
Mrgprg	0.8056	162.16	No	Yes	0.13239
Inmt	0.8241	153.44	No	Yes	0.05950
Gm10032	0.8692	144.19	Yes	No	0.08004
Kng2	0.9500	134.77	Yes	No	0.00148
Tmem82	0.7729	123.21	No	Yes	0.11378
Slc25a34	0.7829	120.46	No	Yes	0.09853
Ucp1	0.9336	118.61	Yes	No	0.01327
Agt	0.7515	116.61	No	Yes	0.04151
Cidea	0.9173	112.24	Yes	No	0.00286
Acsm3	0.7877	109.09	Yes	No	0.08715
Fabp3	0.9629	107.93	Yes	No	0.14098
Cpn2	0.9256	97.77	Yes	No	0.02364
Gm11827	0.8651	92.44	No	Yes	0.18728
Rgs2	0.7726	91.78	No	Yes	0.00422
Igfbp3	0.8926	91.50	No	Yes	0.37679
Pnpla3	0.7805	90.36	Yes	No	0.01464
Cldn22	0.8317	89.69	No	Yes	0.31986
Cox7a1	0.9595	89.60	Yes	No	0.02117
Atp5j2	0.8465	88.99	Yes	No	0.09325
Trp53inp1	0.8510	87.81	No	Yes	0.15538
Gpx3	0.8629	86.86	No	Yes	0.00277
Acot11	0.8123	85.89	Yes	No	0.02253
Cpt1b	0.9615	83.31	Yes	No	0.00236
Prodh	0.8297	80.15	No	Yes	0.86559
Adssl1	0.7801	79.76	No	Yes	0.30046

Interestingly this table contained genes that showed a higher coefficient of variation compared to the selected reference genes. However this list showed a heterogeneous pattern when comparing the mean expression of both strains at P20. On the one hand, genes were represented that had a significantly higher expression at P20 in 129S6sv/ev compared to C57BL6/N and *vice versa*. Representative genes for those categories are Kng2 and Rgs2. While Kng2 was significantly higher expressed in 129S6sv/ev compared to C57BL6/N, Rgs2 was significantly higher expressed in C57BL6/N. On the other hand, genes were represented that are not significantly higher expressed at P20 in one of those strains. A representative gene was Prodh that showed a similar expression in both strains (Fig. 36).

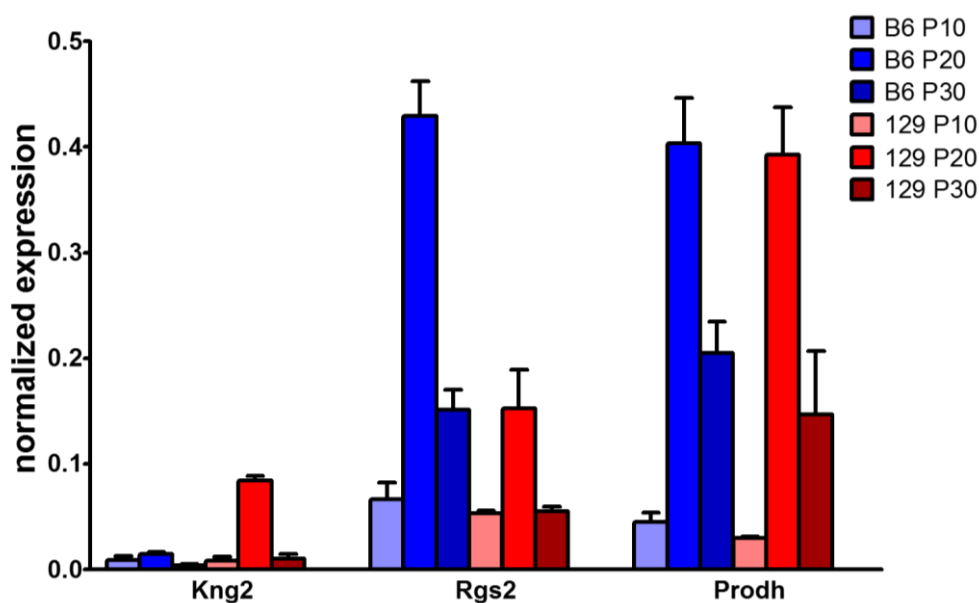


Figure 36 Normalized expression of candidate genes in postnatal retroperitoneal white adipose tissue (rWAT) of C57BL6/N (B6) and 129S6sv/ev (129) mice.

Shown is the normalized expression of the NGS based transcriptome analysis of reference genes of retroperitoneal white adipose tissue. Bars depict mean values \pm SD of $n = 3$ individual samples per group.

Mice of the 129S6sv/ev strain showed higher britening in rWAT compared to C57BL6/N. Possibly, genes that are higher expressed in 129S6sv/ev are associated with britening or enhance britening and represent possible brite marker. The other way around, genes that are higher expressed in C57BL6/N, are possibly associated with inhibiting britening of white adipose tissue. Investigating which transcripts are higher expressed in 129S6sv/ev or C57BL6/N, the transcripts were sorted by comparing the mean of normalized expression at P20 in both strains. For both strains the resulting genes were arranged in descending order by the coefficient of variation (Tab. 19 & 20).

Table 19 List of candidates with a higher mean at P20 in 129S6sv/ev

Mean of correlation (mean cor) and coefficient of variation (CV%) were calculated for individual normalized expression data from P10 to P30 of C57BL6/N and 129S6sv/ev. A strain difference at P20 is analyzed by comparing the respective mean values of both strains. A student t-test illustrates whether a strain difference at P20 is significant.

Symbol	mean cor	CV [%]	129P20>B6P20	B6P20>129P20	Ttest
Gm10032	0.8692	144.19	Yes	No	0.08004
Kng2	0.9500	134.77	Yes	No	0.00148
Ucp1	0.9336	118.61	Yes	No	0.01327
Cidea	0.9173	112.24	Yes	No	0.00286
Acsm3	0.7877	109.09	Yes	No	0.08715
Fabp3	0.9629	107.93	Yes	No	0.14098
Cpn2	0.9256	97.77	Yes	No	0.02364
Pnpla3	0.7805	90.36	Yes	No	0.01464
Cox7a1	0.9595	89.60	Yes	No	0.02117
Atp5j2	0.8465	88.99	Yes	No	0.09325
Acot11	0.8123	85.89	Yes	No	0.02253
Cpt1b	0.9615	83.31	Yes	No	0.00236
Mreg	0.9062	78.19	Yes	No	0.01834
Zbtb16	0.8078	77.91	Yes	No	0.98839
Plin5	0.8354	77.63	Yes	No	0.00764
Impdh1	0.8210	77.14	Yes	No	0.08944
Myo5c	0.9471	76.70	Yes	No	0.03810
2310042D19Rik	0.8706	76.45	Yes	No	0.61422
COX3	0.8343	74.44	Yes	No	0.00835
Cox8b	0.9533	71.77	Yes	No	0.04835

Table 20 List of candidates with a higher mean at P20 in C57BL6/N

Mean of correlation (mean cor) and coefficient of variation (CV%) were calculated for individual normalized expression data from P10 to P30 of C57BL6/N and 129S6sv/ev. A strain difference at P20 is analyzed by comparing the respective mean values of both strains. A student t-test illustrates whether a strain difference at P20 is significant.

Symbol	mean cor	CV [%]	129P20>B6P20	B6P20>129P20	Ttest
Mrgprg	0.8056	162.16	No	Yes	0.13239
Inmt	0.8241	153.44	No	Yes	0.05950
Tmem82	0.7729	123.21	No	Yes	0.11378
Slc25a34	0.7829	120.46	No	Yes	0.09853
Agt	0.7515	116.61	No	Yes	0.04151
Gm11827	0.8651	92.44	No	Yes	0.18728
Rgs2	0.7726	91.78	No	Yes	0.00422
Igfbp3	0.8926	91.50	No	Yes	0.37679
Cldn22	0.8317	89.69	No	Yes	0.31986
Trp53inp1	0.8510	87.81	No	Yes	0.15538
Gpx3	0.8629	86.86	No	Yes	0.00277
Prodh	0.8297	80.15	No	Yes	0.86559
Adssl1	0.7801	79.76	No	Yes	0.30046
1700023B13Rik	0.8980	78.20	No	Yes	0.25945
Cdkn1a	0.9060	76.56	No	Yes	0.75568
Aldh3b2	0.8203	75.11	No	Yes	0.05505
Gadd45g	0.8141	74.85	No	Yes	0.13101
Pon1	0.8087	74.48	No	Yes	0.16238
Hif3a	0.8001	73.19	No	Yes	0.58168
Pdk4	0.8577	72.79	No	Yes	0.27588

Similar to the methylation analysis of the UCP1 enhancer region, genes in the NGS based transcriptome analysis showed a transient negative correlation upon the selected marker genes. Possibly, these genes sustain the white adipocyte character of brite adipocytes until they are stimulated and the expression of these genes is reduced during briteing. To illustrate transiently negative correlating genes from P10 to P30, the list was sorted in descending order to the coefficient of variation (Tab. 21). Similar to the list of positively correlating genes, this list showed a heterogeneous pattern. On the one hand, genes were represented that had a significantly higher expression at P20 in 129S6sv/ev compared to C57BL6/N and *vice versa*. Representative genes for those categories are Gpr81 and Rasd1. While Rasd1 was significantly higher expressed in 129S6sv/ev compared to C57BL6/N, Gpr81 was significantly higher expressed in C57BL6/N. On the other hand, genes were represented that are not significantly higher expressed at P20 in one of those strains. A representative gene was Inhbb that showed a similar expression in both strains (Fig. 37).

Table 21 List of candidates with negative correlation sorted by the coefficient of variation

Mean of correlation (mean cor) and coefficient of variation (CV%) were calculated for individual normalized expression data from P10 to P30 of C57BL6/N and 129S6sv/ev. A strain difference at P20 is analyzed by comparing the respective mean values of both strains. A student t-test illustrates whether a strain difference at P20 is significant.

Symbol	mean cor	CV [%]	129P20>B6P20	B6P20>129P20	Ttest
Pth1r	-0.8634	78.35	No	Yes	0.00367
Oscp1	-0.7901	75.98	No	Yes	0.12256
Ephb2	-0.7906	61.17	Yes	No	0.32596
Ffar2	-0.8760	59.21	No	Yes	0.16765
Hmgcs1	-0.7587	58.15	Yes	No	0.04377
Siglec1	-0.8705	57.54	No	Yes	0.01139
Adamts16	-0.7739	56.74	Yes	No	0.77079
Lgals3bp	-0.8318	56.08	No	Yes	0.19196
Unc119	-0.8368	53.11	Yes	No	0.08910
Chsy1	-0.7937	50.93	Yes	No	0.67897
Zwilch	-0.7922	50.58	No	Yes	0.02108
Tshr	-0.8544	49.44	No	Yes	0.03749
Rasd1	-0.8252	49.27	Yes	No	0.00005
Morc4	-0.7596	48.62	Yes	No	0.16097
Ccne1	-0.7748	47.68	No	Yes	0.05822
Fblim1	-0.7627	47.36	No	Yes	0.01397
Inhbb	-0.8005	46.73	No	Yes	0.91425
Ly6h	-0.8042	46.24	No	Yes	0.08905
Niacr1	-0.8677	45.90	No	Yes	0.01531
Tmem120a	-0.8950	45.41	Yes	No	0.36790
Lpgat1	-0.7686	44.53	Yes	No	0.04343
Kcne4	-0.7545	43.15	No	Yes	0.00570
Tspan18	-0.8646	41.34	Yes	No	0.01518
Rcor2	-0.7762	40.96	Yes	No	0.38233
Palm2	-0.7650	40.62	Yes	No	0.13851
Rab32	-0.8495	38.91	Yes	No	0.00670
Lcorl	-0.7599	38.48	No	Yes	0.14068
Arap2	-0.7597	38.06	Yes	No	0.62044
Odz4	-0.7860	37.79	Yes	No	0.82369
Gpr81	-0.9294	36.99	No	Yes	0.02959

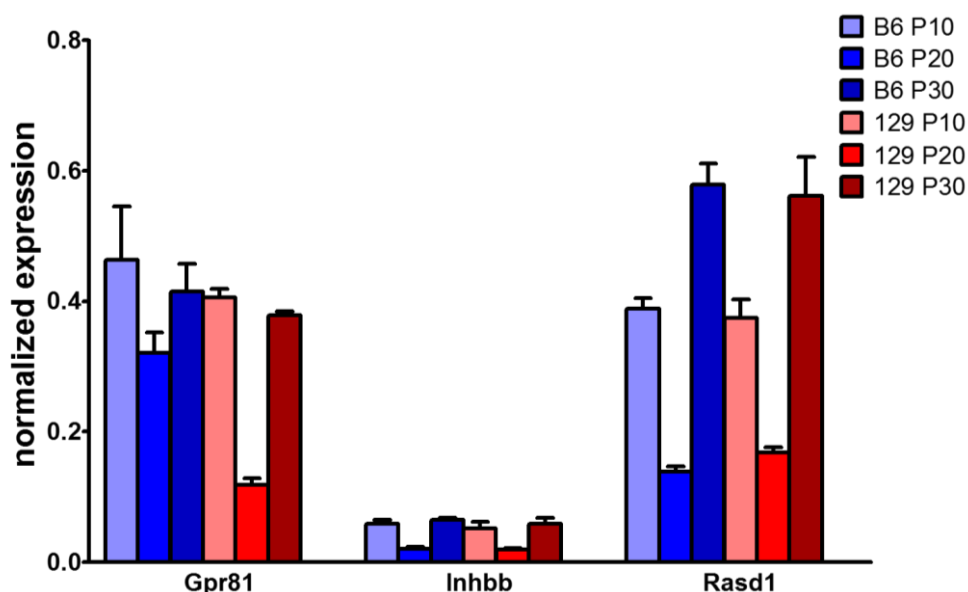


Figure 37 Normalized expression of negatively correlating candidate genes in postnatal retroperitoneal white adipose tissue (rWAT) of C57BL6/N (B6) and 129S6sv/ev (129) mice.

Shown is the normalized expression of the NGS based transcriptome analysis of reference genes of retroperitoneal white adipose tissue. Bars depict mean values \pm SD of $n = 3$ individual samples per group.

Taken together, the NGS based transcriptome analysis of retroperitoneal white adipose tissue of C57BL6/N and 129S6sv/ev mice during postnatal development showed several candidates that are positively or negatively correlated with the transient browning. However, positive and negative correlated transcripts showed a transient expression pattern with a maximum or minimum at P20. By comparing the gene expression at P20 between both strains, transcripts could be observed that were higher expressed in mice of the C57BL6/N strains and lower in mice of the 129S6sv/ev strain. Mice of the 129S6sv/ev strain showed a higher browning potential in white adipose tissue at P20 compared to C57BL6/N mice. Presumably, this correlation to brown adipose tissue markers revealed new genes that are involved in browning as well. However positive correlated genes that are higher expressed in C57BL6/N mice, represented genes that possibly inhibit browning. Negative correlated genes that had a lower expression at P20 in 129S6sv/ev mice possibly sustain the white adipocyte character of brite adipocytes. Presumably, during stimulation the expression of these genes was diminished to enable browning in retroperitoneal white adipose tissue.

4 Discussion

This investigation comparing C57BL6/N and 129S6sv/ev mice during postnatal development was initiated to understand whether postnatal briteening is connected to changes in fat and body mass. The aim of this project is to utilize the transition of postnatal briteening as a model to study its mechanisms, functions and impact on fat pad development. Here it is hypothesized that maternal behavior or a genetic predisposition affect the emergence of brite adipocytes in both strains during postnatal development.

C57BL6/N and 129S6sv/ev are inbred mouse strains with different origin. C57BL6/N were developed 1921 by C.C. Little in the Charles River Laboratory's from a mating of Abby Lathrop's stock (Silver, 1995). 129S6sv/ev mice were developed by Dr. Martin Evan in 1992 from Dunn's stock 1928 and were sent from GenPharm International to Taconic (Silver, 1995). Progenitors of 129S6sv/ev were used to establish embryonic stem cell lines for various knockout mutations. Both strains are phenotypically different. While C57BL6/N is often used as a model for diet-induced obesity, 129S6sv/ev shows a resistant to a high fat challenge (Almind and Kahn, 2004).

This study validates previous known studies performed by Xue et al. 2007 and expands the findings by showing new details in the postnatal development of white, brown and brite fat of different strains under certain conditions. In the relevant traits the strains C57BL6/N and 129S6sv/ev do not largely differ: pups of both strains are first completely covered by fur at day 8 and first leave the warm nest to explore their environment around day 12. Between day 12 and 20 pups from both strains begin to steady replace suckled milk by eating regular chow diet. The typical weaning date, at which young mice are assumed to be completely self-reliant, is at postnatal day 21 in all used strains. On the genetic level those two strains largely differ. A genome wide single nucleotide polymorphism scan of 102 *Mus musculus* strains categorizes them into seven clusters of genetic similarities, whereas C57BL6/N and 129S6sv/ev are part of different clusters (Petkov et al., 2004). The clusters of 129S6sv/ev and C57BL6/N differ in over 4.58 million SNP's with 886136 insertions and deletions those result in approximately 29153 structural variants (Keane et al., 2011).

The present study illustrates differences in the postnatal development of body mass and fat mass in pups of C57BL6/N and 129S6sv/ev. Both strains rapidly increase body mass from

postnatal day 20 to 30 (P20 and P30), known as pubertal growth spurt. While body mass at postnatal day 10 (P10) and P20 show no difference in both strains, body composition already differs with a reduced fat development in C57BL6/N compared to 129S6sv/ev (Fig. 7 B). While lean mass is increased in C57BL6/N at P20 and P30 fat mass is reduced compared to 129S6sv/ev (Fig. 7). However in both strains lean mass is proportionally increasing with the individual body mass. For fat mass development in both strains a proportional growth from P10 to P30 could not be observed. Also on the level of individual fat pad weights 129S6sv/ev mice displayed an increased mass gain in eWAT, iWAT and rWAT compared to C57BL6/N at P20 and P30, while in iBAT subtle differences were visible (Fig. 9). To determine if the lack of proportionality in fat mass is the result of disproportionality in fat pad development, the individual fat pad masses were correlated against the individual body mass. Epididymal white adipose tissue mass was proportionally increasing with body mass at all three measured time points. That was not the case for iWAT and rWAT. Both fat pads were proportional to body mass at each separate time point, the gain of body mass from P10 to P20 was not reflected in higher fat pad masses. It seems that the gain of fat mass in these tissues is attenuated between P10 and P20. In this study the growth attenuation of iWAT and rWAT is described for the first time. Possibly, this growth attenuation in these adipose tissues is the reason of britening.

The rWAT depot of C57BL6/J and A/J mice endured drastic morphological changes during postnatal development (Xue et al., 2007). A transient appearance of multilocular adipocytes with a maximum at P20 is described. The current study replicated this phenomenon in C57BL6/N and 129S6sv/ev mice and showed additionally a similar pattern in iWAT. The morphologic transition from an unilocular appearance to a multilocular was accompanied by a simultaneous attenuation in body mass specific fat pad mass growth (Fig. 10). Histology and gene expression revealed a stronger britening of white adipose tissue during the postnatal development of 129S6sv/ev mice as compared to C57BL6/N. It is hypothesized that the reduction of white fat britening at P30 is diluted by increased adipogenesis. Histology revealed the multilocular islet formation in both strains from P10 to P20. Especially immunohistochemistry showed UCP1 expressing adipocytes forming islets within the respective white adipose tissue at P20. These islet of brite adipocytes could not be observed in rWAT at P30. Additionally iWAT displayed islet formation at P30 but the cells had larger lipid droplets and the majority of UCP1 cells resembled an unilocular appearance (Fig. 12). Using transgenic mice that express a fusion protein of diphtheria toxin receptor and GFP under the

control of the UCP1 promoter, histological slides emphasize the islet formation upon postnatal briteing (Fig. 13). Therefore, a dilution effect at P30 could not be observed, but these data show a cellular plasticity resulting in a transition from a white to a brown like adipocyte and *vice versa*. Possibly, the amount of UCP1 per cell may differ in brite adipocytes of C57BL6/N and 129S6sv/ev mice. Using immunohistochemistry detection, 3,3'-Diaminobenzidine (DAB) is oxidized by the horseradish peroxidase coupled to the secondary antibody and produce a brown staining. The oxidation of DAB on the sections was stopped by water at the same time. An increased UCP1 amount per cell would result in a stronger colorization. However, both strains displayed the same brown intensity after DAB treatment. Therefore, brite adipocytes of both strains had similar amounts of UCP1.

Compared to C57BL6/N, mice from the 129S6sv/ev strain had a stronger briteing capability at P20. To determine if other strains also display a different briteing potential at P20, the fat pad development and brown fat specific gene expression like UCP1 and CIDEA were measured in AKR/J and SWR/J. These strains are known for their different propensity towards diet induced diabetes. Mice from the strain AKR/J are prone to diet induced obesity. Contrary SWR/J are called resistant. However, AKR/J mice had a similarly reduced fat pad development compared to C57BL6/N mice at P20. Also UCP1 and CIDEA gene abundance were at the similar low level. SWR/J mice resemble 129S6sv/ev and showed an elevated fat pad mass development at P20, while UCP1 expression was similar to 129S6sv/ev. CIDEA abundance was lower than 129S6sv/ev but still higher compared to C57BL6/N or AKR/J. This implicates a strong briteing potential during postnatal development that correlates to a diet induced obesity resistance in adulthood. However, the use of other strains illustrated that the postnatal development and the transient briteing are strain related. Because of the similarity of the four strains correlating to the development of diet induced obesity during adulthood, the strains C57BL6/N and 129S6sv/ev were mainly used for experiments.

Undoubtedly, brown adipose tissue maintains normothermia in a cold environment by providing non-shivering thermogenesis (NST). The same function is assumed for brite adipocytes. A study of isolated mitochondria of iWAT from cold exposed mice show that an increase of UCP1 abundance correlates to a higher thermogenic functionality by exhibiting an UCP1 dependent thermogenesis (Shabalina et al., 2013). Beyond question the occurrence of brite adipocytes in white fat is promoted by cold stimulation (Young et al., 1984). Brite cell

appearance in adult mice is reversed within a few weeks of warm adaptation. However, cold recruited brite adipocytes convert into cells similar to white adipocytes after warm acclimatization. Exactly these cells can reconvert to a brown adipocyte like morphology after an additional cold stimulation (Rosenwald et al., 2013). In the postnatal britening model, the first appearance of brite adipocytes in white adipose tissue might resemble a brite cell anlage. This anlage might determine the britening capacity of white adipose tissues in adulthood. The direct comparison of body and fat mass development with brite cell recruitment in the two mouse strains revealed a remarkable coincidence. Many published studies report an association of an increased brite cell number with a resistance to diet induced obesity, increased metabolic rate and decreased fat and body mass (Almind and Kahn, 2004; Almind et al., 2007; Bostrom et al., 2012; Coulter et al., 2003; Guerra et al., 1998; Kopecky et al., 1995). Nevertheless during postnatal development 129S6sv/ev obtain a higher fat mass than C57BL6/N when comparing weight matched mice of both strains, especially in tissues where brite cells occur, like rWAT and iWAT. This natural occurrence of postnatal britening illustrates an association of an elevated brite cell number with a higher fat mass and is an example for an increased brite cell occurrence that is not connected to fat and body mass loss.

Possibly, postnatal treatment of the offspring influences britening and its adaption in regard to adulthood. In humans, several studies aim to manipulate fat mass in early development to prevent diet induced obesity in adulthood (Ekelund et al., 2006; Karaolis-Danckert et al., 2008; Mundt et al., 2006). This early intervention might also affect the britening capacity, either in mice. In rats, maternal feeding dependent on fat and fat species impairs postnatal weight gain and the thermogenic capacity during suckling (Priego et al., 2013). The strain difference in postnatal britening between C57BL6/N and 129S6sv/ev is possibly affected by maternal behavior, like suckling, grooming or by providing a certain thermal microenvironment.

Cross-fostering, i.e. raising pups of one strain by a foster mother of the other strain, allows distinguishing maternal care from inherited effects. It is hypothesized that cross-fostering and thereby the change of maternal care reverse the strain difference, resulting in higher fat pad masses and expression levels of brown adipocyte marker genes in cross-fostered C57BL6/N compared to cross-fostered 129S6sv/ev. Cross-fostered mice did not show any major strain differences in body mass development from P10 to P30, while normal fostered mice do. However, individual fat pad development during postnatal development was affected

compared to normal fostered animals. The prevalent increase of fat mass development from P10 to P20 in 129S6sv/ev compared to C57BL6/N seemed to be reduced during cross-fostering. Cross-fostered C57BL6/N mice displayed a higher fat mass, while cross-fostered 129S6sv/ev mice showed a reduced fat mass (Tab. 15). At P30, cross-fostered 129S6sv/ev mice developed higher eWAT and iWAT masses but in a moderate manner compared to normal fostered mice. Nevertheless both strains showed an attenuated fat pad growth from P10 to P20 accompanied by browning of rWAT and iWAT. Especially gene expression data of UCP1, CIDEA and COX7A1 in rWAT and iWAT were strongly affected by cross fostering. In rWAT a transient gene expression with a maximum of the mitochondrial associated genes UCP1 and COX7A1 at P20 was not detectable for both strains. The lipid coating protein CIDEA was not impaired by mitochondrial biogenesis and showed a transient expression from P10 to P30 with its maximum at P20 that was stronger in 129S6sv/ev compared to C57BL6/N. The expression profile in iWAT of both strains did not reflect the strain specific difference at P20. It seems that cross fostering reduce the expression of brown fat markers in iWAT of 129S6sv/ev. C57BL6/N animals seem to be unaffected by this change. The increase of brown adipocyte marker genes at P10 in both cross-fostered strains might be an adaptation towards an early cold stress. After switching the pups from one mother to the other, the foster mother needed a certain time to recollect the new litter.

Surprisingly the UCP1 expression in both tissues at P10 of cross-fostered mice is drastically elevated. This could be a result of switching the pups from one mother to the other. The foster mothers may be distrustful by changing the pups and may leave the nest more often during the first days that would result in a longer exposure of the pups towards a low ambient temperature. However, approximately 30 min after switching the pups and distributing them in the cage independently of strain, the foster mother had collected them and brought them back into the nest. The elevated expression of mitochondrial related genes in 129S6sv/ev at P10 indicates a higher mitochondrial content per tissue. Considering the increase of individual fat pad mass in cross-fostered C57BL6/N compared to normal fostered animals, the expression of brown fat marker genes is unaffected by an increased adipogenesis. Again, this observation does not confirm a possible dilution by an increased white adipocyte number. *Vice versa*, this outcome suggests higher brite cell recruitment in white fat. However the changes of fat pad development as well as gene expression are stronger affected in 129S6sv/ev and show that these mice are more sensitive towards environmental changes compared to C57BL6/N. Still,

it is illusive how the expression at P20 in 129S6sv/ev is reduced comparing to normal fostered animals. Cross-fostering is often used to analyze animal behavior or a possible maternal inheritance of severe syndromes, e.g. alcohol abuse (Bartolomucci et al., 2004; Bohman et al., 1981; Cox et al., 2010; Priebe et al., 2005). However, no studies have directly investigated the effect of cross-fostering on early adipose tissue development. But cross-fostering could not completely explain the strain difference, observed in normal fostered mice. This project describes for the first time a cross-foster effect on postnatal adipose tissue development and the effect of maternal care on postnatal browning at P20.

Possibly, another factor influencing postnatal browning, is the thermal microenvironment provided by the mother. It is stated that lactating mice show a suppressed brown fat thermogenesis (Trayhurn et al., 1982; Trayhurn and Jennings, 1987). A comparison of wild type and *ob/ob* mice illustrates a suppressed brown fat activity within the mother during the physiological hyperphagia of lactation that results in a reduction in energy requirements (Trayhurn and Jennings, 1987). Due to maternal activity the periods of warming the pups may differ between strains, as in C57BL6/N and 129S6sv/ev. It is hypothesized that raising pups at 30 °C reduces browning in both strains. Raising pups in 30 °C largely increases fat mass and individual fat pad mass in both strains compared to animals raised at normal temperature. The higher fat mass and fat pad development in 129S6sv/ev mice compared to C57BL6/N mice raised at normal temperature remains similar to mice raised in 30 °C but with a stronger increase in masses of 129S6sv/ev. Gene expression data at P20 of mice kept in 30 °C show a significant reduction of the brown fat marker UCP1 and CIDEA in both strains. However, the strain difference in gene expression levels at P20 is still higher in 129S6sv/ev compared to C57BL6/N. By diminishing the effect of the thermal microenvironment that is provided by the mother and the reduction of browning emphasizes an inherited strain difference. Probably, a genetic predisposition exists that cannot be influenced by maternal care or thermal environment.

In eukaryotic cells, gene expression is controlled in many ways. An epigenetic tool that is used by eukaryotic cells to regulate gene expression is DNA methylation. It occurs on CpG sites, cytosines followed by a guanine can be methylated to 5-methylcytosine. These methyl-residues block promoters at which activating transcription factors should bind (Bird, 2007). DNA regions that can be methylated show two alternatively stages correlating to their

grade of methylation. A potentially active gene is correlated to low methylation as well as a silent gene is correlated to a high methylation (Eckhardt et al., 2006; Rakyan et al., 2004). However, the grade of methylation that resembles an active gene is still illusive (Suzuki and Bird, 2008). Here it is hypothesized, that methylation is negatively correlated with the transient britening pattern. To illustrate whether inheritance or epigenetic mechanisms caused by a genetic predisposition affect the postnatal development of both strains, a combined methylation sensitive high resolution melting (MS-HRM) and pyrosequencing on the UCP1 enhancer region was performed.

This enhancer region was first described in rats by Cassard-Doulcier A.M. et al. in 1993 (Cassard-Doulcier et al., 1993). This approximately 390 bp long region can also be found in mice 2.8 kbp before the UCP1 transcriptional start site and inherits several cAMP-responsive elements (Kozak et al., 1994). In a previous study, this region was described in which methylation occurs at six CpG sites. This study could not show any differences upon methylation in WAT or BAT by comparing room temperature kept mice with mice kept in a cold environment (Shore et al., 2010).

Here, focusing on the britening during postnatal development shows a transiently reduced methylation of the UCP1 enhancer with a minimum at P20 in all six CpG sites in rWAT of both strains. The reduction in methylation correlates with a higher gene expression of UCP1. Uncontroversial methylation regulates gene activity (Baylin et al., 2001; Furst et al., 2012a; Heller et al., 2013; Tate and Bird, 1993). Methylation in 129S6sv/ev mice was stronger reduced at P20 compared to C57BL6/N. This reduction in 129S6sv/ev correlates to the increased UCP1 expression. The reduced rate of methylation in 129S6sv/ev at P20 implicates a higher activity in this region.

In brown adipose tissue, a change of methylation during postnatal development could not be observed in both strains. Nevertheless iBAT constitutively express UCP1 during postnatal development (Xue et al., 2007). Also western blots of iBAT of both strains from P10 to P30 did not show remarkable differences. Therefore the methylation rate of iBAT seems to be a suitable reference for an active gene expression. Comparing the methylation rate of iBAT with the methylation rate of rWAT at P20, rWAT displayed a similar rate observed in iBAT. However this enhancer region analysis emphasizes that the methylation cannot clearly explain the strain differences. Beyond question multiple genes are involved and necessary for brown

adipocyte formation in white adipose tissue. But this analysis shows that an epigenetic mechanism affect the strain specific difference in briteing.

Next to the brown adipocyte marker genes UCP1, CIDEA and COX7A1, other genes are known that are largely expressed in brown adipocytes, like CPT1b and FABP3 (Britton et al., 1997; Vergnes et al., 2011). A state-of-the-art technology to search for new candidates that might interact with postnatal briteing is the Next Generation Sequencing (NGS) based transcriptome analysis. This technique uses parallel sequencing to allow a genome wide transcriptome analysis. It has a higher resolution compared to microarray-based methods (Nagalakshmi et al., 2010). It is hypothesized that a genome wide transcriptome analysis exhibits new candidates that are involved in briteing and are differentially expressed in both strains. The NGS based transcriptome analysis on postnatal rWAT samples of C57BL6/N and 129S6sv/ev revealed several candidates that are positively or negatively correlating with the brown adipocyte markers UCP1, CIDEA, COX7A1, CPT1b and FABP3. All five reference genes are higher expressed at postnatal day 20 in 129S6sv/ev.

The resulting list after correlating to the reference genes surprisingly consists genes that except few genes like PRODH showed a strain specific expression at postnatal day 20. PRODH is a mitochondrial proline dehydrogenase that displayed a transient expression from P10 to P30 in both strains. It is involved in calcineurin-NFAT signaling, induction of apoptosis and cell cycle regulation and acts in oxygen and ROS metabolism (Depke et al., 2008; Lettieri Barbato et al., 2014; Swindell, 2011). Ablations or mutations in this gene in humans result in a disturbed proline degradation and are associated with hyperprolinemia type 1 (Jacquet et al., 2002). Possibly, this gene is an essential mitochondrial marker that just increase upon mitochondrial biogenesis in both strains at the same extend. However, postnatal briteing is stronger in 129S6sv/ev. By comparing a heterogeneous tissue that displays more brite adipocytes in 129S6sv/ev, implicates a higher mitochondrial content in this strain and should result in an increased PRODH expression compared to C57BL6/N. Presumably, PRODH is a mitochondrial marker that is not directly linked to brite adipocyte metabolism and is therefore not regulated by factors that inhibit brite cell occurrence.

Several genes that are higher expressed in 129S6sv/ev are located in the mitochondria, like COX3, ACSM3 or COX8b. This increased occurrence of mitochondrial associated genes possibly originate from a higher mitochondrial content in 129S6sv/ev compared to C57BL6/N or show

a strain specific mitochondrial function. A higher expression of these genes indicates an enhanced activity of mitochondrial lipid metabolism and the respiratory chain. These functions are also essential for active brown adipose tissue (Cannon and Nedergaard, 2004, 2011; Wang et al., 2003). However, it is illusive whether these genes are simultaneously expressed with mitochondrial biogenesis to maintain mitochondrial function, or whether these genes are selectively expressed to increase a certain mitochondrial function, e.g. thermogenesis.

Genes that are higher expressed in C57BL6/N at P20 may constitute to a negative feedback loop and modulate the browning in white adipose tissue. Such negative feedback loops are known in other tissues, e.g. SOCS3 inhibiting the JAK-STAT pathway after activation by STAT3 in neuronal circuits (Bjorbak et al., 2000). Taking the coefficient of variation into account, genes were identified that had a higher difference from P10 to P30 compared to the reference genes, like *Mrgprg*, *Inmt*, *Gm10032* and *Kng2*. MAS-Related GPR member G (MRGPRG) is an orphan G-protein coupled receptor. A supposed function is the regulation and development of nociception (Vassilatis et al., 2003). Indolethylamine N-Methyltransferase (INMT) is a class 1 transmethylation enzyme. It is known for its production of N,N-dimethyltryptamine, but biological mechanisms remain unknown (Chu et al., 2014). *Gm10032* is a noncoding element on chromosome 14. Its position is approximately 12 kbp after the adrenergic receptor alpha 1a (*ADRAA1*), that is higher expressed in 129S6sv/ev. A direct interaction of these genes has not been shown yet. Kininogens, like kininogen 2 (*KNG2*) is a precursor for kinin. Kininogen can be spliced in high-molecular-weight kininogen (HMWK) or low-molecular-weight kininogen (LMWK). They are associated in the regulation of matrix metalloproteases in vascular smooth muscle cells (Okamoto et al., 1998; Vosgerau et al., 2010; Wang et al., 2010). The function of these genes upon browning is elusive. Studies on monogenetic knockouts in brown and white adipose tissue of these genes would clarify the function of these genes on browning. Nevertheless, this study gives new insights in the natural browning that is not influenced or mediated upon chemical treatments like β_3 -adrenergic agonists.

Mice of the C57BL6/N and 129S6sv/ev strains kept at room temperature show a transient postnatal browning in white adipose tissue depots from P10 to P30. This phenomenon is a natural occurrence that is not induced by additional cold stimulation, application of agents promoting browning like β_3 -agonists or by genetic modifications. Postnatal browning seems to

be a suitable model to analyze white adipocyte occurrence in white adipose tissue. 129S6sv/ev mice show a stronger white cell occurrence accompanied by higher adipose tissue depot masses compared to C57BL6/N mice. Still it is hard to distinguish whether maternal imprinting or a genetic predisposition is the dominant factor modulating the strain difference of postnatal whitening. The cross-fostering experiment shows a maternal influence on postnatal fat pad development. A foster mother of a strain that has lower adipose tissue masses and a reduced white adipocyte occurrence during postnatal development, like C57BL6/N, decreases adipose tissue mass gain and whitening in pups of a strain that shows increased whitening, like 129S6sv/ev. Additionally the thermoneutral experiment shows a necessity of the thermal environment that is needed for postnatal whitening. The adipose tissue development is increased in both strains by possibly reducing the metabolic rate. However, whitening of white adipose tissue is reduced in those strains. Thus whitening is a regulator of energy expenditure during postnatal development. Nevertheless the UCP1 enhancer methylation and especially the NGS based transcriptome analysis show trends towards the hypothesis of a genetic predisposition. In 129S6sv/ev methylation of the UCP1 enhancer region is lower in three of six CpG sites. But it is still unclear which CpG site is important for gene expression. The NGS based transcriptome analysis displayed several genes that are positively correlating with postnatal whitening in both strains. Nevertheless, most of these genes are differentially expressed comparing both strains. It is shown that maternal behavior during development has a strong influence on stress levels of the offspring in later life. This maternal imprinting is a result of lasting epigenetic modifications (De Kloet et al., 1998; Liu et al., 1997; Weaver, 2007; Weaver et al., 2004). Despite the inherent stability of the epigenomic marks, the gene expression can be altered during development and also later in life to potentially reverse these modifications (Weaver et al., 2006). Thus, postnatal whitening is a strain specific phenomenon and underlies a genetic inheritance but it can be modulated by changing the maternal care.

5 References

- Almind, K., and Kahn, C.R. (2004). Genetic determinants of energy expenditure and insulin resistance in diet-induced obesity in mice. *Diabetes* *53*, 3274-3285.
- Almind, K., Manieri, M., Sivitz, W.I., Cinti, S., and Kahn, C.R. (2007). Ectopic brown adipose tissue in muscle provides a mechanism for differences in risk of metabolic syndrome in mice. *Proceedings of the National Academy of Sciences of the United States of America* *104*, 2366-2371.
- Aquila, H., Link, T.A., and Klingenberg, M. (1985). The uncoupling protein from brown fat mitochondria is related to the mitochondrial ADP/ATP carrier. Analysis of sequence homologies and of folding of the protein in the membrane. *The EMBO journal* *4*, 2369-2376.
- Bar-Shalom, R., Gaitini, D., Keidar, Z., and Israel, O. (2004). Non-malignant FDG uptake in infradiaphragmatic adipose tissue: a new site of physiological tracer biodistribution characterised by PET/CT. *European journal of nuclear medicine and molecular imaging* *31*, 1105-1113.
- Barbatelli, G., Murano, I., Madsen, L., Hao, Q., Jimenez, M., Kristiansen, K., Giacobino, J.P., De Matteis, R., and Cinti, S. (2010). The emergence of cold-induced brown adipocytes in mouse white fat depots is determined predominantly by white to brown adipocyte transdifferentiation. *American journal of physiology Endocrinology and metabolism* *298*, E1244-1253.
- Bartolomucci, A., Gioiosa, L., Chirieleison, A., Ceresini, G., Parmigiani, S., and Palanza, P. (2004). Cross fostering in mice: behavioral and physiological carry-over effects in adulthood. *Genes, brain, and behavior* *3*, 115-122.
- Baylin, S.B., Esteller, M., Rountree, M.R., Bachman, K.E., Schuebel, K., and Herman, J.G. (2001). Aberrant patterns of DNA methylation, chromatin formation and gene expression in cancer. *Human molecular genetics* *10*, 687-692.
- Bieber, L.L., Pettersson, B., and Lindberg, O. (1975). Studies on norepinephrine-induced efflux of free fatty acid from hamster brown-adipose-tissue cells. *European journal of biochemistry / FEBS* *58*, 375-381.
- Bird, A. (2007). Perceptions of epigenetics. *Nature* *447*, 396-398.
- Bjorbak, C., Lavery, H.J., Bates, S.H., Olson, R.K., Davis, S.M., Flier, J.S., and Myers, M.G., Jr. (2000). SOCS3 mediates feedback inhibition of the leptin receptor via Tyr985. *The Journal of biological chemistry* *275*, 40649-40657.
- Bohman, M., Sigvardsson, S., and Cloninger, C.R. (1981). Maternal inheritance of alcohol abuse. Cross-fostering analysis of adopted women. *Archives of general psychiatry* *38*, 965-969.
- Borecky, J., Maia, I.G., and Arruda, P. (2001). Mitochondrial uncoupling proteins in mammals and plants. *Bioscience reports* *21*, 201-212.
- Bostrom, P., Wu, J., Jedrychowski, M.P., Korde, A., Ye, L., Lo, J.C., Rasbach, K.A., Bostrom, E.A., Choi, J.H., Long, J.Z., *et al.* (2012). A PGC1-alpha-dependent myokine that drives brown-fat-like development of white fat and thermogenesis. *Nature* *481*, 463-468.
- Bourova, L., Pesanova, Z., Novotny, J., Bengtsson, T., and Svoboda, P. (2000). Differentiation of cultured brown adipocytes is associated with a selective increase in the short variant of g(s)alpha protein. Evidence for higher functional activity of g(s)alphaS. *Molecular and cellular endocrinology* *167*, 23-31.
- Britton, C.H., Mackey, D.W., Esser, V., Foster, D.W., Burns, D.K., Yarnall, D.P., Froguel, P., and McGarry, J.D. (1997). Fine chromosome mapping of the genes for human liver and muscle carnitine palmitoyltransferase I (CPT1A and CPT1B). *Genomics* *40*, 209-211.
- Cannon, B., and Nedergaard, J. (2004). Brown adipose tissue: function and physiological significance. *Physiological reviews* *84*, 277-359.
- Cannon, B., and Nedergaard, J. (2011). Nonshivering thermogenesis and its adequate measurement in metabolic studies. *The Journal of experimental biology* *214*, 242-253.
- Cao, W., Daniel, K.W., Robidoux, J., Puigserver, P., Medvedev, A.V., Bai, X., Floering, L.M., Spiegelman, B.M., and Collins, S. (2004). p38 mitogen-activated protein kinase is the central regulator of cyclic AMP-dependent transcription of the brown fat uncoupling protein 1 gene. *Molecular and cellular biology* *24*, 3057-3067.

- Chaudhry, A., MacKenzie, R.G., Georgic, L.M., and Granneman, J.G. (1994). Differential interaction of beta 1- and beta 3-adrenergic receptors with Gi in rat adipocytes. *Cellular signalling* 6, 457-465.
- Chu, U.B., Vorperian, S.K., Satyshur, K., Eickstaedt, K., Cozzi, N.V., Mavlyutov, T., Hajipour, A.R., and Ruoho, A.E. (2014). Noncompetitive Inhibition of Indolethylamine-N-methyltransferase by N,N-Dimethyltryptamine and N,N-Dimethylaminopropyltryptamine. *Biochemistry*.
- Cohade, C., Osman, M., Pannu, H.K., and Wahl, R.L. (2003). Uptake in supraclavicular area fat ("USA-Fat"): description on 18F-FDG PET/CT. *Journal of nuclear medicine : official publication, Society of Nuclear Medicine* 44, 170-176.
- Coulter, A.A., Bearden, C.M., Liu, X., Koza, R.A., and Kozak, L.P. (2003). Dietary fat interacts with QTLs controlling induction of Pgc-1 alpha and Ucp1 during conversion of white to brown fat. *Physiological genomics* 14, 139-147.
- Cox, K.H., Gatewood, J.D., Howeth, C., and Rissman, E.F. (2010). Gestational exposure to bisphenol A and cross-fostering affect behaviors in juvenile mice. *Hormones and behavior* 58, 754-761.
- Cypess, A.M., Chen, Y.C., Sze, C., Wang, K., English, J., Chan, O., Holman, A.R., Tal, I., Palmer, M.R., Kolodny, G.M., *et al.* (2012). Cold but not sympathomimetics activates human brown adipose tissue in vivo. *Proceedings of the National Academy of Sciences of the United States of America* 109, 10001-10005.
- Cypess, A.M., Lehman, S., Williams, G., Tal, I., Rodman, D., Goldfine, A.B., Kuo, F.C., Palmer, E.L., Tseng, Y.H., Doria, A., *et al.* (2009). Identification and importance of brown adipose tissue in adult humans. *The New England journal of medicine* 360, 1509-1517.
- De Kloet, E.R., Vreugdenhil, E., Oitzl, M.S., and Joels, M. (1998). Brain corticosteroid receptor balance in health and disease. *Endocrine reviews* 19, 269-301.
- Delahaye, F., Lukaszewski, M.A., Watzet, J.S., Cisse, O., Dutriez-Casteloot, I., Fajardy, I., Montel, V., Dickes-Coopman, A., Laborie, C., Lesage, J., *et al.* (2010). Maternal perinatal undernutrition programs a "brown-like" phenotype of gonadal white fat in male rat at weaning. *American journal of physiology Regulatory, integrative and comparative physiology* 299, R101-110.
- Depke, M., Fusch, G., Domanska, G., Geffers, R., Volker, U., Schuett, C., and Kiank, C. (2008). Hypermetabolic syndrome as a consequence of repeated psychological stress in mice. *Endocrinology* 149, 2714-2723.
- Eckhardt, F., Lewin, J., Cortese, R., Rakyan, V.K., Attwood, J., Burger, M., Burton, J., Cox, T.V., Davies, R., Down, T.A., *et al.* (2006). DNA methylation profiling of human chromosomes 6, 20 and 22. *Nature genetics* 38, 1378-1385.
- Ekelund, U., Ong, K., Linne, Y., Neovius, M., Brage, S., Dunger, D.B., Wareham, N.J., and Rossner, S. (2006). Upward weight percentile crossing in infancy and early childhood independently predicts fat mass in young adults: the Stockholm Weight Development Study (SWEDES). *The American journal of clinical nutrition* 83, 324-330.
- Enslin, H., Raingeaud, J., and Davis, R.J. (1998). Selective activation of p38 mitogen-activated protein (MAP) kinase isoforms by the MAP kinase kinases MKK3 and MKK6. *The Journal of biological chemistry* 273, 1741-1748.
- Fleury, C., Neverova, M., Collins, S., Raimbault, S., Champigny, O., Levi-Meyrueis, C., Bouillaud, F., Seldin, M.F., Surwit, R.S., Ricquier, D., *et al.* (1997). Uncoupling protein-2: a novel gene linked to obesity and hyperinsulinemia. *Nature genetics* 15, 269-272.
- Furst, R.W., Kliem, H., Meyer, H.H., and Ulbrich, S.E. (2012a). A differentially methylated single CpG-site is correlated with estrogen receptor alpha transcription. *The Journal of steroid biochemistry and molecular biology* 130, 96-104.
- Furst, R.W., Meyer, H.H., Schweizer, G., and Ulbrich, S.E. (2012b). Is DNA methylation an epigenetic contribution to transcriptional regulation of the bovine endometrium during the estrous cycle and early pregnancy? *Molecular and cellular endocrinology* 348, 67-77.
- Gerhardt, C.C., Gros, J., Strosberg, A.D., and Issad, T. (1999). Stimulation of the extracellular signal-regulated kinase 1/2 pathway by human beta-3 adrenergic receptor: new pharmacological profile and mechanism of activation. *Molecular pharmacology* 55, 255-262.

- Gesta, S., Tseng, Y.H., and Kahn, C.R. (2007). Developmental origin of fat: tracking obesity to its source. *Cell* 131, 242-256.
- Granneman, J.G., Burnazi, M., Zhu, Z., and Schwamb, L.A. (2003). White adipose tissue contributes to UCP1-independent thermogenesis. *American journal of physiology Endocrinology and metabolism* 285, E1230-1236.
- Guerra, C., Koza, R.A., Yamashita, H., Walsh, K., and Kozak, L.P. (1998). Emergence of brown adipocytes in white fat in mice is under genetic control. Effects on body weight and adiposity. *The Journal of clinical investigation* 102, 412-420.
- Hahn, P., and Skala, J. (1972). Changes in interscapular brown adipose tissue of the rat during perinatal and early postnatal development and after cold acclimation. 3. Some cytoplasmic enzymes. *Comparative biochemistry and physiology B, Comparative biochemistry* 41, 147-155.
- Hausman, D.B., DiGirolamo, M., Bartness, T.J., Hausman, G.J., and Martin, R.J. (2001). The biology of white adipocyte proliferation. *Obesity reviews : an official journal of the International Association for the Study of Obesity* 2, 239-254.
- Heaton, G.M., Wagenvoort, R.J., Kemp, A., Jr., and Nicholls, D.G. (1978). Brown-adipose-tissue mitochondria: photoaffinity labelling of the regulatory site of energy dissipation. *European journal of biochemistry / FEBS* 82, 515-521.
- Heller, G., Babinsky, V.N., Ziegler, B., Weinzierl, M., Noll, C., Altenberger, C., Mullauer, L., Dekan, G., Grin, Y., Lang, G., *et al.* (2013). Genome-wide CpG island methylation analyses in non-small cell lung cancer patients. *Carcinogenesis* 34, 513-521.
- Himms-Hagen, J. (1985). Defective brown adipose tissue thermogenesis in obese mice. *International journal of obesity* 9 Suppl 2, 17-24.
- Himms-Hagen, J. (1989). Brown adipose tissue thermogenesis and obesity. *Progress in lipid research* 28, 67-115.
- Hirschberg, V. (2012). Analysis of uncoupling protein 1 and CideA function in two mammalian cell lines. In *Fakultät Wissenschaftszentrum Weihenstephan (TU München)*, pp. 128.
- Hondares, E., Rosell, M., Gonzalez, F.J., Giral, M., Iglesias, R., and Villarroya, F. (2010). Hepatic FGF21 expression is induced at birth via PPARalpha in response to milk intake and contributes to thermogenic activation of neonatal brown fat. *Cell metabolism* 11, 206-212.
- Inokuma, K., Okamatsu-Ogura, Y., Omachi, A., Matsushita, Y., Kimura, K., Yamashita, H., and Saito, M. (2006). Indispensable role of mitochondrial UCP1 for antiobesity effect of beta3-adrenergic stimulation. *American journal of physiology Endocrinology and metabolism* 290, E1014-1021.
- Jacquet, H., Raux, G., Thibaut, F., Hecketsweiler, B., Houy, E., Demilly, C., Haouzir, S., Allio, G., Fouldrin, G., Drouin, V., *et al.* (2002). PRODH mutations and hyperprolinemia in a subset of schizophrenic patients. *Human molecular genetics* 11, 2243-2249.
- Karaolis-Danckert, N., Buyken, A.E., Kulig, M., Kroke, A., Forster, J., Kamin, W., Schuster, A., Hornberg, C., Keil, T., Bergmann, R.L., *et al.* (2008). How pre- and postnatal risk factors modify the effect of rapid weight gain in infancy and early childhood on subsequent fat mass development: results from the Multicenter Allergy Study 90. *The American journal of clinical nutrition* 87, 1356-1364.
- Kawabata, F., Inoue, N., Masamoto, Y., Matsumura, S., Kimura, W., Kadowaki, M., Higashi, T., Tominaga, M., Inoue, K., and Fushiki, T. (2009). Non-pungent capsaicin analogs (capsinoids) increase metabolic rate and enhance thermogenesis via gastrointestinal TRPV1 in mice. *Bioscience, biotechnology, and biochemistry* 73, 2690-2697.
- Keane, T.M., Goodstadt, L., Danecek, P., White, M.A., Wong, K., Yalcin, B., Heger, A., Agam, A., Slater, G., Goodson, M., *et al.* (2011). Mouse genomic variation and its effect on phenotypes and gene regulation. *Nature* 477, 289-294.
- Kopecky, J., Clarke, G., Enerback, S., Spiegelman, B., and Kozak, L.P. (1995). Expression of the mitochondrial uncoupling protein gene from the aP2 gene promoter prevents genetic obesity. *The Journal of clinical investigation* 96, 2914-2923.
- Kozak, U.C., Kopecky, J., Teisinger, J., Enerback, S., Boyer, B., and Kozak, L.P. (1994). An upstream enhancer regulating brown-fat-specific expression of the mitochondrial uncoupling protein gene. *Molecular and cellular biology* 14, 59-67.

- Laemmli, U.K. (1970). Cleavage of structural proteins during the assembly of the head of bacteriophage T4. *Nature* 227, 680-685.
- Lasar, D., Julius, A., Fromme, T., and Klingenspor, M. (2013). Browning attenuates murine white adipose tissue expansion during postnatal development. *Biochimica et biophysica acta* 1831, 960-968.
- Lee, P., Werner, C.D., Kebebew, E., and Celi, F.S. (2014). Functional thermogenic beige adipogenesis is inducible in human neck fat. *Int J Obes (Lond)* 38, 170-176.
- Lee, Y.H., Petkova, A.P., Mottillo, E.P., and Granneman, J.G. (2012). In vivo identification of bipotential adipocyte progenitors recruited by beta3-adrenoceptor activation and high-fat feeding. *Cell metabolism* 15, 480-491.
- Lettieri Barbato, D., Aquilano, K., Baldelli, S., Cannata, S.M., Bernardini, S., Rotilio, G., and Ciriolo, M.R. (2014). Proline oxidase-adipose triglyceride lipase pathway restrains adipose cell death and tissue inflammation. *Cell death and differentiation* 21, 113-123.
- Liu, D., Diorio, J., Tannenbaum, B., Caldji, C., Francis, D., Freedman, A., Sharma, S., Pearson, D., Plotsky, P.M., and Meaney, M.J. (1997). Maternal care, hippocampal glucocorticoid receptors, and hypothalamic-pituitary-adrenal responses to stress. *Science* 277, 1659-1662.
- Lockie, S.H., Heppner, K.M., Chaudhary, N., Chabenne, J.R., Morgan, D.A., Veyrat-Durebex, C., Ananthakrishnan, G., Rohner-Jeanrenaud, F., Drucker, D.J., DiMarchi, R., *et al.* (2012). Direct control of brown adipose tissue thermogenesis by central nervous system glucagon-like peptide-1 receptor signaling. *Diabetes* 61, 2753-2762.
- M. Klingenspor, T.F. (2011). Brown Adipose Tissue, Chapter 3. In *Adipose tissue biology*, M.E. Symonds, ed. (New York: Springer).
- Matthias, A., Ohlson, K.B., Fredriksson, J.M., Jacobsson, A., Nedergaard, J., and Cannon, B. (2000). Thermogenic responses in brown fat cells are fully UCP1-dependent. UCP2 or UCP3 do not substitute for UCP1 in adrenergically or fatty acid-induced thermogenesis. *The Journal of biological chemistry* 275, 25073-25081.
- Matyskova, R., Maletinska, L., Maixnerova, J., Pirnik, Z., Kiss, A., and Zelezna, B. (2008). Comparison of the obesity phenotypes related to monosodium glutamate effect on arcuate nucleus and/or the high fat diet feeding in C57BL/6 and NMRI mice. *Physiological research / Academia Scientiarum Bohemoslovaca* 57, 727-734.
- Meyer, C.W., Korthaus, D., Jagla, W., Cornali, E., Grosse, J., Fuchs, H., Klingenspor, M., Roemheld, S., Tschop, M., Heldmaier, G., *et al.* (2004). A novel missense mutation in the mouse growth hormone gene causes semidominant dwarfism, hyperghrelinemia, and obesity. *Endocrinology* 145, 2531-2541.
- Meyer, C.W., Willershauser, M., Jastroch, M., Rourke, B.C., Fromme, T., Oelkrug, R., Heldmaier, G., and Klingenspor, M. (2010). Adaptive thermogenesis and thermal conductance in wild-type and UCP1-KO mice. *American journal of physiology Regulatory, integrative and comparative physiology* 299, R1396-1406.
- Minotti, A.J., Shah, L., and Keller, K. (2004). Positron emission tomography/computed tomography fusion imaging in brown adipose tissue. *Clinical nuclear medicine* 29, 5-11.
- Morrison, S.F., Madden, C.J., and Tupone, D. (2012). Central control of brown adipose tissue thermogenesis. *Frontiers in endocrinology* 3.
- Mundt, C.A., Baxter-Jones, A.D., Whiting, S.J., Bailey, D.A., Faulkner, R.A., and Mirwald, R.L. (2006). Relationships of activity and sugar drink intake on fat mass development in youths. *Medicine and science in sports and exercise* 38, 1245-1254.
- Nagalakshmi, U., Waern, K., and Snyder, M. (2010). RNA-Seq: a method for comprehensive transcriptome analysis. *Current protocols in molecular biology / edited by Frederick M Ausubel [et al]* Chapter 4, Unit 4 11 11-13.
- Nedergaard, J., Bengtsson, T., and Cannon, B. (2007). Unexpected evidence for active brown adipose tissue in adult humans. *American journal of physiology Endocrinology and metabolism* 293, E444-452.

- Nedergaard, J., Golozoubova, V., Matthias, A., Asadi, A., Jacobsson, A., and Cannon, B. (2001). UCP1: the only protein able to mediate adaptive non-shivering thermogenesis and metabolic inefficiency. *Biochimica et biophysica acta* *1504*, 82-106.
- Nedergaard, J., and Lindberg, O. (1979). Norepinephrine-stimulated fatty-acid release and oxygen consumption in isolated hamster brown-fat cells. Influence of buffers, albumin, insulin and mitochondrial inhibitors. *European journal of biochemistry / FEBS* *95*, 139-145.
- Nisoli, E., Tonello, C., and Carruba, M.O. (1998). Nerve growth factor, beta3-adrenoceptor and uncoupling protein 1 expression in rat brown fat during postnatal development. *Neuroscience letters* *246*, 5-8.
- Nordstrom, E.A., Ryden, M., Backlund, E.C., Dahlman, I., Kaaman, M., Blomqvist, L., Cannon, B., Nedergaard, J., and Arner, P. (2005). A human-specific role of cell death-inducing DFFA (DNA fragmentation factor-alpha)-like effector A (CIDEA) in adipocyte lipolysis and obesity. *Diabetes* *54*, 1726-1734.
- Okamoto, H., Yayama, K., Shibata, H., Nagaoka, M., and Takano, M. (1998). Kininogen expression by rat vascular smooth muscle cells: stimulation by lipopolysaccharide and angiotensin II. *Biochimica et biophysica acta* *1404*, 329-337.
- Ono, K., Tsukamoto-Yasui, M., Hara-Kimura, Y., Inoue, N., Nogusa, Y., Okabe, Y., Nagashima, K., and Kato, F. (2011). Intra-gastric administration of capsiate, a transient receptor potential channel agonist, triggers thermogenic sympathetic responses. *Journal of applied physiology* *110*, 789-798.
- Petkov, P.M., Ding, Y., Cassell, M.A., Zhang, W., Wagner, G., Sargent, E.E., Asquith, S., Crew, V., Johnson, K.A., Robinson, P., *et al.* (2004). An efficient SNP system for mouse genome scanning and elucidating strain relationships. *Genome research* *14*, 1806-1811.
- Petrovic, N., Walden, T.B., Shabalina, I.G., Timmons, J.A., Cannon, B., and Nedergaard, J. (2010). Chronic peroxisome proliferator-activated receptor gamma (PPARgamma) activation of epididymally derived white adipocyte cultures reveals a population of thermogenically competent, UCP1-containing adipocytes molecularly distinct from classic brown adipocytes. *The Journal of biological chemistry* *285*, 7153-7164.
- Pittenger, M.F., Mackay, A.M., Beck, S.C., Jaiswal, R.K., Douglas, R., Mosca, J.D., Moorman, M.A., Simonetti, D.W., Craig, S., and Marshak, D.R. (1999). Multilineage potential of adult human mesenchymal stem cells. *Science* *284*, 143-147.
- Priebe, K., Romeo, R.D., Francis, D.D., Sisti, H.M., Mueller, A., McEwen, B.S., and Brake, W.G. (2005). Maternal influences on adult stress and anxiety-like behavior in C57BL/6J and BALB/cJ mice: a cross-fostering study. *Developmental psychobiology* *47*, 398-407.
- Priego, T., Sanchez, J., Garcia, A.P., Palou, A., and Pico, C. (2013). Maternal dietary fat affects milk fatty acid profile and impacts on weight gain and thermogenic capacity of suckling rats. *Lipids* *48*, 481-495.
- Prusiner, S.B., Cannon, B., and Lindberg, O. (1968). Oxidative metabolism in cells isolated from brown adipose tissue. 1. Catecholamine and fatty acid stimulation of respiration. *European journal of biochemistry / FEBS* *6*, 15-22.
- Rakyan, V.K., Hildmann, T., Novik, K.L., Lewin, J., Tost, J., Cox, A.V., Andrews, T.D., Howe, K.L., Otto, T., Olek, A., *et al.* (2004). DNA methylation profiling of the human major histocompatibility complex: a pilot study for the human epigenome project. *PLoS biology* *2*, e405.
- Rangwala, S.M., and Lazar, M.A. (2000). Transcriptional control of adipogenesis. *Annual review of nutrition* *20*, 535-559.
- Renshaw, S. (2007). *Immunohistochemistry* (Bloxham, Oxfordshire: Scion).
- Ricquier, D., and Kader, J.C. (1976). Mitochondrial protein alteration in active brown fat: a sodium dodecyl sulfate-polyacrylamide gel electrophoretic study. *Biochemical and biophysical research communications* *73*, 577-583.
- Robidoux, J., Cao, W., Quan, H., Daniel, K.W., Moukdar, F., Bai, X., Floering, L.M., and Collins, S. (2005). Selective activation of mitogen-activated protein (MAP) kinase kinase 3 and p38alpha MAP kinase is essential for cyclic AMP-dependent UCP1 expression in adipocytes. *Molecular and cellular biology* *25*, 5466-5479.

- Rosen, E.D., and MacDougald, O.A. (2006). Adipocyte differentiation from the inside out. *Nature reviews Molecular cell biology* 7, 885-896.
- Rosenwald, M., Perdikari, A., Rulicke, T., and Wolfrum, C. (2013). Bi-directional interconversion of brite and white adipocytes. *Nature cell biology* 15, 659-667.
- Saito, M., Okamatsu-Ogura, Y., Matsushita, M., Watanabe, K., Yoneshiro, T., Nio-Kobayashi, J., Iwanaga, T., Miyagawa, M., Kameya, T., Nakada, K., *et al.* (2009). High incidence of metabolically active brown adipose tissue in healthy adult humans: effects of cold exposure and adiposity. *Diabetes* 58, 1526-1531.
- Sanchez-Gurmaches, J., Hung, C.M., Sparks, C.A., Tang, Y., Li, H., and Guertin, D.A. (2012). PTEN loss in the Myf5 lineage redistributes body fat and reveals subsets of white adipocytes that arise from Myf5 precursors. *Cell metabolism* 16, 348-362.
- Seale, P., Bjork, B., Yang, W., Kajimura, S., Chin, S., Kuang, S., Scime, A., Devarakonda, S., Conroe, H.M., Erdjument-Bromage, H., *et al.* (2008). PRDM16 controls a brown fat/skeletal muscle switch. *Nature* 454, 961-967.
- Seale, P., Kajimura, S., Yang, W., Chin, S., Rohas, L.M., Uldry, M., Tavernier, G., Langin, D., and Spiegelman, B.M. (2007). Transcriptional control of brown fat determination by PRDM16. *Cell metabolism* 6, 38-54.
- Shabalina, I.G., Petrovic, N., de Jong, J.M., Kalinovich, A.V., Cannon, B., and Nedergaard, J. (2013). UCP1 in brite/beige adipose tissue mitochondria is functionally thermogenic. *Cell reports* 5, 1196-1203.
- Sharp, L.Z., Shinoda, K., Ohno, H., Scheel, D.W., Tomoda, E., Ruiz, L., Hu, H., Wang, L., Pavlova, Z., Gilsanz, V., *et al.* (2012). Human BAT possesses molecular signatures that resemble beige/brite cells. *PloS one* 7, e49452.
- Silva, J.E. (1995). Thyroid hormone control of thermogenesis and energy balance. *Thyroid : official journal of the American Thyroid Association* 5, 481-492.
- Silver, L.M. (1995). *Mouse genetics : concepts and applications* (New York: Oxford University Press).
- Skala, J., Barnard, T., and Lindberg, O. (1970). Changes in interscapular brown adipose tissue of the rat during perinatal and early postnatal development and after cold acclimation. II. Mitochondrial changes. *Comparative biochemistry and physiology* 33, 509-528.
- Spalding, K.L., Arner, E., Westermark, P.O., Bernard, S., Buchholz, B.A., Bergmann, O., Blomqvist, L., Hoffstedt, J., Naslund, E., Britton, T., *et al.* (2008). Dynamics of fat cell turnover in humans. *Nature* 453, 783-787.
- Spiegelman, B.M., and Flier, J.S. (1996). Adipogenesis and obesity: rounding out the big picture. *Cell* 87, 377-389.
- Suzuki, M.M., and Bird, A. (2008). DNA methylation landscapes: provocative insights from epigenomics. *Nature reviews Genetics* 9, 465-476.
- Swindell, W.R. (2011). Metallothionein and the biology of aging. *Ageing research reviews* 10, 132-145.
- Tate, P.H., and Bird, A.P. (1993). Effects of DNA methylation on DNA-binding proteins and gene expression. *Current opinion in genetics & development* 3, 226-231.
- Thonberg, H., Fredriksson, J.M., Nedergaard, J., and Cannon, B. (2002). A novel pathway for adrenergic stimulation of cAMP-response-element-binding protein (CREB) phosphorylation: mediation via alpha1-adrenoceptors and protein kinase C activation. *The Biochemical journal* 364, 73-79.
- Truong, M.T., Erasmus, J.J., Munden, R.F., Marom, E.M., Sabloff, B.S., Gladish, G.W., Podoloff, D.A., and Macapinlac, H.A. (2004). Focal FDG uptake in mediastinal brown fat mimicking malignancy: a potential pitfall resolved on PET/CT. *AJR American journal of roentgenology* 183, 1127-1132.
- van Marken Lichtenbelt, W.D., Vanhomerig, J.W., Smulders, N.M., Drossaerts, J.M., Kemerink, G.J., Bouvy, N.D., Schrauwen, P., and Teule, G.J. (2009). Cold-activated brown adipose tissue in healthy men. *The New England journal of medicine* 360, 1500-1508.
- Vassilatis, D.K., Hohmann, J.G., Zeng, H., Li, F., Ranchalis, J.E., Mortrud, M.T., Brown, A., Rodriguez, S.S., Weller, J.R., Wright, A.C., *et al.* (2003). The G protein-coupled receptor repertoires of human and

- mouse. *Proceedings of the National Academy of Sciences of the United States of America* *100*, 4903-4908.
- Vergnes, L., Chin, R., Young, S.G., and Reue, K. (2011). Heart-type fatty acid-binding protein is essential for efficient brown adipose tissue fatty acid oxidation and cold tolerance. *The Journal of biological chemistry* *286*, 380-390.
- Virtanen, K.A., Lidell, M.E., Orava, J., Heglind, M., Westergren, R., Niemi, T., Taittonen, M., Laine, J., Savisto, N.J., Enerback, S., *et al.* (2009). Functional brown adipose tissue in healthy adults. *The New England journal of medicine* *360*, 1518-1525.
- Vosgerau, U., Lauer, D., Unger, T., and Kaschina, E. (2010). Cleaved high molecular weight kininogen, a novel factor in the regulation of matrix metalloproteinases in vascular smooth muscle cells. *Biochemical pharmacology* *79*, 172-179.
- Vosselman, M.J., van der Lans, A.A., Brans, B., Wierdsma, R., van Baak, M.A., Schrauwen, P., and van Marken Lichtenbelt, W.D. (2012). Systemic beta-adrenergic stimulation of thermogenesis is not accompanied by brown adipose tissue activity in humans. *Diabetes* *61*, 3106-3113.
- Walden, T.B., Hansen, I.R., Timmons, J.A., Cannon, B., and Nedergaard, J. (2012). Recruited vs. nonrecruited molecular signatures of brown, "brite," and white adipose tissues. *American journal of physiology Endocrinology and metabolism* *302*, E19-31.
- Wang, L., Chen, Y., Yang, M., Zhou, M., Chen, T., Sui, D.Y., and Shaw, C. (2010). Peptide DV-28 amide: An inhibitor of bradykinin-induced arterial smooth muscle relaxation encoded by *Bombina orientalis* skin kininogen-2. *Peptides* *31*, 979-982.
- Wang, Y.X., Lee, C.H., Tjep, S., Yu, R.T., Ham, J., Kang, H., and Evans, R.M. (2003). Peroxisome-proliferator-activated receptor delta activates fat metabolism to prevent obesity. *Cell* *113*, 159-170.
- Weaver, I.C. (2007). Epigenetic programming by maternal behavior and pharmacological intervention. *Nature versus nurture: let's call the whole thing off. Epigenetics : official journal of the DNA Methylation Society* *2*, 22-28.
- Weaver, I.C., Cervoni, N., Champagne, F.A., D'Alessio, A.C., Sharma, S., Seckl, J.R., Dymov, S., Szyf, M., and Meaney, M.J. (2004). Epigenetic programming by maternal behavior. *Nature neuroscience* *7*, 847-854.
- Whiting, S., Derbyshire, E., and Tiwari, B.K. (2012). Capsaicinoids and capsinoids. A potential role for weight management? A systematic review of the evidence. *Appetite* *59*, 341-348.
- Wu, J., Bostrom, P., Sparks, L.M., Ye, L., Choi, J.H., Giang, A.H., Khandekar, M., Virtanen, K.A., Nuutila, P., Schaart, G., *et al.* (2012). Beige adipocytes are a distinct type of thermogenic fat cell in mouse and human. *Cell* *150*, 366-376.
- Xue, B., Rim, J.S., Hogan, J.C., Coulter, A.A., Koza, R.A., and Kozak, L.P. (2007). Genetic variability affects the development of brown adipocytes in white fat but not in interscapular brown fat. *Journal of lipid research* *48*, 41-51.
- Yoneshiro, T., Aita, S., Kawai, Y., Iwanaga, T., and Saito, M. (2012). Nonpungent capsaicin analogs (capsinoids) increase energy expenditure through the activation of brown adipose tissue in humans. *The American journal of clinical nutrition* *95*, 845-850.
- Young, P., Arch, J.R., and Ashwell, M. (1984). Brown adipose tissue in the parametrial fat pad of the mouse. *FEBS letters* *167*, 10-14.
- Zhou, Q., and Melton, D.A. (2008). Extreme makeover: converting one cell into another. *Cell stem cell* *3*, 382-388.
- Zhou, Z., Yon Toh, S., Chen, Z., Guo, K., Ng, C.P., Ponniah, S., Lin, S.C., Hong, W., and Li, P. (2003). Cidea-deficient mice have lean phenotype and are resistant to obesity. *Nature genetics* *35*, 49-56.

IV Acknowledgments

I feel obliged to many people for their support and encouragement which was invaluable for the success of this PhD thesis. In the following lines some of them are gratefully acknowledged. However, I am aware that there are many more and my words cannot express my respect and gratitude I feel for those.

First and foremost I thank Prof. Dr. Martin Klingenspor for establishing this project within the context of the ZIEL PhD College for “Ernährungsphysiologische Anpassung und epigenetische Mechanismen”. I am grateful for his supervisory support and especially his vigorous efforts to improve myself as a scientist. At the same time I like to express my gratitude to my supervisor Dr. Tobias Fromme. As a tower of strength, he managed to support me 24/7, even during his own stressful times. I like him and his family a bunch. I owe special thanks to our technicians Anika Zimmerman and Sabine Mocek. Their efforts allowed a trouble-free daily routine. Special thanks go to my office members Theresa Schöttl, Kerstin Haas, Christoph Hoffman and Patrice Mengue. Our vividly discussions, also about science, were an enjoyable distraction. I like to thank all the other lab members and colleagues of the institute for the nice time that we shared together.

Furthermore I like to thank Prof. Dr. Susanne Ulbrich for her supervision of the ZIEL PhD College and the collaboration in context of the methylation analysis of the UCP1 enhancer region that was accomplished by Veronika Pistek. In this context I like to thank Jana Hemmerling, Kirsten Übel and again Veronika Pistek for the enjoyable time during this PhD College.

I would particularly like to thank my family, especially my parents Ursula and Heinrich Lasar and my brother Andreas Lasar for their moral support. You laid the foundation of my recent life. In the same context I like to express my greatest respect to my two best friends and best men Philipp and Heinrich that remained steadfastly at my side for at least 25 years. They were always there for me and showed me that there is also a life next to science.

Last but not least I like to thank my beloved wife Jasmin for being at my side. Luckily for me she, besides Tobias, corrected this work and had to endure my grumpy behavior during the time writing it. I love you and especially here my words cannot express my gratitude for you, supporting me in prosperity and adversity.

V Curriculum Vitae

David Lasar

PhD student

Personal information:

Name: David Martin Lasar
Address: Grundstr. 20
CH-8600 Dübendorf
Switzerland
Phone: 0049791761331
E-mail: david-lasar@ethz.ch
Date of birth: 19th February 1983
Place of birth: Cologne, Germany
Profession: PhD student



Scientific interests: In my current PhD thesis I am interested in the transition from white adipocytes into brown like adipocytes in white adipose tissue of murine neonates in different mouse strains. Finding a way to understand the mechanism, this transition phenomenon could be a possible way to treat obesity. To analyze the browning phenomenon I use histological methods and state-of the art genetic and biochemical tools.

In my previous diploma thesis I analyzed the role of inflammation and endoplasmatic reticulum stress in the dysregulation of hypothalamic control of energy homeostasis during obesity and the normal aging process. In general, I am very interested in the development of the metabolic syndrome and the regulation of signal transduction pathways.

Scientific skills: Trained in cell culture, molecular *in vitro* and *in vivo* analysis of mouse models, including intracerebroventricular cannula surgery and icv injections (in mice), glucose and insulin tolerance tests. Trained in biochemical methods such as HPLC, Western blotting, real-time PCR, Immuno-Fluorescent and Histochemistry. Proficient in Windows, Word, Excel, PowerPoint, Sigma Stat and Graph Pad Prism.

Academic Background:

- May 2014 – **research fellow:**
Workgroup of Prof.dr. C. Wolfrum, I.f.Lebensmittelwiss, ETH Zürich
Reference: Prof.dr. C. Wolfrum christian-wolfrum@ethz.ch
- Aug 2010 – Jan 2014 **PhD thesis:**
Workgroup of Prof.dr. M. Klingenspor, Institute for Molecular Nutritional Medicine, department Z I E L Research Center for Nutrition and Food Sciences, Technische Universität München

Subject: The developmental role of brown adipose tissue and brown-like adipocytes (brites) in murine neonates
Reference: Prof.dr. M. Klingenspor mk@tum.de

Associate in the Epigenetic Kolleg “Nutritional Adaptation”
Reference: dr. S.E. Ulbrich ulbrich@wzw.tum.de

Associate in the “Graduierten Zentrum Weihenstephan”
Reference: dr. A. Schieder arne.schieder@wzw.tum.de
Mentor: Prof.dr. C. Wolfrum christian-wolfrum@ethz.ch
- Apr – May 2013 **Academic commutation during PhD thesis:**
Jun 2013 Workgroup of Prof.dr. C. Wolfrum, I.f.Lebensmittelwiss, ETH Zürich
Workgroup of Prof.dr. J. Auwerx, Laboratory of Integrative Systems Physiology, EPFL Lausanne
- Aug 2009 – July 2010 **Diploma thesis:**
Workgroup of Prof.dr. J.C. Brüning, Institute of Genetics, department for Mouse Genetics and Metabolism, University of Cologne

Subject: The Effect of Inflammatory Cytokines and Fatty Acids on Hypothalamic Regulation of Energy Homeostasis
Reference: Prof.dr. J.C. Brüning Jens.Bruening@uni-koeln.de
- May 2009 **Diploma oral examination:**
Principal subject: Genetics (1.0)
Minor subjects: Biochemistry (1.3) and Pharmacology (2.0)
- Jan 2009 – May 2009 **Internship in the workgroup of Prof.dr. J.C. Brüning**
Institute of Genetics, University of Cologne

Subject: Learning of biochemical and molecular methods
Reference: Prof.dr. J.C. Brüning Jens.Bruening@uni-koeln.de
- Apr 2006 – Mar 2010 **Student assistant of em.Prof.dr. B. Müller-Hill**
Institute for Genetics, University of Cologne

Subject: correspondence clerk
Reference: em.Prof.dr. B. Müller-Hill muellerhill@uni-koeln.de

Jul 2008 – Sep 2008 **Internship in the workgroup of Dr.med. C. Müller**
Therapeutical Drug Monitoring, Institute of Pharmacology, University
Hospital of Cologne

Subject: Establishment and validation of an analytical HPLC Method
for the detection of Amisulpride in blood serum

Reference: Prof.dr. C. Müller c.mueller@uni-koeln.de

Mar 2006/2007/2008 **Student assistant and academic advisor for 1st year students**

Teaching methods:

- Handling of bacterial cultures (*E.coli*)
- Cloning
- Restriction analysis

Reference: Dr. B. Kisters-Woike b.kisters@uni-koeln.de

Publications:

D. Lasar, A. Julius, T. Fromme, M. Klingenspor: Browning attenuates murine white adipose tissue expansion during postnatal development **Biochim Biophys Acta**. 2013 Jan 30. pii: S1388-1981(13)00035-8. doi: 10.1016/j.bbaliip.2013.01.016.

Yongguo Li, **David Lasar**, Tobias Fromme, Martin Klingenspor: White, Brite and Brown Adipocytes: The Evolution and Function of a Heater Organ in Mammals, **Canadian Journal of Zoology**, review, Published on the web 21 October 2013, 10.1139/cjz-2013-0165

Presentations:

Jan – Feb Poster presentation at the meeting on Adipose Tissue Biology (J5), in Keystone Resort in Keystone, Colorado

Grants & awards:

Oct 2012 Keystone scholarship: meeting on Adipose Tissue Biology (J5), Jan 27 - Feb 1, 2013, in Keystone Resort in Keystone, Colorado

Teaching: Mentoring of bachelor and master students

Military Service:

Jul 2003 – Aug 2004 Heinrich-Hertz-Kaserne in Daun
(last service grade: „Hauptgefreiter“)

Education:

2004 – 2010 Diploma student in the University of Cologne

1999 – 2003 Wirteltor-Gymnasium, Düren

Abitur Ø2,9

1993 – 1999 Heinrich-Mann-Gymnasium, Cologne

1989 – 1993 Gemeinschaftsgrundschule, Cologne

Personal Interests: In my spare time I play soccer, basketball and do ballroom dance.

VI A Statement under Oath/Eidesstattliche Erklärung

Ich erkläre an Eides statt, dass ich die bei der Fakultät Wissenschaftszentrum Weihenstephan für Ernährung, Landnutzung und Umwelt (promotionsführende Einrichtung) der TUM zur Promotionsprüfung vorgelegten Arbeit mit dem Titel:

The developmental role of brown adipose tissue and brown-like
adipocytes (brite) in murine neonates

am Lehrstuhl für Molekulare Ernährungsmedizin unter der Anleitung und Betreuung durch Prof. Dr. Martin Klingenspor ohne sonstige Hilfe erstellt und bei der Abfassung nur die gemäß § 6 Abs. 6 & 7 Satz 2 angegebenen Hilfsmittel benutzt habe.

Ich habe keine Organisation eingeschaltet, die gegen Entgelt Betreuerinnen und Betreuer für die Anfertigung von Dissertationen sucht, oder die mir obliegenden Pflichten hinsichtlich der Prüfungsleistungen für mich ganz oder teilweise erledigt.

Ich habe die Dissertation in dieser oder ähnlicher Form in keinem anderen Prüfungsverfahren als Prüfungsleistung vorgelegt.

Ich habe den angestrebten Doktorgrad noch nicht erworben und bin nicht in einem früheren Promotionsverfahren für den angestrebten Doktorgrad endgültig gescheitert.

Die öffentlich zugängliche Promotionsordnung der TUM ist mir bekannt, insbesondere habe ich die Bedeutung von § 28 (Nichtigkeit der Promotion) und § 29 (Entzug des Doktorgrades) zur Kenntnis genommen. Ich bin mir der Konsequenzen einer falschen Eidesstattlichen Erklärung bewusst.

Mit der Aufnahme meiner personenbezogenen Daten in die Alumni-Datei bei der TUM bin ich einverstanden.

.....
(Ort, Datum, Unterschrift)